



저작자표시-비영리-변경금지 2.0 대한민국

이용자는 아래의 조건을 따르는 경우에 한하여 자유롭게

- 이 저작물을 복제, 배포, 전송, 전시, 공연 및 방송할 수 있습니다.

다음과 같은 조건을 따라야 합니다:



저작자표시. 귀하는 원저작자를 표시하여야 합니다.



비영리. 귀하는 이 저작물을 영리 목적으로 이용할 수 없습니다.



변경금지. 귀하는 이 저작물을 개작, 변형 또는 가공할 수 없습니다.

- 귀하는, 이 저작물의 재이용이나 배포의 경우, 이 저작물에 적용된 이용허락조건을 명확하게 나타내어야 합니다.
- 저작권자로부터 별도의 허가를 받으면 이러한 조건들은 적용되지 않습니다.

저작권법에 따른 이용자의 권리는 위의 내용에 의하여 영향을 받지 않습니다.

이것은 [이용허락규약\(Legal Code\)](#)을 이해하기 쉽게 요약한 것입니다.

[Disclaimer](#)

Master's Thesis

Modeling and Evaluation of the Volumetric Errors  
for the 5-Axis Machine Tool

Taesoo Jang

Department of Mechanical Engineering

Ulsan National Institute of Science and Technology

2023

# Modeling and Evaluation of the Volumetric Errors for the 5-Axis Machine Tool

Taesoo Jang

Department of Mechanical Engineering

Ulsan National Institute of Science and Technology

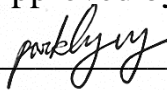
# Modeling and Evaluation of the Volumetric Errors for the 5-Axis Machine Tool

A thesis/dissertation submitted to  
Ulsan National Institute of Science and Technology  
in partial fulfillment of the  
requirements for the degree of  
Master of Science

Taesoo Jang

12/08/2022

Approved by



---

Advisor

Hyung-Wook Park

# Modeling and Evaluation of the Volumetric Errors for the 5-Axis Machine Tool

Taesoo Jang

This certifies that the thesis/dissertation of Taesoo Jang is approved.


12/08/2022

Signature



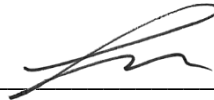
\_\_\_\_\_  
Advisor: Hyung-Wook Park

Signature



\_\_\_\_\_  
Thesis Committee: Namhun Kim

Signature



\_\_\_\_\_  
Thesis Committee: Im Doo Jung

## ABSTRACT

CNC Machine tools are among the most important means of production in metalworking industries and/ have been most widely used. Since an increasing demand for machinery parts with geometric complexity in high efficiency, multi-axialization and multi-functionalization emerged as technology trends in the machine tools field. As a result, 5-axis machine tools have been extensively used in various manufacturing applications requiring higher machining accuracy. In reality, demand in aerospace, medical, electric vehicle, and precision&semiconductor industries are driving. Based on the order composition of machine tools, the proportion of five-axis machine tools has become large remarkably, and also this trend is expected to continue in the future.

While this high flexibility to machine complex parts efficiently could have led the 5-axis machine tool to become a great solution in the metalworking industry, at the same time, 5-axis machine tools have encountered challenges that have to overcome hurdles that come from this flexibility and freedom. As is well known, machine tools' accuracy is one of the most important indicators for the performance of machine tools, and 5-axis machine tools accompany more complexities and require more elements and more assembly processes, so encounter more accuracy problems indispensably.

Overcoming these challenges and under the motivation to high-accuracy 5-axis machine tools, modeling and evaluating the volumetric errors for a 5-axis machine tool was set as this research objective. Specifically, in order to model the volumetric error, a study on the kinematic structures and identification for systematic error is carried out beforehand, and based on this, the goal aims to establish an error model of the 5-axis machine tool. Then, the error model established for a 5-axis machine tool is applied to a practical machine tool, and the errors propagating sensitively to volumetric error are determined as key errors. Also, the resultant effect of the individual errors and key errors is evaluated in advance through estimation of volumetric error. To estimate the volumetric error in virtual, stochastic estimation with random variables was conducted to obtain tool points' coordinates within a workspace, and statistical analysis has carried out. Through these analysis processes, whether machine tools' volumetric error is enhanced under the condition when key errors were specified and assembled is confirmed.

Lastly, to confirm the utility of modeling and evaluation for volumetric error in advance, the demonstration was conducted on two actual 5-axis machine tools, and each machine tool had been manufactured under the management to be assembled with the tolerance used in virtual evaluations as same as possible. Depending on whether or not the specified key error tolerance range is fulfilled, it has clearly confirmed the superiority and inferiority of 5-axis machine tools' volumetric error. And also by comparing estimation and experimental results, it is found that the approach and methods used in this study were useful and could be applied to the actual 5-axis machine tool manufacturing process.



## CONTENTS

<b>1. INTRODUCTION</b> .....	12
1.1 Problem Definition .....	12
1.2 Research Objective .....	13
1.3 Organization of Thesis .....	14
<b>2. LITERATURE REVIEW</b> .....	16
2.1 Kinematic Structure and Systematic Geometric Error of 5-Axis Machine Tools .....	16
2.1.1 Classification of Kinematic Structure of 5-Axis Machine Tools .....	16
2.1.2 Classification of Systematic Geometric Error of 5-Axis Machine Tools .....	17
2.2 Techniques for Error Modeling of Multi-Axis Machine Tools .....	20
2.3 Technique for Measurement of Volumetric Error of Machine Tools .....	22
2.4 Summary .....	25
<b>3. MODELING VOLUMETRIC ERROR FOR 5-AXIS MACHINE TOOLS</b> .....	27
3.1 Kinematic Structure and Chain of 5-Axis Machine Tools .....	27
3.2 Homogeneous Coordinate Representation for 5-Axis Machine Tools .....	30
3.3 Homogeneous Transformation Matrix for 5-Axis Machine Tools .....	31
3.3.1 Homogeneous Transformation Matrix of Linear Motion Components .....	31
3.3.2 Homogeneous Transformation Matrix of Rotary Motion Components .....	34
3.3.3 Homogeneous Transformation Matrix of Errors by Inaccurate Link .....	37
<b>4. EVALUATION OF VOLUMETRIC ERROR FOR A 5-AXIS MACHINE TOOL</b> .....	41
4.1 Formulation of Error Model for a Practical 5-Axis Machine Tool .....	41
4.2 Determination of Key Error for a Practical 5-Axis Machine Tool .....	46
4.3 Estimation of Volumetric Error for a Practical 5-Axis Machine Tool .....	56
<b>5. EXPERIMENTAL RESULTS AND DISCUSSION</b> .....	62
5.1 Experiment Setup .....	62
5.2 Experiment Results of a 5-Axis Machine Tool, DVF5000 .....	66
5.2.1 Assessment for Errors Before Application of Proposed Tolerance .....	66
5.2.2 Assessment for Errors After Application of Proposed Tolerance .....	69
5.3 Comparison of Experiment Results and Discussion .....	72
<b>6. CONCLUSION AND FUTURE WORKS</b> .....	75
<b>REFERENCES</b> .....	77
<b>ACKNOWLEDGEMENT</b> .....	82



## LIST OF FIGURES

Fig. 1-1 Flow chart of thesis configuration .....	11
Fig. 2-1 Example of classification for practical 5-axis machine tools into main group and subgroup .....	16
Fig. 2-2 Influencing factors on geometric and kinematic deviations of machine tools .....	17
Fig. 2-3 Schematics of the motion and errors elements in (a) X-axis, (b) C-axis .....	18
Fig. 2-4 Position and orientation errors of (a) linear axis(e.g., Z-axis), and (b) rotary axis(e.g., C-axis) .....	20
Fig. 2-5 Procedure for the calibration of rotary axes, C-axis, using a tracking interferometer in three positions (I–III) and four reflector locations (1–4) .....	25
Fig. 3-1 Configuration of 5-axis machine tool(Group of main: RRTTT, sub: G3/G'2) .....	28
Fig. 3-2 Concept of kinematic chain and structural loop for the 5-axis machine tool .....	28
Fig. 3-3 Motion and errors in an X-axis linear motion(translatory joint) .....	32
Fig. 3-4 Motion and errors in a C-axis rotation motion(rotary joint) .....	35
Fig. 3-5 Influence of orientation and location errors of the rotary axes .....	40
Fig. 4-1 Kinematic chain diagram for DVF5000; the subject machine tool of this study .....	41
Fig. 4-2 Distribution of coordinate frames in each rigid body; (a) Isometric view, (b) Right side view, and (c) Plane view .....	45
Fig. 4-3 The analysis result of sensitive error parameters for $E_v$ .....	51
Fig. 4-4 The analysis result of sensitive error parameters for $E_{vx}$ , $E_{vy}$ , and $E_{vz}$ .....	51
Fig. 4-5 The analysis result of sensitive error parameters for $E_v$ of rotary axes .....	55
Fig. 4-6 The analysis result of sensitive error parameters for $E_{vx}$ , $E_{vy}$ , and $E_{vz}$ of rotary axes .....	55
Fig. 4-7 Illustration of the simulation of the traces at arbitrary point; (a) tool point, (b) workpiece point .....	58
Fig. 4-8 Frequency distribution of predicting volumetric errors propagated through (a) the tool side loop, (b) the workpiece side loop under the general tolerance .....	59
Fig. 4-9 Frequency distribution of predicting volumetric errors propagated through (a) the tool side loop,	

(b) the workpiece side loop under the condition of suppressing the key errors .....	60
Fig. 5-1 Preparation for experiments using the environmental chamber; (a) installation of DVF5000 before tests, (d) state of the environmental chamber during the experiment .....	62
Fig. 5-2 Experimental setup for measuring linear errors of (a) X-axis, (b) Y-axis, and (c) Z-axis .....	64
Fig. 5-3 A measured error profile affected by the squareness error dominantly .....	64
Fig. 5-4 Experimental setup for the circular test of each plane of (a) XY, (b) XZ, and (c) YZ .....	65
Fig. 5-5 Experimental setup of laser trace for assessing the volumetric error .....	65
Fig. 5-6 Geometric errors along the X-axis before applying the proposed tolerance .....	66
Fig. 5-7 Geometric errors along the Y-axis before applying the proposed tolerance .....	67
Fig. 5-8 Geometric errors along the Z-axis before applying the proposed tolerance .....	67
Fig. 5-9 Squareness errors between the Y- and Z-axis before applying the proposed tolerance .....	68
Fig. 5-10 Result of volumetric errors before applying the proposed tolerance .....	69
Fig. 5-11 Geometric errors of the (a) X-, (b) Y-, and (c) Z- axis, after applying the proposed tolerance .....	70
Fig. 5-12 Result of volumetric errors after applying the proposed tolerance .....	71
Fig. 5-13 Comparison of key errors for individual motions of two machine tools tested .....	72
Fig. 5-14 Comparison of key errors for mutually simultaneous motions of two machine tools tested .....	73

## LIST OF TABLES

Table 2-1 List of geometric error parameters for 5-axis machine tools (ISO notation) .....	19
Table 4-1 Relative coordinate values between the origin of each coordinate frame .....	47
Table 4-2 List of considered error parameters for 5-axis machine tool .....	47
Table 4-3 Error gain matrix for translatory axes of a 5-axis machine tool, DVF5000 .....	50
Table 4-4 Error gain matrix for rotary axes of a 5-axis machine tool, DVF5000 .....	54
Table 4-5 Chance of a value falling within $k \sigma$ of its expected value for random processes .....	57
Table 4-6 Ranges of sampling tolerance of geometric and kinematic errors; general case .....	58
Table 4-7 Key errors and ranges of sampling tolerance; case considering coefficient of errors .....	59
Table 5-1 Specification of a Walk-in environmental chamber and setup condition .....	63
Table 5-2 Performance specification of an XM-60, a multi-axis calibrator .....	63
Table 5-3 Results of squareness errors between the linear axes before applying the proposed tolerance .....	68
Table 5-4 Results of squareness errors between the linear axes after applying the proposed tolerance .....	71
Table 5-5 Comparison of key errors and the resulting volumetric error of two machine tools tested .....	74



Fig. 1-1 Flow chart of thesis configuration

## Chapter 1. INTRODUCTION

### 1. 1 Problem Definition

CNC Machine tools are among the most significant means of manufacturing and have been widely used in the metalworking industry(e.g., aerospace, automobile, die&mold industry, etc.). Over the past few decades as the increasing complexity of parts and the demand for high-performance machine tools is extended, 5-axis machine tools have been increasingly attracting attention compared to conventional 3-axis machine tool. To allow the flexibility of orientations between a workpiece and cutting tool, almost all 5-axis machine tools are composed of add two rotational axes (R) to three translational axes (T) identical to the configuration of the existing 3-axis machine tools and can be divided into three configurations: TTTRR, RTTTR, and RRTTT[1]. Due to these combinations of axes, the 5-axis machine tools can achieve higher accuracy by machining in a single set-up even if parts need to be machined are geometrically complicated. And also shorten production lead time by integrating multiple processes. In other words, the high flexibility and the degree of freedom to machine complex parts efficiently have led 5-axis machine tools to become a great solution in the metalworking industry.

While 5-axis machine tools have some disadvantages caused by the flexibility and degree of freedom of the machine configuration mentioned above. Particularly, in the perspective of accuracy, 5-axis machine tools builders or users might often encounter more problems such as dimensional inaccuracy than 3-axis machine tools, due to the simultaneous motions involved by 5-axes increase risks related to machine volumetric errors[2], which is defined as relative position error between a cutting tool and a workpiece. In recent decades, the volumetric error has become one of the significant indexes of the quality of the machine tool, as perceptions increase that the volumetric error indicates the machine tools' overall error. Such a volumetric error of machine tools is affected by various error sources occurring in the machine tools' components; the error sources can broadly be classified into three major classes namely quasi-static, thermally induced, and dynamic errors. Among them, quasi-static errors are defined as errors that change slowly over time and are one of the most important factors in volumetric errors of machine tools since they account for about 70% of all errors attributable to a machine tool.[3],[4]. Therefore the process to identify and eliminate quasi-static errors in advance is a key measure that must be carried out to achieve improved volumetric accuracy of 5-axis machine tools. In order to execute this procedure, the 5-axis machine tools' machine builders need to understand a comprehensive knowledge of the relationships between the kinematic and geometric properties of the machine elements and volumetric error in the workspace.

Nevertheless investigating the effect of propagation of quasi-static errors including geometric and

kinematic errors with respect to the volumetric error has been often omitted or accepted as difficult to be quantified in the stage of design for 5-axis machine tools. That is because there are two impediments to conquer. First, the modeling process for volumetric errors of 5-axis machines is more complex than that of 3-axis machines[5]. Second, it is inevitable volumetric errors of 5-axis machines could arise in different axis directions and varying extents depending on the machine configuration, even if the same errors occur in certain machine components[6]. Thus the key requirements for enhancing the machine tools' volumetric inaccuracy are establishing an appropriate mathematical model for volumetric error and distinguishing crucial errors that most influence the relations of position and orientation between a workpiece and a cutting tool. In efforts to reveal these prerequisites, enormous research for identifying and enhancing the machine tools' volumetric error has been conducted and verified successfully. As a result, many studies have been presented in the literature related to the modeling for machine tools' volumetric error to identify individual geometric errors and to find out the resultant spatial accuracy over the past few decades[7-17].

For enhancing the machine tools' volumetric accuracy, there are two approaches to minimizing the end-effect of geometric errors occurring in each component. One is error avoidance which is focused on managing the precision of the machine to the utmost through stages of design, manufacturing, and installation in advance. Another is error compensation which identifies and corrects the resultant discrepancy between the nominal and actual coordinate using specialized measuring instruments(e.g., touch probe) as post-processing[3]. Commonly, manufacturers possessing the technique to properly control the underlying deviation occurring on each machine component of machine tools have been earning a reputation as competitive machine builders. As mentioned earlier, although a tremendous amount of study and demonstrations corresponding to the machine tools' volumetric accuracy have been carried out, almost all the research was concentrated on deriving the methodologies to compensate for the inaccuracy in three-dimensional space caused by geometric errors. In other words, there is still a lack of methodical approaches to avoid comprehensive error by controlling individual geometric error sources on machine tools' components from a stage of design or assembly.

## **1. 2 Research Objective**

To obtain a comprehensive insight into the preemptive measures to minimize the volumetric error propagated from diverse geometric errors occurring on each machine tool component, this thesis focuses on analyzing the various geometric error sources that are usually encountered on 5-axis machine tools and investigating routes of magnification to volumetric inaccuracy. Lastly, it also verifies the effectiveness of error avoidance that can be achieved by employing the analysis results in the stage for building actual machines. Based on this background, the volumetric error modeling using homogenous

transformation matrix for the DVF5000 which is one of the 5-axis machine tool models was established to identify the interrelationship between individual components of 5-axis machine tools and end-effectors (e.g. tool-tip, workpiece), and then it was utilized to classify crucial error parameters that are magnified sensitively to volumetric inaccuracy. In addition, the tendency of volumetric error predicted when individual geometric error parameters are generated in uniformly distributed random numbers form was examined using simulation. And based on these results, the range for assembly tolerance of geometric errors required to achieve the target level of volumetric error was selected and then it experimentally verified whether the volumetric error enhances by controlling the actual assembly tolerance and process.

### **1.3 Organization of This Thesis**

In Chapter 2, previous research conducted on the categorization according to the kinematic structure of 5-axis machine tools and classifications of systematic geometric errors arising from the machine tool components are examined. In addition, research on techniques for error modeling to determine the final effect by synthesizing the parameters of the individual error, and also techniques for measuring and evaluating errors occurring in machine tools are also examined.

In Chapter 3, to construct the 5-axis machine tools' volumetric error model, the individual error parameters that could occur in the 5-axis machine tool are classified into errors due to linear motion components, rotary motion components, and their linkage relationships. Then each matrix composed of these error parameters is defined, and the error model using a homogeneous transformation matrix and rigid body motion kinematics is established based on a kinematic chain of 5-axis machine tools.

In Chapter 4, an error model of the practical 5-axis machine tools, DVF5000, is developed by deriving the gain equation for volumetric error. And the coefficients of the error gain equation are compared for each variable, and the errors propagating sensitively to volumetric errors were determined as key errors through the key error analysis. Then the range of tolerances for key errors is selected considering kinematic characteristics, and the effect of applying the measures to restrain the key geometric errors is predicted through simulation within the working space.

In Chapter 5, In order to demonstrate whether the volumetric error is improved through the process for determination and suppression of key errors, experiments for each error assessment are conducted on two machine tools. Error evaluation under two conditions of machine tools, which are before applying the proposed tolerance and after undergoing measures that satisfied the proposed tolerance, is conducted for comparison. Whether each key error parameter was properly suppressed is evaluated using a laser interferometer which can measure six-degree-of-freedom error and a double ball bar. And

then, the volumetric error, which is the means for resultant error evaluation, is measured using a laser tracer, a commercial volumetric error measuring instrument. Through the comparison of the measurement results of two machine tools, the effectiveness is confirmed that the volumetric error can be enhanced if key error parameters of 5-axis machine tools can be identified in advance and then suppressed properly during the assembly process of machine tools.



## Chapter 2. LITERATURE REVIEW

### 2.1 Kinematic Structure and Systematic Geometric Error of 5-Axis Machine Tools

#### 2.1.1 Classification of Kinematic Structure of 5-Axis Machine Tools

The categorization of 5-axis machine tools can be made into 4 main groups based on a kinematic structure which is represented as combinations of Translatory (T) and Rotary (R) axes; (i) 3 T axes and 2 R axes, (ii) 2 T axes and 3 R axes, (iii) 1 T axis and 4 R axes, (iv) five R axes. In general, almost all 5-axis machine tools belong to the (i) group consisting of 3 'T' axes and 2 'R' axes, and the most typically used configurations are as follows.

- **RRTTT**: As the most common configuration, it consists of 2 rotary axes that constitute a rotational table in which the workpiece is supported, and then 3 sequential translatory axes for tool carrying. The rotational degree of freedom is provided only workpiece by the rotational table.
- **RTTTR**: The configuration can be constructed in combination with 1 rotary, 3 translatory axes, and then 1 rotary axis in which the workpiece is mounted by a rotary linkage and the tool is held by a tilting(rotary) head. The rotational freedom is provided for either workpiece or tool individually.
- **TTTTR**: As the configuration to handle very heavy workpieces, it consists of 3 translatory axes and then 2 rotary axes sequentially, in which the cutting tool is held by a spindle head that has two rotational linkages, one for swivel and another for tilting. The rotational freedom is only provided to the tool by the spindle head.

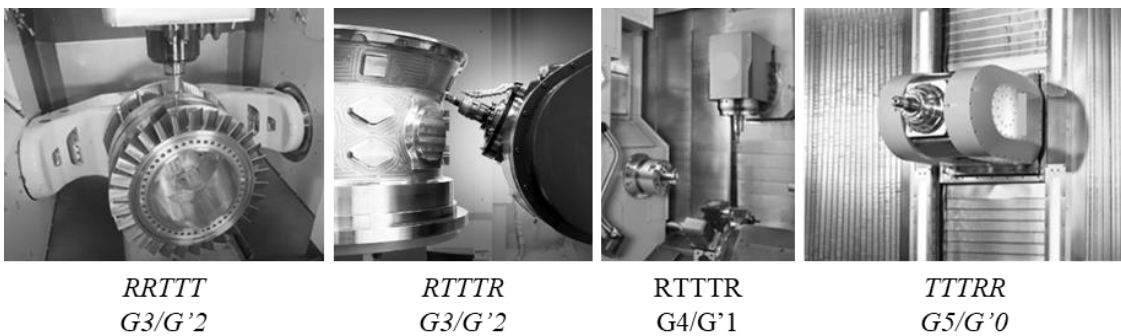


**Fig. 2-1** Example of classification for practical 5-axis machine tools into main group and subgroup

Theoretically, all configurations of 5-axis machines with one tool carrying axis are able to make 720 combinations according to the permutation of axes. As well as 360 combinations that can position or orient the cutting tool within the workspace simultaneously are possible, even considering only typical

5-axis machine tools composed of 3 translatory (T) and 2 rotary (R) motion axes. Based on sequences of carrying axes for workpiece or tool, common 5-axis machines can be classified into 6 subgroups; (i)  $G0/G'5$ , (ii)  $G1/G'4$ , (iii)  $G2/G'3$ , (iv)  $G3/G'2$ , (v)  $G4/G'1$ , (vi)  $G5/G'0$ . Where the set  $Gt/G'w$  of 5-axis machine tools' combinations is characterized by the number of tool-carrying axes like a 't' and workpiece-carrying axes like a 'w'(w=5-t)[32]. These main groups and subgroups can be classified in various ways according to the purpose of use and concept of the 5-axis machine tool, Fig. 2-1 is an example of classifying representative commercial 5-axis machine tools according to the kinematic structure and sequence of carrying axes for the workpiece and cutting tools. It should keep in mind that these various combinations and possibilities can be acted as not only the pros of increasing freedom for 5-axis machine tools but also the cons of multiplying the design and manufacturing complexity of machine tools.

### 2.1.2 Classification of Systematic Geometric Error of 5-Axis Machine Tools

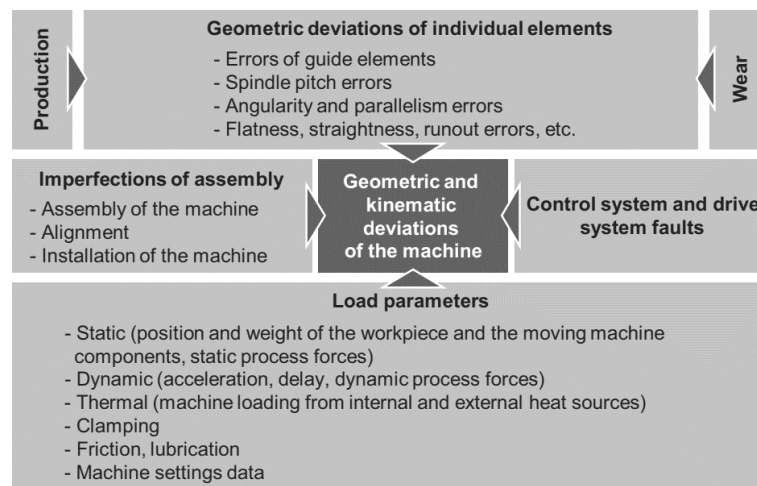


Fig. 2-2 Influencing factors on geometric and kinematic deviations of machine tools[33]

The volumetric error which is the most representative measure of the machine tools' comprehensive accuracy can be expressed as discrepancies between the actual position of the cutting point and the nominal coordinate selected to machine a workpiece in the machine tools' working volume. As shown in Fig. 2-2, the geometric and kinematic deviations as an origin of machine tools' volumetric error have different underlying causes[33], among roots of machine tools' inaccuracy, 75% of the initial error of machine tools are the geometric error of the individual elements that occurred during the production process and the Imperfections in the assembly process[18]. This integrated error is propagated by the incremental accumulation of individual geometric errors caused by mechanical imperfections or geometrical misalignments. These geometrical integrated errors are revealed as forms of translation

inaccuracy at functional points such as a positioning or straightness error of each axis and are mainly caused by errors of flatness, angular motion(e.g., roll, pitch, and yaw), straightness, and linkage errors like squareness or parallelism errors.

In general, the errors of a precision machine that controls positioning behavior are categorized into two groups depending on reproducibility. One is a random error which is defined as an error that does not always have the same value under obviously equal conditions in a given position and is bound to be statistically expressed. Another is systematic error defined as an error that always has the same value and sign under a given position and condition[19]. These error sources mentioned as geometric errors consistently change the dimensional or geometric properties of the machine tools' components and so can be considered errors with systematic characteristics according to the classification into reproducibility stated above. Hence, these systematic geometric errors can often be calibrated to a certain degree through the technological developments of design or manufacture, identifying the geometric errors in advance and making effort to eliminate them is essential to manufacture high-accuracy machine tools that are with high spatial performance.

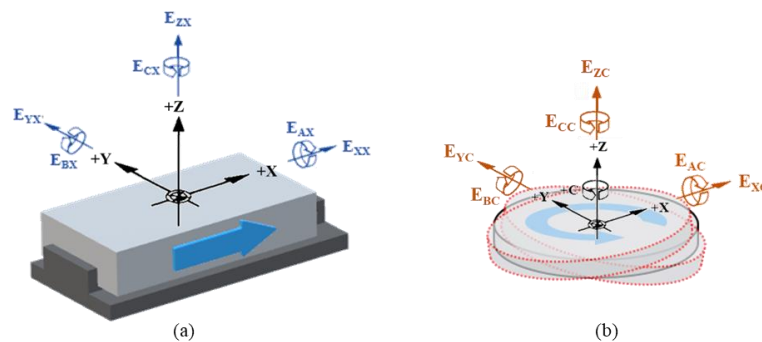


Fig. 2-3 Schematics of the motion and errors elements in (a) X-axis, (b) C-axis

As is well known, it is obvious that there are a total of 21 sources of geometric errors in typical machinery consisting of three linear axes orthogonal to each other(e.g., machine tools, CMM, etc.)[19]. Contrariwise, it is confirmed that the number of error elements applied for each research conducted to error identification for 5-axis machine tools depends on the methodology adopted in modeling for the 5-axis machine tools' error[13]. The most widely used number of error factors in the previous studies is 37 or 39 which can be independently handled considering the individual components of a machine as a rigid body, and the difference between the two numbers depends on whether or not the rotation axis offset error is considered. ISO 230-1[34], international standards of the test code for machine tools, has specified that the classification of machine tools' error motions of translatory and rotary axes assuming it has rigid body behavior, in this regard, the 5-axis machine tool can have a total of 45 independent geometric error elements taking into account the components as a rigid body theoretically; 6 error

elements separately intrinsic in 5 individual components for motion, a total of 7 error elements associated with non-orthogonality of the 5-axis machine tools' coordinate system, and 2 position offset errors per each rotary axis. These geometric error components can be grouped into two; 'PDGE'(abbreviation for 'Position Dependent Geometric Error'), and 'PIGE'(abbreviation for 'Position Independent Geometric Error') depending on the characterization of errors from individual motion or relative linkage. The PDGEs are geometric errors existing in the form of 6-degrees of freedom errors, 3 angular and 3 translational, along the axis of rotation or linear motion. For translatory feed axes, 3 translational errors exist as 1 positioning error and 2 straightness errors, and 3 angular error components are as forms of 1 yaw error, 2 wobbling motion errors, so-called pitch, and roll as pictured in Fig. 2-3 (a). In contrast to that, for rotary motion axes, 3 angular error elements are forms of 1 positioning error and 2 wobbling motion errors, and 3 translational errors appear as forms of 1 axial and 2 radial errors so-called runout as pictured in Fig. 2-3 (b). The 'PIGEs' are a kind of kinematic error defined as errors of the position and orientation between the machine coordinate systems originating from mutual linkages and are mostly caused by the imperfect during assembly of machinery parts such as linkage misalignment, angular tilt, and rotary axes' eccentricity. 'PIGEs' occurring between the linear axes are resulting from relative motion on sequential translatory linkage and are represented by a form of a vector referring to the reference coordinate system's zero position. Therefore, position and orientation errors of translatory linkages are as pictured in Fig. 2-4 (a), only the three orientation errors which contain an orientational deviation on the Y-axis(i.e.,  $E_{C0Y}$ ), and two orientational deviations on the Z-axis(i.e.,  $E_{A0Z}$  and  $E_{B0Z}$ ) are used for representing orthogonality, and only one location error is described as a zero position error(i.e.,  $E_{Z0Z}$ ) in addition. Likewise, in position and orientation errors of rotary joints, irregularities of actual motion and position with respect to the nominal state are defined by a total of 5 error parameters which include 2 location errors (i.e.,  $E_{X0C}$  and  $E_{Y0C}$ ), 2 orientation errors (i.e.,  $E_{A0C}$  and  $E_{B0C}$ ), and a zero angular position (i.e.,  $E_{C0C}$ ) as pictured in Fig. 2-4 (b). And the simplified list of geometric error parameters for the 5-axis machine tools classified based on ISO 230-1 is shown in Table 2-1.

Axis	PIGEs	Number of errors	PDGEs	Number of errors
X	$E_{XX}, E_{YX}, E_{ZX}, E_{AX}, E_{BX}, E_{CX}$	6	-	-
Y	$E_{YY}, E_{XY}, E_{ZY}, E_{BY}, E_{CY}, E_{AY}$	6	$E_{C0Y}, E_{Y0Y}$	2
Z	$E_{ZZ}, E_{XZ}, E_{YZ}, E_{CZ}, E_{BZ}, E_{AZ}$	6	$E_{A0Z}, E_{B0Z}, E_{Z0Z}$	3
A	$E_{XA}, E_{YA}, E_{ZA}, E_{AA}, E_{BA}, E_{CA}$	6	$E_{A0A}, E_{B0A}, E_{C0A}, E_{Y0A}, E_{Z0A}$	5 (i.e., 1+2+2)
B	$E_{XB}, E_{YB}, E_{ZB}, E_{BB}, E_{AB}, E_{CB}$	6	$E_{A0B}, E_{B0B}, E_{C0B}, E_{X0B}, E_{Z0B}$	5 (i.e., 2+1+2)
C	$E_{XC}, E_{YC}, E_{ZC}, E_{CC}, E_{AC}, E_{BC}$	6	$E_{A0C}, E_{B0C}, E_{C0C}, E_{X0C}, E_{Y0C}$	5 (i.e., 2+2+1)

Table 2-1 List of geometric error parameters for 5-axis machine tools (ISO notation)

For reference, the notation of elements of geometric errors(i.e. PIGEs, PDGEs) has the following meanings. 'E' is abbreviation for error error, a character after 'E' refers to the direction of the corresponding error in the machine tools' coordinate system, the '0' attributes the location error, and the last character on the far right is the concerning axis of motion[35].

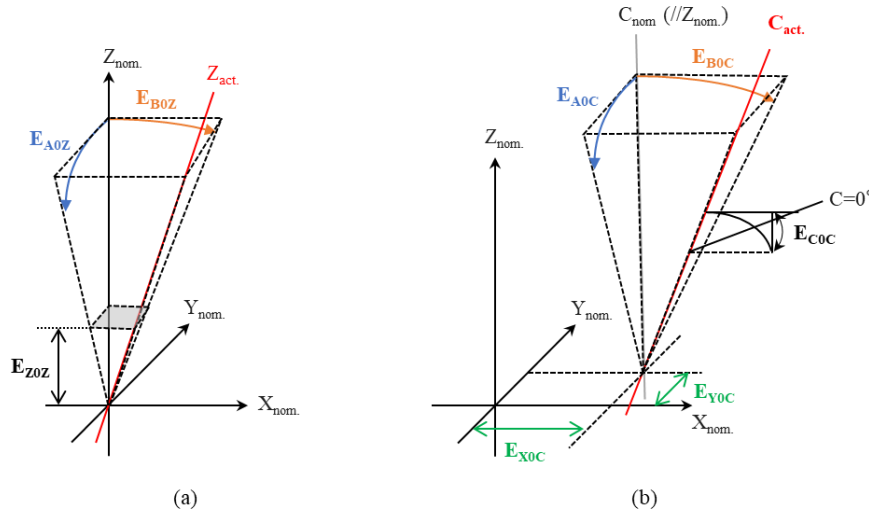


Fig. 2-4 Position and orientation errors of (a) linear axis(e.g., Z-axis), and (b) rotary axis(e.g., C-axis)

## 2.2 Techniques for Error Modeling of Multi-Axis Machine Tools

A substantial amount of study on error modeling of multi-axis machine tools to reveal the resultant error which is caused by the relation of individual components and then manifested as a deviation between tool and workpiece has been carried out; These approaches are based on analyzing how individual errors are propagated with magnification or suppression through the machine tools' kinematic loop system to influence spatial performance within the machine tools' working volume. The technical methods of error modeling for multi-axis machine tools can provide a methodical, and appropriate system to construct the error model which is useful to design and manufacture the machine tools. Among the approaches developed by the previous researchers, the error matrix method, rigid body kinematics, and D-H method are the most representative, and the second-order method, neural network method, and variational method are the others[18]. Considering individual motion components of a machine as rigid body kinematics is very useful to analyze the motion between machine components. The method using homogeneous transform can describe spatial relations between the nominal and actual coordinate represented mutual components composing the machine tools. The pioneering works of these areas were in form of a model using an ideal kinematic based on a homogeneous transformation matrix presented by J. Denavit, et al., and then P. P. Paul, et al. later laid the foundation of analytical inquiry for error model generalization considering a reference frame later[20],[21]. And also a more

generalized methodology for estimating machine tools' spatial errors using a homogenous transformation matrix(HTM) and alleviating its effect through compensation is presented by Donmez, et al., and then demonstrated the validity of the model and methodology[22]. An analytical methodology through a quadratic model for predicting machine tools' geometric errors and contribution analysis was proposed by P. M. Ferreira, et al. Novelty of the proposed models are that rigid body kinematics was utilized to establish an error model that observes error vectors at a certain functional point like a cutting tool point in its coordinates of the machine's working volume, and tracking for the variation of errors along each joint of the machine tool are allowed through that model[23],[24]. Then the model was analyzed to show that the individual coefficients of the models can be assessed by monitoring a few error vectors at functional points. K. F. Ehmann[25] insisted that multi-axis machine tools' position and orientation errors are the effects of the individual axes' errors themselves and also the results of interplays between them. And then presented a model of machine tools' volumetric error through procedures of kinematic modeling which adopted strategies for error compensating based on error propagation models. A general approach based on kinematic chains between a cutting tool and a workpiece to define relative locations is developed by J. A. Soons, et al. and utilized direct kinematics and piecewise polynomials to accomplish this[26]. And claimed that the utilities of these polynomials in combining the pick of important factors with the least squares estimation are meaningful. A viable method adopting the Denavit-Hartenberg (so-called D-H) method for modeling and visualization of each axes' positioning error effects on the volumetric accuracy of a 5-axis machine tool was developed by V. S. B. Kiridena, et al., and it proves that this is a useful tool to utilize as a design tool for error allocation and optimization of machine tools' accuracy[27]. K. G. Ahn, et al.[28] used the model applying homogeneous transformation matrices of adjacent links in machine tools' kinematic chain to find a total volumetric error including effects of backlash error, and the novel approach which proved that the backlash error is a function of position and feed-rate through backlash assessment is worthy. Y. Lin, et al.[29] presented a geometric error model of 5-axis machine tools which is sufficiently common to deal with almost typical 5-axis machine types by utilizing the approach of matrix summation. Although this approach has some merits compared with the homogeneous transformation matrix approach, several demerits existed that more burden follows to should construct each model for definitions of every different configuration and axis. A Multi-Body System(so-called MBS) kinematics to settle the limit of the universal error model established by rigid body kinematics of machine tools is proposed by J. W. Fan, et al., and a general methodology for making machine tools' kinematic model was presented[30]. And then the experimental result that the machine tools' machining accuracy achieved improvement by more than 60% was reported. This remarkable result, however, is limited to a method that the actual cutter points are moved along the ideal cutter path using only error-correcting strategies based on numerical control, so discussions on the methodology for fundamental error reduction of machine tools were rather insufficient. Chen, Guoda, et al.[31] pointed out deficiencies of

previous studies that less attention was paid to the sensitivity and key parameter analysis for 5-axis machines' volumetric error from design views of machine tools particularly. And a volumetric error model for a 5-axis machine tool involving 37 error parameters was constructed based on kinematics assuming a rigid body motion, and a homogenous transformation matrix. And then sensitivity analysis for spatial error considering all individual geometric error parameters was conducted respectively. And it suggested that these analysis results can be utilized from the design and manufacture process of high-accuracy 5-axis machine tools through the experiments of fine surface machining. However, detailed methods or procedure for how to control each error factor that can be applied in actual machine tools was not presented.

As stated above, the research to enhance the errors of machine tools has been done for a long time and extensively, especially the systematic error characterizations in these studies have led to the development of many various approaches for improving the machine tools' comprehensive accuracy. Among these improvement methods, 2 main techniques which are most well-known and widely used are 'Error compensation' and 'Error avoidance'. First, error compensation can be defined as a method for minimizing the effects of geometric errors by either direct or indirect error measurements. Second, error avoidance can be defined as a method for attempting to eliminate systematic errors by predicting them in advance and then suppressing them. Therefore, in order to increase the machine tools' accuracy, establishing an accurate error model regardless of these methodologies is a key factor that must be preceded to successfully identify and control systematic geometric errors.

### **2.3 Technique for Measurement of Volumetric Error of Machine Tools**

The volumetric error of machine tools can be defined as one of the most important factors affecting the accuracy of a machined part. So, evaluations related to machine tools' spatial performance so-called volumetric error have been widely adopted as a useful tool for assessing the comprehensive accuracy of machine tools, and a preemptive action to improve machining accuracy[36, 37, 38]. The main aim of techniques for evaluating the volumetric error is the acquisition of the crucial factor causing the machining inaccuracies. Thus, the measurement for related volumetric error is not only the first but also the most important stage in the process of achieving the objective. Methods for measuring the machine tools' accuracies can be split up 2 ways, 'direct measurements' and 'indirect measurements', depending on whether focus on individual errors themselves or the effects of errors.

First, direct measurement represents measuring and analyzing geometric errors directly as singular errors, such as positioning and angular motion errors of each linear or rotary motion axis[39]. Measuring the position accuracy of a linear motion axis utilizing a laser interferometer or the squareness error using a granite square are representative instances. In reality, many direct measurement methodologies

are tools widely and effectively used by machine tool fields. Measuring volumetric error through direct measurement, however, can have adverse issues in the aspect of efficiency. Even for a typical orthogonal 3-axis machine, in order to evaluate the volumetric error all 21 errors (i.e., summing the number of each 3 linear position, 6 straightness, 3 squareness, and 6 angular motion errors) must be measured by different setups and need to construct the appropriate kinematic model for the machine as well.

Secondly, indirect measurement, which focuses on the combined effects of single errors, represents measuring and analyzing the location or trajectory of certain points like a tooltip. In the early, indirect measurements have been developed for purpose of quickly checking the motioning accuracy of machine tools, a representative instance of indirect measurement broadly adopted by machine tool companies is the circular interpolation performance test employing the double ball bar or grid encoder[41]. The circular interpolation performance test, described in ISO 230-4[40], is most broadly used by machine tool companies and machine tool users for verifying the geometrical characteristics between linear axes under orthogonal configuration as an indirect measurement. It is mainly implemented by utilizing the double ball bar so-called DBB, for particular measurements such as small-radius or high-speed tests a two-dimensional digital scale like a grid encoder is often used. The circular interpolation performance test enables the purpose of checking circular motion accuracy quickly, and also allows the individual errors of the linear axis to be quantitatively calibrated as well[42]. Based on circular tests, identification of the kinematic model is possible, in particular, it is excellent at being able to identify the squareness error by fitting the deviation of contour profiles between a nominal circle and the actual in which shapes of a slanting ellipsoid are measured[43],[44]. The diagonal test, described in ISO 230-6, mainly evaluates the deviation of certain functional points like TCP (Tool Center Point) along the direction to the body diagonal or the face diagonal of the machine tools' working volume utilizing devices based on a laser interferometer. Although diagonal tests are suitable for estimating machine tools' orthogonality between linear motion axes[45],[46],[47], it is not able to evaluate each error parameter related to geometric irregularity through procedures measuring 4 body diagonal length only. And in the case that an aspect ratio of the measuring workspace is extended the measurement error sensitivity or noise increases as well[48]. Therefore, it should be noted that the diagonal test allows estimation of the volumetric performance of a machine tool, machine tools' spatial performance so-called volumetric accuracy can be estimated by diagonal tests but can not diagnose the effects of individual geometric error in itself[45].

Recently, measurement technologies that can estimate the volumetric error in combination with data measured using instruments like the laser tracker or the laser tracer within the working volume of machine tools have been widely applied. A tracking interferometer so-called laser tracker is a sort of laser interferometer adopting a mechanical steering mechanism that controls the laser beam's direction



to track the paths of a target retroreflector. These advanced measurement technologies formed the basis of spatial performance measurement for positioning accuracy of linear motion or rotary axis and are implemented by multi-axis coordinate measurement methodologies including triangulation and multilateration[58]. These technologies have considerable advantages, including the performance to measure even a large volume with high precision and determine individual errors by virtue of the inherent algorithms and techniques of model identification. As previously stated, since almost all 5-axis machine tools consist of three T axes and two R axes, the technique of measurement for kinematics with rotary axes is needed to consider verifying the volumetric error of 5-axis machine tools. Similar to the verification for volumetric error of linear axis, a measurement using a double ball bar is being widely adopted. Tests for interpolation performance of rotary axis are described ISO/CD 10791-6[50], which mainly focus on the measurement technique for location errors calibration of rotary axes, many investigation attempts and results have been presented on the measurement utilizing a double ball bar to identify these rotary axes' location errors[51],[52]. The double ball bar test for trajectories which involves synchronous 5-axis motion can be treated equally to the machining test for the cone frustum described in ISO 10791-6. The tests related to simultaneous motions between rotary and linear axis with dynamic synchronization error were presented by Lei et al.[53]. However, a method measuring rotary axes using a ball bar can gain results one-dimensional each measurement step, hence it repeatedly requires each measurement setup differently to identify all of the rotary motion components' location errors. Unlike the ball bar test, which uses two precision spheres and one linear variable displacement transducer(i.e., LVDT) above, each 3-dimensional coordinate of the precision sphere so-called ball tool can be measured by using a ball cup embedding more than 3 linear displacement detecting sensors. Based on this basis, S. Weikert[54], Bringmann, and Knapp[55] presented a device for measurement, 'R-Test', with a novel concept. A precision sphere as a reference ball mounted at the machine tools' head is located in overlap with the nest in which 3 linear displacement detecting sensors are placed on the rotating table, and then the coordinate based on a 3-dimensional displacement of the reference ball is tracked and acquired by machine tools' motion. therefore, R-test can identify rotary axes' location errors by fitting obtained data to the 5-axis machine tools' motion through a kinematic model. The measurement using the R-test measure the TCP under the mutually synchronous motion between linear and rotary motion axes. The measured coordinate of this trajectory is, thus, influenced by the error of rotary motion and linear motion comprehensively. For this reason, many previous studies for the calibration of rotary axes assume that the linear motions' errors are close to the integrity or insignificant, uncertainty analysis is vital for assessing the reliability of rotary axis calibration under the condition that can not exclude influences of linear motions error[56],[57]. Measuring error with the tracking interferometer for rotary motions' accuracy at arbitrary positions without the mutually synchronous movement of linear motion axes was reviewed by Schwenke, H., et al.[58]. The procedure for measuring error parameters of rotary motions is similar to the measurement process for the linear motion

axis based on acquiring path distances between the traceable laser interferometer and a retro-reflector so-called cat-eye mounted on the spindle nose. The main body of a laser interferometer is mounted on the rotary table and its measuring beam tracks the reflector moving in accordance with the movement between the spindle and the work table. Fig. 2-5 shows a sequential combination of 4 locations of the retro-reflector and 3 installation locations of the main body of a traceable interferometer. Each distance of path is obtained at pre-set angles of the rotary axis driven, these configurations and procedures enable all of the individual errors of rotary motion defined by ISO 230-1[34] to be calculated. Hence, tracking laser interferometers(e.g., LaserTRACER, etc.) are confirmed to be the only measuring system that can be conducted for the total measuring and calibrating errors for linear motion and rotary motion axes of a 5-axis machine tool without additional instruments.

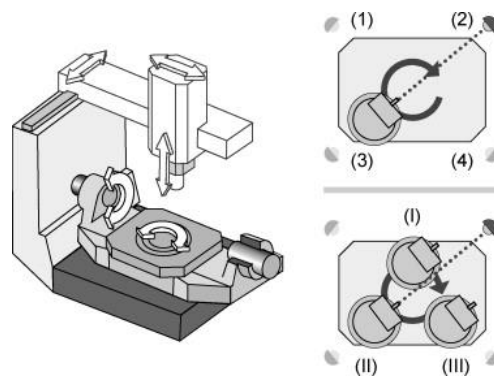


Fig. 2-5 Procedure for the calibration of rotary axes, C-axis, using a tracking interferometer in three positions (I–III) and four reflector locations (1–4)[58]

## 2.4 Summary

In this chapter, an outline of the literature on the schemes of kinematic structure, systematic geometric error, volumetric error modeling, and error measurement related to the 5-axis machine tool have been presented. Although a great deal of research on error modeling, error measuring, and error identification has been accomplished previously, a measure related to error elimination there still remains much work to be done to develop a feasible and substantive way to improve the machine tools' machining accuracy which can also be used in environments of the machine builder or shop.

Many researchers worked on identifying and modeling geometric or kinematic errors which is the first step in increasing the comprehensive accuracy of machine tools. The approaches which are capable of handling all of the error parameters including the PDGEs and PIGEs (position dependent and position independent geometric errors), 21 errors for a 3-axis machine tool, and 37 errors for a 5-axis machine tool, can improve the accuracy of a certain functional point such as TCP. Although the volumetric model of the machines was studied extensively, methods for correction by modifying the

NC program have been concentrated in previous studies.

Therefore, this study aims to develop a methodology to enhance the spatial accuracy of 5-axis machine tools from the design and manufacturing stage by developing and empirically verifying the mathematical error model of the machine tool which defines the relationship between individual components' geometric and kinematic errors, and the resultant error within the machine tools' working volume. Predicting the individual geometric errors of linear and rotary motion in the mathematical model provides the ranges that should be controlled to the machine in order to get better volumetric accuracy by minimizing any geometric errors. For this purpose, modeling techniques using homogeneous transformation matrix manipulations based on assumptions made with rigid body kinematics and small angle approximation are applied to DNS DVF5000 which is a subject machine of this research.

Error measurement is always the most practical and accurate way to determine the errors of machine tools. Direct measurements of the errors are usually used to provide the necessary data for error identification and also the capability of verifying the error analysis process. The laser interferometers are the most widely useful devices with high accuracy and resolution for this task. Indirect measurement focuses on the combined effects of single errors, and measures and analyzes the location or trajectory of certain points. Indirect measurements have been developed for quickly checking the accuracy of machine tools, a typical example of indirect measurement broadly adopted is the circular interpolation performance test using the double ball bar or grid encoder. A tracking interferometer so-called laser tracker is a sort of laser interferometer adopting a mechanical steering mechanism that controls the laser beam's direction to track the paths of a target retroreflector, can be used for the complete measurement and calibration of linear and rotary axes of a 5-axis machine tool without additional devices. R-test can identify rotary axes' location errors by fitting obtained data to the 5-axis machine tools' motion through a kinematic model. In this research, a laser interferometer is the chosen tool to measure individual errors of linear axes, double ball bar is used for verifying the geometrical characteristics between linear axes under orthogonal configuration such as squareness errors. And laser tracer is utilized for estimating the volumetric error of linear axes and identifying all of the individual errors of rotary motion.

## Chapter 3.

### MODELING VOLUMETRIC ERROR FOR 5-AXIS MACHINE TOOLS

The 5-axis machine tools can be classified based on combinations of translatory (T) and rotary (R) axes, called a kinematic structure, and typical 5-axis machine tools are configured with 3 'T' axes, 2 'R' axes that provide rotational degrees of freedom to the workpiece or tool. Each component that constitutes the axes of the machine tool contains various error parameters according to each motion (e.g., translatory, rotary motion), and 5-axis machines with more parts and more complicated relations between axes than 3-axis machines are inevitably affected by errors occurring in each machine tool. Indeed 3-axis machine tools which own only 3 translatory axes accommodate a total of 21 geometric error parameters. Whereas, typical 5-axis machine tools embedded 3 translatory and 2 rotary axes in various configurations of sequential manners contain 37 or 39 systematic geometric errors whose tricky to deal with [13],[19]. Thus, quantifying the effects of individual errors of the 5-axis machine tools on its spatial error within its working volume has become more significant in order to enhance the machine tools' comprehensive accuracy. The first step to identifying and controlling these various errors is establishing a proper and robust model for machine tools' volumetric error. Unfortunately, since the error modeling depends on the kinematic structure and topology of machine tools' components, the generic model which is sufficient for modeling all machine tools is not presented yet [15]. Based on this background, in this chapter, a 5-axis machine tool that is a type of vertical is selected, then in order to enhance the machine tool's spatial performance so-called volumetric error through numericalization, a mathematical model that can reflect the influences of the individual axes' geometric error on the comprehensive errors within a working volume is constructed utilizing a homogenous transformation matrix based on rigid body kinematics.

#### 3.1 Kinematic Structure and Chain of 5-Axis Machine Tools

The 5-axis machine tool used in this paper contains 3 translatory (X-, Y-, and Z-) and 2 rotary (B- and C-) axes respectively, which are utilized to establish an error model and carry out the experiments as a subject machine. and is the configuration of RRTTT according to kinematic structure classification. As shown in Fig. 3-1, this machine has 2 rotary axes (B- and C-axis) that constitute a tilting-rotary table in which the workpiece is mounted, and 3 translatory axes (X-, Y-, and Z-axis) for tool carrying. The kinematic chain which is adopted to model geometric errors of a subject machine tool is depicted in Fig. 3-2 and can be represented as (w)CBFXYZ(t) according to the sequence of the component's linkage from a workpiece to a tool. For reference, the letters before 'F' means the joints allowing motions of the

workpiece whereas the characters after 'F' means the joints allowing motions of the tool. Using the fundamental concept of this kinematic chain, the location of a certain functional point on a tooltip and a workpiece,  $P^t$  and  $P^w$  respectively, can be identified with respect to a reference coordinate frame  $\{R\}$ . As well as, a structural closed-loop based on a kinematic chain allows easy conversion between two relatively difficult points to be identified (e.g., moving points, TCP, etc.) using a homogeneous transformation between fixed objects or two adjacent objects that are relatively easy to measure.

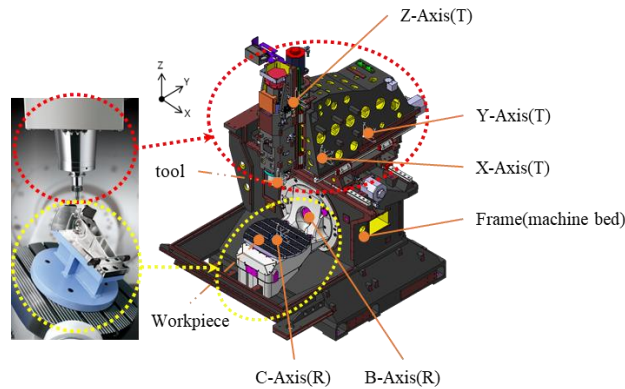


Fig. 3-1 Configuration of 5-axis machine tool(Group of main: RRTTT, sub: G3/G'2)

In the methodology of modeling for volumetric error, hence, the vector representing an error between 2 points of interest can be calculated by constructing the structural closed-loop chain in the frame system of the machine tool, which allows the computation of the errors at any interest certain point within the working volume by measuring or simulating errors caused in individual components. These each errors inherent in links and joints composing the machine tools are constituted by 4 vectors, i.e., vector of position, motion, and error of position and motion, for a joint with relation to its adjacent joint in a structural loop. The resultant error vector which resulted from the propagation of individual errors can be gained by arranging them in order and by representing vectors in form of a homogenous transformation matrix and then batching these matrices into one another.

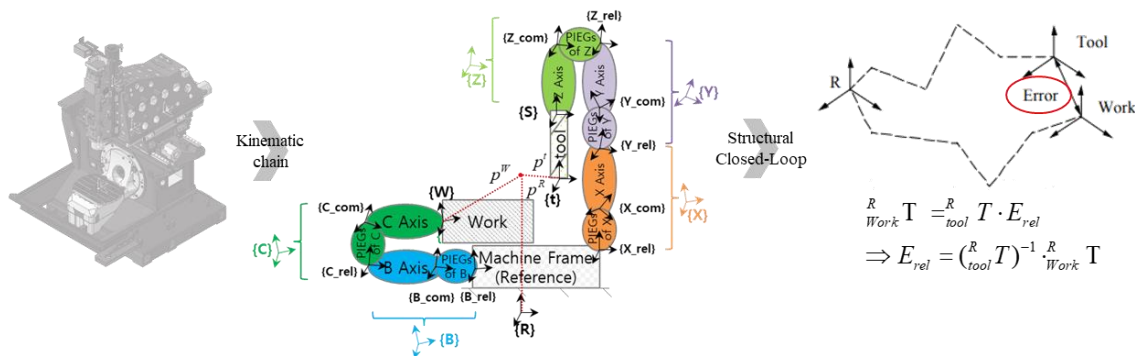


Fig. 3-2 Concept of Kinematic chain and structural loop for the 5-axis machine tool

According to a theorem of the rigid body kinematics based on structural loop, position or orientation containing any errors at points from a certain joint to its adjacent joint can be expressed by multiplying the homogenous transformation matrix between the neighboring joints. The 5-axis machine tool, which is the type of RRTTT and is depicted in Fig. 3-2, has arbitrary points in the machine tools' coordinate frame. For the sequential arrangement for error modeling, the structural kinematic chain loop for the machine tools can be split up into 2 paths considering the machine tools' fixed frame (e.g., machine bed, etc.) as a reference frame. One path of the structural kinematic chain loop is from the reference (fixed) coordinate frame to a certain point at the cutting tool coordinate frame consisting of 3 translatory joints, X-axis expressed as {X}, Y-axis expressed as {Y}, Z-axis expressed as {Z}, spindle expressed as {S} and cutting tool expressed as {t}. Another path is leading from a reference frame to a point at the workpiece consisting of rotary joints, B-axis {B}, C-axis {C}, and workpiece {W}, which will contact the tool.

First, 'T' represents the coordinate transformation, and the workpiece coordinate frame {w} in relation with respect to reference coordinate frame {R} can be described as;

$${}^R T_W = {}^R T_B \cdot {}^B T_C \cdot {}^C T_W \quad (3-1)$$

Second, the cutting tool coordinates frame {t} in relation with respect to reference coordinate frame {R} can be expressed as;

$${}^R T_t = {}^R T_X \cdot {}^X T_Y \cdot {}^Y T_Z \cdot {}^Z T_S \cdot {}^S T_t \quad (3-2)$$

And also, from the nature of the closed loop, coordinate transformations of the cutting tool coordinate frame {t} in relation with respect to the reference coordinate frame {R} can be described as;

$${}^R T_t = {}^R T_W \cdot {}^W T_t \quad (3-3)$$

Eventually, from the above equations, the general error matrix,  $E_{rel}$ , equals the coordinate vector between the coordinate frame from cutting tool {t} to workpiece {W} and can be determined by transposition from Eq. 3-3.

$$E_{rel} = {}^W T_t = ({}^R T_W)^{-1} \cdot {}^R T_t \quad (3-4)$$

In this study, in order to simplification of the machine tools' error modeling, assume that the backlash

error is excluded since it was compensated beforehand and also thermal deformation is excluded since it was preserved constantly during the experiment.

### 3.2 Homogeneous Coordinate Representation for 5-Axis Machine Tools

In common, a representation for a homogeneous coordinate is defined as a form of an N-dimensional position vector with an (N+1) component. The physical N-dimensional vector is a value obtained by dividing the homogeneous coordinates by the (N+1)<sup>th</sup> coordinates. Therefore, the position vector of the points defined in the coordinates in the 3-dimensional space is below;

$$p = [p_x \quad p_y \quad p_z]^T \quad (3-5)$$

is defined, then, in the homogenous coordinate representation by the augmented vector;

$$p = [Wp_x \quad Wp_y \quad Wp_z \quad W]^T \quad (3-6)$$

Where, the 4<sup>th</sup> coordinate component,  $W$ , is a non-zero scaling factor. The representation for a homogenous coordinate transform of points in 3-dimensional Euclidean space is helpful to construct transformation matrices including rotation, translation(or positioning), scaling, and perspective.

A homogenous transformation matrix,  $T$ , in 3-dimensional space is described as a 4×4 matrix that is for the purpose of mapping a homogenous position vector from one coordinate frame to another. The homogenous transformation matrix is composed of four submatrices  $R$ ,  $P$ ,  $W$ , and  $F$  of dimensions 3×3, 3×1, 1×1, and 1×3 respectively. It has the form following;

$$T = \begin{bmatrix} R_{3 \times 3} & P_{3 \times 1} \\ F_{1 \times 3} & W_{1 \times 1} \end{bmatrix} = \begin{bmatrix} \text{rotation matrix} & \text{position vector} \\ \text{perspective transformation} & \text{scaling factor} \end{bmatrix} \quad (3-7)$$

The rotation matrix, upper left 3×3 sub-matrix expressed  $R_{3 \times 3}$ , denotes the direction cosine of one frame with respect to the other, and the position vector, upper right 3×1 sub-matrix, denotes the position of one frame's origin to the other coordinate frame. Then, for kinematics of mechanisms, a scaling factor is taken to be 1 and the 3 elements of the perspective transformation are zeros, hence the homogenous transformation matrix is given by;

$$T = \begin{bmatrix} R & P \\ 0 & 0 & 0 & 1 \end{bmatrix} \quad (3-8)$$

The homogenous transformation can be utilized to describe the geometric relationship between the 2 coordinate frames, for example,  $P_{xyz}$  and  $P_{uvw}$  such that:

$$\begin{aligned} [p_x \ p_y \ p_z \ 1]^T &= T \cdot [p_u \ p_v \ p_w \ 1]^T \\ [p_u \ p_v \ p_w \ 1]^T &= T^{-1} \cdot [p_x \ p_y \ p_z \ 1]^T \end{aligned} \quad (3-9)$$

For axes with a sequential combination of motions, such as for machine tools composed of multi-axis, the Homogenous Transformation Matrix(so-called HTM) corresponding to each frame can be multiplied serially to acquire a single form of HTM for the resultant motion. This is helpful to identify diverse error sources that occurred at any kinematic joints. Using this homogeneous transformation approach, machine tools' system frame can be decomposed into a series of individual motion components with each coordinate transformation matrix. These matrices describe the relative posture and location(position) between each motion component and any transitory coordinate frames that may generate in the modeling procedure. The modeling can start at the cutting tool point or workpiece or reference coordinate frame and also can arrive all the way around to any point at a cutting tool or a workpiece coordinate system depending on the starting point. For example, if N rigid bodies are linked serially and the corresponding homogenous transformation matrices between related motion components (axes) are awarded properly, the location(position) and orientation(posture) of the end-point ( $N^{\text{th}}$  components) in the criteria of the reference coordinate frame is estimated as the sequential multiplying of all homogenous transformation matrix and becomes below;

$${}^{0(R)}T_N = \prod_{m=1}^N {}^{m-1}T_m = {}^0T_1 {}^1T_2 {}^2T_3 \dots {}^{N-1}T_N \quad (3-10)$$

### 3.3 Homogeneous Transformation Matrix for 5-Axis Machine Tools

#### 3.3.1 Homogeneous Transformation Matrix of Linear Motion Components

The generalized mathematical model for error can break a machine tool system down into individual motion components such as rigid linkage connected to each other by movable joints[22]. In this way, it can assign coordinate frames to each slide component and use a homogeneous transformation matrix to describe the motion of the slide in the reference frame[59]. The error matrix for a linear motion slide of machine tools consists of three rotational and three translational errors can be expressed as Eq. 3-17.





Under the assumption that second-order terms can be negligible and the approximation can be used (i.e.  $\cos \varepsilon = 1$ ,  $\sin \varepsilon = \varepsilon$ ) since angles are too small and the multiplication of two errors is assumed to equal zero since small enough to be ignored, the rotational error matrix becomes;

$${}^X T_{rot} = \begin{bmatrix} 1 & -\varepsilon_{zX} & \varepsilon_{yX} & 0 \\ \varepsilon_{zX} & 1 & -\varepsilon_{xX} & 0 \\ -\varepsilon_{yX} & \varepsilon_{xX} & 1 & 0 \\ 0 & 0 & 0 & 1 \end{bmatrix} \quad (3-13)$$

Where,  $\varepsilon_{xX}$  is the rotational error around X-axis along motion on the X-axis and is defined as the roll.

$\varepsilon_{yX}$  is the rotational error around Y-axis along motion on the X-axis and is defined as the pitch.

$\varepsilon_{zX}$  is the rotational error around Z-axis along motion on the X-axis and is defined as the yaw.

Besides, the translational error matrix,  $T_{TRANS}$ , consists of three components which are translatory deviations along the three axes orthogonal to each other, and this translational error matrix is derived in an alike way to that used to derive the rotational error matrix;

$${}^X T_{trans} = \begin{bmatrix} 1 & 0 & 0 & \delta_{xX} \\ 0 & 1 & 0 & 0 \\ 0 & 0 & 1 & 0 \\ 0 & 0 & 0 & 1 \end{bmatrix} \begin{bmatrix} 1 & 0 & 0 & 0 \\ 0 & 1 & 0 & \delta_{yX} \\ 0 & 0 & 1 & 0 \\ 0 & 0 & 0 & 1 \end{bmatrix} \begin{bmatrix} 1 & 0 & 0 & 0 \\ 0 & 1 & 0 & 0 \\ 0 & 0 & 1 & \delta_{zX} \\ 0 & 0 & 0 & 1 \end{bmatrix} \quad (3-14)$$

The resulting rotational error matrix becomes below:

$${}^X T_{trans} = \begin{bmatrix} 1 & 0 & 0 & \delta_{xX} \\ 0 & 1 & 0 & \delta_{yX} \\ 0 & 0 & 1 & \delta_{zX} \\ 0 & 0 & 0 & 1 \end{bmatrix} \quad (3-15)$$

Where,  $\delta_{xX}$  is the error of the X-direction while moving X-axis and is defined as the positioning error.

$\delta_{yX}$  is the error of the Y-direction while moving X-axis and is defined as the straightness error.

$\delta_{zX}$  is the error of the Z-direction while moving X-axis and is defined as the straightness error.

The total error matrix of components, E, representing the errors of a component for the X-directional

linear slide becomes below;

$$E = {}_X T_{rot} \cdot {}_X T_{trans} = {}_X T_{ce}$$

$$= \begin{bmatrix} 1 & -\varepsilon_{zX} & \varepsilon_{yX} & 0 \\ \varepsilon_{zX} & 1 & -\varepsilon_{xX} & 0 \\ -\varepsilon_{yX} & \varepsilon_{xX} & 1 & 0 \\ 0 & 0 & 0 & 1 \end{bmatrix} \begin{bmatrix} 1 & 0 & 0 & \delta_{xX} \\ 0 & 1 & 0 & \delta_{yX} \\ 0 & 0 & 1 & \delta_{zX} \\ 0 & 0 & 0 & 1 \end{bmatrix} \quad (3-16)$$

$${}_X T_{ce} = \begin{bmatrix} 1 & -\varepsilon_{zX} & \varepsilon_{yX} & \delta_{xX} \\ \varepsilon_{zX} & 1 & -\varepsilon_{xX} & \delta_{yX} \\ -\varepsilon_{yX} & \varepsilon_{xX} & 1 & \delta_{zX} \\ 0 & 0 & 0 & 1 \end{bmatrix} \quad (3-17)$$

For reference, each term in the error matrix above is a function of the position on the X-axis.

Therefore, the form of homogenous transformation representation can be used for machine tools' all slide components to establish the general mathematical error modeling for any error within the machine tool's workspace. With this generalized error matrix, the actual or nominal location(position) and orientation(posture) of the functional component can be identified while slide motion in the reference coordinate frame.

### 3.3.2 Homogeneous Transformation Matrix of Rotary Motion Components

Typical 5-axis machine tools which consist of 3 linear motion axes and 2 rotary motion axes can provide rotational motions as well as linear motions, 3 linear axes make 3 linear motions in 3 orthogonal coordinate directions(i.e., X-, Y-, and Z-axis) and the 2 rotary axes make possible to 2 rotational motions(i.e., two out of A-, B-, and C-axis). Considering the generalized mathematical model for rotary joint components such as depicted in Fig. 3-4 is vital in order to construct a volumetric error model for 5-axis machine tools. Ideally, the rotary components which assumed the rigid body motion have to rotate around the rotational axis without any errors. The actual rotary component, however, rotates with containing a total of 6 geometric error parameters, an axial motion error  $\delta_{zC}$ , 2 radial motion errors  $\delta_{xC}$  and  $\delta_{yC}$ , 2 tilt motion errors causing wobble motion  $\varepsilon_{xC}$  and  $\varepsilon_{yC}$ , and a positioning error  $\varepsilon_{zC}$ , around an axis of the reference coordinate frame.

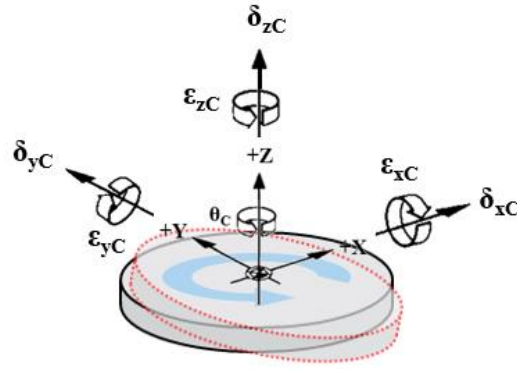


Fig. 3-4 Motion and errors in a C-axis rotation motion(rotary joint)

For the rotational component, assuming that errors related to all the angles are small enough to neglect their multiplications is unreasonable because the intended motion is rotation movement about an axis. Thus, it needs to be considered since the angle related to rotation which is the intended motion around an axis cannot be assumed to be small. For example, if the rotation axis is around at the center of the Z-direction such as the C-axis in machine tools,  $\theta_C$  is not small enough to make a small angle negligible.

The general error matrix for an individual rotary component can be also described as a product between the error matrix of the translational and the rotational. The rotational error matrix,  ${}_cT_{rot}$ , represents the error parameters coming from the angular deviations during rotation around C-axis.

$${}_cT_{rot} = \begin{bmatrix} 1 & 0 & 0 & 0 \\ 0 & \cos \varepsilon_{xC} & -\sin \varepsilon_{xC} & 0 \\ 0 & \sin \varepsilon_{xC} & \cos \varepsilon_{xC} & 0 \\ 0 & 0 & 0 & 1 \end{bmatrix} \begin{bmatrix} \cos \varepsilon_{yC} & 0 & \sin \varepsilon_{yC} & 0 \\ 0 & 1 & 0 & 0 \\ -\sin \varepsilon_{yC} & 0 & \cos \varepsilon_{yC} & 0 \\ 0 & 0 & 0 & 1 \end{bmatrix} \begin{bmatrix} \cos(\theta_C + \varepsilon_{zC}) & -\sin(\theta_C + \varepsilon_{zC}) & 0 & 0 \\ \sin(\theta_C + \varepsilon_{zC}) & \cos(\theta_C + \varepsilon_{zC}) & 0 & 0 \\ 0 & 0 & 1 & 0 \\ 0 & 0 & 0 & 1 \end{bmatrix} \quad (3-18)$$

The general result of error matrix becomes below:

$${}_C T_{rot} = \begin{bmatrix} \cos \varepsilon_{yC} \cos(\theta_C + \varepsilon_{zC}) & \sin \varepsilon_{xC} \sin \varepsilon_{yC} \cos(\theta_C + \varepsilon_{zC}) + \cos \varepsilon_{xC} \sin(\theta_C + \varepsilon_{zC}) & -\cos \varepsilon_{xC} \sin \varepsilon_{yC} \cos(\theta_C + \varepsilon_{zC}) + \sin \varepsilon_{xC} \sin(\theta_C + \varepsilon_{zC}) & 0 \\ -\cos \varepsilon_{yC} \sin(\theta_C + \varepsilon_{zC}) & \sin \varepsilon_{yC} & 0 \\ -\sin \varepsilon_{xC} \sin \varepsilon_{yC} \sin(\theta_C + \varepsilon_{zC}) + \cos \varepsilon_{xC} \cos(\theta_C + \varepsilon_{zC}) & -\sin \varepsilon_{xC} \cos \varepsilon_{yC} & 0 \\ \cos \varepsilon_{xC} \sin \varepsilon_{yC} \sin(\theta_C + \varepsilon_{zC}) + \sin \varepsilon_{xC} \cos(\theta_C + \varepsilon_{zC}) & \cos \varepsilon_{xC} \cos \varepsilon_{yC} & 0 \\ 0 & 0 & 1 \end{bmatrix} \quad (3-19)$$

After the simplification assuming that the angular errors about the axes other than the axis of rotation are negligible and the approximation can be used (i.e.  $\cos \varepsilon = 1$ ,  $\sin \varepsilon = \varepsilon$ ) since angles are too small and the multiplication of two errors is assumed to equal zero since small enough to be ignored, the transformation matrix representing the rotational error can be expressed as the following equation;

$${}_C T_{rot} = \begin{bmatrix} \cos(\theta_C + \varepsilon_{zC}) & -\sin(\theta_C + \varepsilon_{zC}) & \varepsilon_{yC} & 0 \\ \sin(\theta_C + \varepsilon_{zC}) & \cos(\theta_C + \varepsilon_{zC}) & -\varepsilon_{xC} & 0 \\ -\varepsilon_{yC} \cos(\theta_C + \varepsilon_{zC}) + \varepsilon_{xC} \sin(\theta_C + \varepsilon_{zC}) & \varepsilon_{yC} \sin(\theta_C + \varepsilon_{zC}) + \varepsilon_{xC} \cos(\theta_C + \varepsilon_{zC}) & 1 & 0 \\ 0 & 0 & 0 & 1 \end{bmatrix} \quad (3-20)$$

Where,  $\varepsilon_{xC}$  is the rotational error around X-axis along motion on the C-axis.

$\varepsilon_{yC}$  is the rotational error around Y-axis along motion on the C-axis.

$\varepsilon_{zC}$  is the rotational positioning error along motion on the C-axis.

The total error matrix, E, representing the errors of a component for the rotation becomes below;

$$E = {}_C T_{rot} \cdot {}_C T_{trans} = {}_C T_{ce}$$

$$= \begin{bmatrix} \cos(\theta_C + \varepsilon_{zC}) & -\sin(\theta_C + \varepsilon_{zC}) & \varepsilon_{yC} & 0 \\ \sin(\theta_C + \varepsilon_{zC}) & \cos(\theta_C + \varepsilon_{zC}) & -\varepsilon_{xC} & 0 \\ -\varepsilon_{yC} \cos(\theta_C + \varepsilon_{zC}) + \varepsilon_{xC} \sin(\theta_C + \varepsilon_{zC}) & \varepsilon_{yC} \sin(\theta_C + \varepsilon_{zC}) + \varepsilon_{xC} \cos(\theta_C + \varepsilon_{zC}) & 1 & 0 \\ 0 & 0 & 0 & 1 \end{bmatrix} \quad (3-21)$$

$$\begin{bmatrix} 1 & 0 & 0 & \delta_{xC} \\ 0 & 1 & 0 & \delta_{yC} \\ 0 & 0 & 1 & \delta_{zC} \\ 0 & 0 & 0 & 1 \end{bmatrix}$$

$${}^c T_{ce} = \begin{bmatrix} \cos(\theta_C + \varepsilon_{zC}) & -\sin(\theta_C + \varepsilon_{zC}) & & \\ \sin(\theta_C + \varepsilon_{zC}) & \cos(\theta_C + \varepsilon_{zC}) & & \\ \varepsilon_{xC} \sin(\theta_C + \varepsilon_{zC}) - \varepsilon_{yC} \cos(\theta_C + \varepsilon_{zC}) & \varepsilon_{yC} \sin(\theta_C + \varepsilon_{zC}) + \varepsilon_{xC} \cos(\theta_C + \varepsilon_{zC}) & & \\ 0 & 0 & & \end{bmatrix} \quad (3-22)$$

$$\begin{bmatrix} \varepsilon_{yC} & \delta_{xC} \\ -\varepsilon_{xC} & \delta_{yC} \\ 1 & \delta_{zC} \\ 0 & 1 \end{bmatrix}$$

Where,  $\delta_{xC}$ , and  $\delta_{yC}$  are the radial error of the X-, and Y-direction respectively while rotating C-axis.

$\delta_{zC}$  is the axiaa error of the Z-direction while rotating C-axis.

### 3.3.3 Homogeneous Transformation Matrix of Errors by Inaccurate Link

In general, multi-axis machine tools are composed of various linkages of components for axes with a sequential combination in order to generate simultaneous motion. The process of assembling linkages with inaccuracies due to misalignment or components' improper geometry causes errors, and these are defined as kinematic errors. Typical examples of kinematic errors of machine tools, which defined form as spatial position and orientation errors, contain orthogonality(i.e., squareness error) and parallelism error between axes, translational offset errors within the workspace of axes are also a kind of kinematic error[19]. The components' actual location and dimensions of the axis can also cause a certain point at a cutting tool or a workpiece to be shifted to where they are not intended to be, so, can be also defined as a kinematic error. But fortunately, these translational errors so-called offset errors are usually compensated easily in the Cartesian coordinates machine tools by using functions for a tool offset correction.

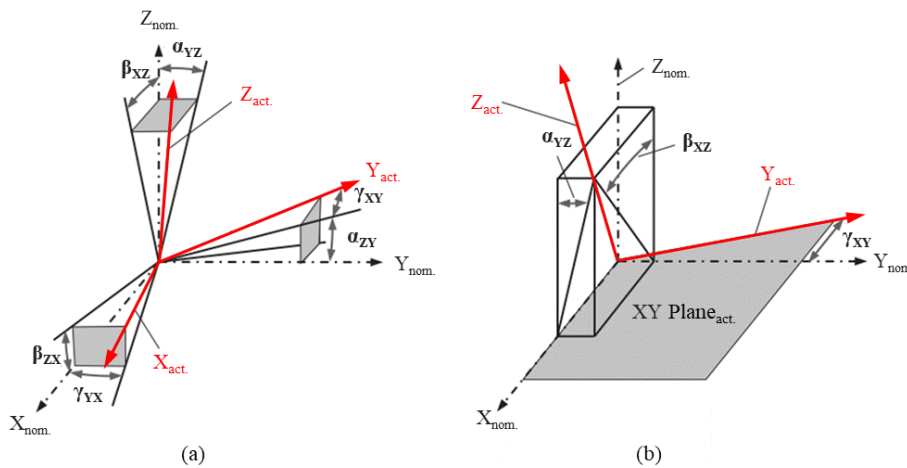


Fig. 3-5 Orientation errors between the linear axes of mutual motion

Theoretically, in the axis of machinery moving along multi-linear axes, angles  $\beta_{ZX}$  and  $\gamma_{YX}$  identify as the orientation errors of the X-axis. And also in accordance with angles  $\alpha_{ZY}/\gamma_{XY}$  and  $\alpha_{YZ}/\beta_{XZ}$  define axis orientation errors of the Y-axis and Z-axis around the respective axes of the reference coordinate frame such as depicted in Fig. 3-5 (a). Particularly, in the configuration of the serial XYZ axis of typical machine tools, X-axis is designated as the reference axis and the XY plane is designated as the reference plane. Therefore considering that the orientation angles are independent of the X-coordinate and orientation angles are respectively defined referring from the X-axis sequentially, only 3 orientation errors,  $\gamma_{XY}$ ,  $\beta_{XZ}$ , and  $\alpha_{YZ}$ , are identified as the actual orientation error of machine tools composed of 3 linear axes as depicted in Fig. 3-5 (b).

The orientation error matrix of the linear axes,  ${}_{Linear}T_{oe}$ , represents the error parameters coming from the angular deviations of mutual motion.

$${}_{Linear}T_{oe} = \begin{bmatrix} 1 & 0 & 0 & 0 \\ 0 & \cos \alpha_{YZ} & -\sin \alpha_{YZ} & 0 \\ 0 & \sin \alpha_{YZ} & \cos \alpha_{YZ} & 0 \\ 0 & 0 & 0 & 1 \end{bmatrix} \begin{bmatrix} \cos \beta_{XZ} & 0 & \sin \beta_{XZ} & 0 \\ 0 & 1 & 0 & 0 \\ -\sin \beta_{XZ} & 0 & \cos \beta_{XZ} & 0 \\ 0 & 0 & 0 & 1 \end{bmatrix} \begin{bmatrix} \cos \gamma_{XY} & -\sin \gamma_{XY} & 0 & 0 \\ \sin \gamma_{XY} & \cos \gamma_{XY} & 0 & 0 \\ 0 & 0 & 1 & 0 \\ 0 & 0 & 0 & 1 \end{bmatrix} \quad (3-23)$$

The resulting a orientation error matrix can be derived as below:

$${}_{Linear}T_{oe} = \begin{bmatrix} \cos \beta_{XZ} \cos \gamma_{XY} & \sin \alpha_{YZ} \sin \beta_{XZ} \cos \gamma_{XY} + \cos \alpha_{YZ} \sin \gamma_{XY} & -\cos \alpha_{YZ} \sin \beta_{XZ} \cos \gamma_{XY} + \sin \alpha_{YZ} \sin \gamma_{XY} & 0 \\ -\cos \beta_{XZ} \sin \gamma_{XY} & -\sin \alpha_{YZ} \sin \beta_{XZ} \sin \gamma_{XY} + \cos \alpha_{YZ} \cos \gamma_{XY} & \cos \alpha_{YZ} \sin \beta_{XZ} \sin \gamma_{XY} + \sin \alpha_{YZ} \cos \gamma_{XY} & 0 \\ \sin \beta_{XZ} & -\sin \alpha_{YZ} \cos \beta_{XZ} & \cos \alpha_{YZ} \cos \beta_{XZ} & 0 \\ 0 & 0 & 0 & 1 \end{bmatrix} \quad (3-24)$$

Under the assumption that second-order terms are negligible and small-angle approximations (i.e.,  $\cos \alpha$  or  $\beta$  or  $\gamma=1$ ,  $\sin \alpha$  or  $\beta$  or  $\gamma=\alpha$  or  $\beta$  or  $\gamma$ ) are used and the multiplication of two errors is assumed to equal zero since small enough to be ignored, the orientation error matrix becomes;

$$Linear T_{oe} = \begin{bmatrix} 1 & -\gamma_{XY} & \beta_{XZ} & 0 \\ \gamma_{XY} & 1 & -\alpha_{YZ} & 0 \\ -\beta_{XZ} & \alpha_{YZ} & 1 & 0 \\ 0 & 0 & 0 & 1 \end{bmatrix} \quad (3-25)$$

These axis orientation errors result in the relative deviation of a functional point, which is directly proportional to the distance of travel within the coordinate frame, within the workspace of machine tools. In the case that the X-axial direction is chosen as a reference axis for each orthogonal axis of the machine tools' coordinate frame, orientation errors are nonexistent related to X-axis. Whereas one squareness error(e.g.,  $\gamma_{XY}$ ) that rotates around Y-axis, and two squareness errors(e.g.,  $\beta_{XZ}$  and  $\alpha_{YZ}$ ) that rotate around Z-axis are existent since the plane through the X-axial direction and Y-axial direction is chosen as a reference plane. The homogenous transformation matrices error by inaccurate link for the Y-axis and Z-axis(i.e.,  ${}_yT_{oe}$  and  ${}_zT_{oe}$ ) representing the orientation errors of the linear axes in machine tools become below;

$${}_yT_{oe} = \begin{bmatrix} 1 & -\gamma_{XY} & 0 & 0 \\ \gamma_{XY} & 1 & -\alpha_{YZ} & 0 \\ 0 & \alpha_{YZ} & 1 & 0 \\ 0 & 0 & 0 & 1 \end{bmatrix} \quad (3-26)$$

$${}_zT_{oe} = \begin{bmatrix} 1 & 0 & \beta_{XZ} & 0 \\ 0 & 1 & -\alpha_{YZ} & 0 \\ -\beta_{XZ} & \alpha_{YZ} & 1 & 0 \\ 0 & 0 & 0 & 1 \end{bmatrix} \quad (3-27)$$

Where,  $\gamma_{XY}$  is the squareness error between X-axial motion and Y-axial motion.

$\beta_{XZ}$  is the squareness error between X-axial motion and Z-axial motion.

$\alpha_{YZ}$  is the squareness error between Y-axial motion and Z-axial motion.



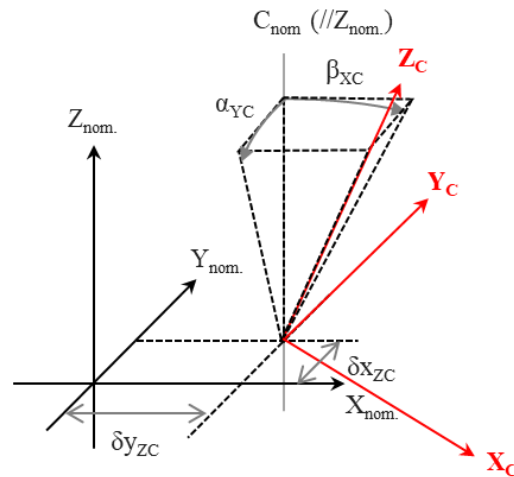


Fig. 3-5 Influence of orientation and location errors of the rotary axes

A distinction is made between 3-axis machine tools and 5-axis machine tools depending on whether have 2 extra rotary axes that enable relative rotational motion freedom between a cutting tool and a workpiece. Hence, 5-axis machine tools' rotary motion axes are typically located at the end-point of a path following a kinematic chain in the directions of the cutting tool or workpiece, taking into account errors by inaccurate links for the rotation axes is important to struct the 5-axis machine tools' kinematic chain. Each rotation axis is aligned parallel or perpendicular to the Cartesian coordinate axes and can be assigned two orientation and location errors around the two perpendicular coordinate axes. So, as shown in Fig. 3-5, the rotation axis of the C-axis is parallel to the ideal Z-axial motion direction and has 2 squareness errors (i.e.,  $\beta_{XC}$ ,  $\alpha_{YC}$ ), and 2 location errors (i.e.,  $\delta_{x_{ZC}}$ ,  $\delta_{y_{ZC}}$ ). As with the linear axes' orientation errors, the orientation errors of rotary motion axes estimated for serial axes have to take transformed into the machine coordinate frame using HTM. Applicable to rotary motion axes such as C-axis is like below:

$${}^c T_{oe} = {}^c T_{ori} \cdot {}^c T_{loc} \begin{bmatrix} 1 & 0 & \beta_{XC} & \delta_{x_{ZC}} \\ 0 & 1 & -\alpha_{YC} & \delta_{y_{ZC}} \\ -\beta_{XC} & \alpha_{YC} & 1 & 0 \\ 0 & 0 & 0 & 1 \end{bmatrix} \quad (3-28)$$

Where,  $\beta_{XC}$  is the squareness error of the C-axis of rotation with respect to X-axis motion.

$\alpha_{YC}$  is the squareness error of the C-axis of rotation with respect to Y-axis motion.

$\delta_{x_{ZC}}$  is x-direction offset of origin of C-axis with respect to the origin of the nominal coordinate.

$\delta_{y_{ZC}}$  is y-direction offset of origin of C-axis with respect to the origin of the nominal coordinate.

## Chapter 4.

# EVALUATION OF VOLUMETRIC ERROR FOR 5-AXIS MACHINE TOOLS

### 4.1 Formulation of Error Model for a Practical 5-Axis Machine Tool

Establishing and formulating the mathematical model for machine tools' volumetric error aims to obtain a robust error model containing all geometric error parameters that can occur at machine tools' components and trace the trajectory at certain functional points(e.g., cutting tool or workpiece point) into a 3-dimensional error map as it moves within the workspace. For this purpose, kinematics assuming rigid body motion and homogenous transformation matrix(HTM) has been used for formulating the 5-axis machine tool's volumetric error model in this research. A 5-axis machine tool that formulated the mathematical model for this study is DVF5000 which is a (w)CBFXYZ(t) type machine tool. The table of this machine tool has rotary motions through the B and C axes with respect to a machine bed designated as a fixed frame and the tool has translatory motion in X-, Y-, and Z-axial directions with respect to the same fixed frame. This 5-axis machine tool can be decomposed of nine components as rigid bodies and whose diagram described kinematic chain is shown in Fig. 4-1. The machine bed is chosen as the fixed reference frame, and each functional component is assumed as a component with a rigid body motion which is expressed by a capital, e.g., 'X' represents the X-axis or 'C' represents the C-axis.

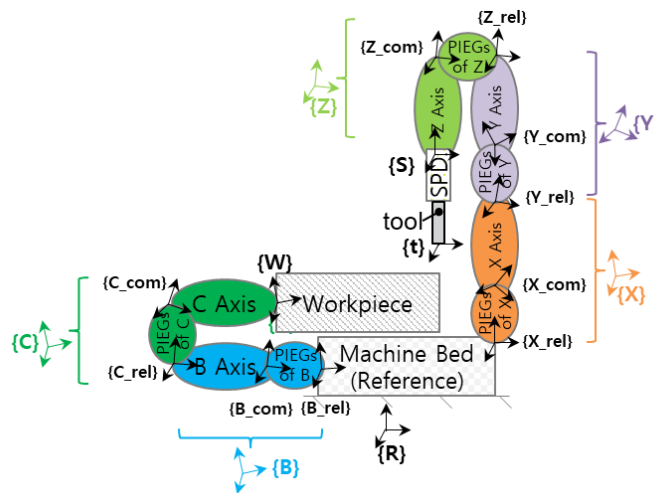


Fig. 4-1 Kinematic chain diagram for DVF5000; the subject machine tool of this study

The two structural loops are existent in this kinematic chain. one is designated as the 'workpiece side loop' which is from the machine bed, reference (fixed) frame, to the workpiece, and another is

designated as the 'tool side loop' which is from the machine bed, reference (fixed) frame, to the cutting tool in this study. And then the homogenous transformation matrix derived for each motion joint is needed to build the mathematical model. The transformation matrix between rigid body 'M' and the adjacent previous-sequence rigid body 'L' is expressed as;

$${}^L T_M = {}^L T_{pc} \cdot {}^L T_{oe} \cdot {}^L T_{ce} \quad (4-1)$$

For reference,  $T_{pc}$ ,  $T_{oe}$ , and  $T_{ce}$  are represented for the transformation matrix of position coordinate, orientation errors, and component errors of rigid body M relative to rigid body L respectively.

Based on Eq. 4-1, formulas for the transformation matrix between rigid bodies in the tool side loop can be obtained as below;

$${}^R T_X = {}^R T_{pc} \cdot {}^R T_{oe} \cdot {}^R T_{ce} = \begin{bmatrix} 1 & 0 & 0 & O_{xX} \\ 0 & 1 & 0 & O_{yX} \\ 0 & 0 & 1 & O_{zX} \\ 0 & 0 & 0 & 1 \end{bmatrix} \begin{bmatrix} 1 & 0 & 0 & 0 \\ 0 & 1 & 0 & 0 \\ 0 & 0 & 1 & 0 \\ 0 & 0 & 0 & 1 \end{bmatrix} \begin{bmatrix} 1 & -\varepsilon_{zX} & \varepsilon_{yX} & X + \delta_{xX} \\ \varepsilon_{zX} & 1 & -\varepsilon_{xX} & \delta_{yX} \\ -\varepsilon_{yX} & \varepsilon_{xX} & 1 & \delta_{zX} \\ 0 & 0 & 0 & 1 \end{bmatrix} \quad (4-2)$$

$${}^X T_Y = {}^X T_{pc} \cdot {}^X T_{oe} \cdot {}^X T_{ce} = \begin{bmatrix} 1 & 0 & 0 & O_{xY} \\ 0 & 1 & 0 & O_{yY} \\ 0 & 0 & 1 & O_{zY} \\ 0 & 0 & 0 & 1 \end{bmatrix} \begin{bmatrix} 1 & -\gamma_{XY} & 0 & 0 \\ \gamma_{XY} & 1 & -\alpha_{YZ} & 0 \\ 0 & \alpha_{YZ} & 1 & 0 \\ 0 & 0 & 0 & 1 \end{bmatrix} \begin{bmatrix} 1 & -\varepsilon_{zY} & \varepsilon_{yY} & \delta_{xY} \\ \varepsilon_{zY} & 1 & -\varepsilon_{xY} & Y + \delta_{yY} \\ -\varepsilon_{yY} & \varepsilon_{xY} & 1 & \delta_{zY} \\ 0 & 0 & 0 & 1 \end{bmatrix} \quad (4-3)$$

$${}^Y T_Z = {}^Y T_{pc} \cdot {}^Y T_{oe} \cdot {}^Y T_{ce} = \begin{bmatrix} 1 & 0 & 0 & O_{xZ} \\ 0 & 1 & 0 & O_{yZ} \\ 0 & 0 & 1 & O_{zZ} \\ 0 & 0 & 0 & 1 \end{bmatrix} \begin{bmatrix} 1 & 0 & \beta_{XZ} & 0 \\ 0 & 1 & -\alpha_{YZ} & 0 \\ -\beta_{XZ} & \alpha_{YZ} & 1 & 0 \\ 0 & 0 & 0 & 1 \end{bmatrix} \begin{bmatrix} 1 & -\varepsilon_{zZ} & \varepsilon_{yZ} & \delta_{xZ} \\ \varepsilon_{zZ} & 1 & -\varepsilon_{xZ} & \delta_{yZ} \\ -\varepsilon_{yZ} & \varepsilon_{xZ} & 1 & Z + \delta_{zZ} \\ 0 & 0 & 0 & 1 \end{bmatrix} \quad (4-4)$$

Assuming that the spindle is ideally assembled and firmly fixed to the z-axis component and that there is only position coordinate information about the z-axis, and that the tool is also fixed to the center of the spindle and only the position coordinate for the tool length, the following transformation matrix related to the spindle and the tool can be obtained below.

$${}^zT = \begin{bmatrix} 1 & 0 & 0 & O_{xS} \\ 0 & 1 & 0 & O_{yS} \\ 0 & 0 & 1 & O_{zS} \\ 0 & 0 & 0 & 1 \end{bmatrix} \quad (4-5)$$

$${}^sT = \begin{bmatrix} 1 & 0 & 0 & O_{xt} \\ 0 & 1 & 0 & O_{yt} \\ 0 & 0 & 1 & O_{zt} \\ 0 & 0 & 0 & 1 \end{bmatrix} \quad (4-6)$$

Using the transformation matrices given from Eq. 4-2 to 4-6 a homogenous transformation from a reference coordinate frame to a cutting tool coordinate can be described by the following matrix;

$${}^R T = {}^R T_X \cdot {}^X T_Y \cdot {}^Y T_Z \cdot {}^Z T_S \cdot {}^S T_t$$

$$= \begin{bmatrix} 1 & -\varepsilon_{zX} & \varepsilon_{yX} & O_{xX} + X + \delta_{xX} \\ \varepsilon_{zX} & 1 & -\varepsilon_{xX} & O_{yX} + \delta_{yX} \\ -\varepsilon_{yX} & \varepsilon_{xX} & 1 & O_{zX} + \delta_{zX} \\ 0 & 0 & 0 & 1 \end{bmatrix} \begin{bmatrix} 1 & -\gamma_{XY} - \varepsilon_{zY} & \varepsilon_{yY} \\ \varepsilon_{zY} + \gamma_{XY} & 1 & -\varepsilon_{xY} \\ -\varepsilon_{yY} & \varepsilon_{xY} & 1 \\ 0 & 0 & 0 \end{bmatrix}$$

$$= \begin{bmatrix} O_{xY} + \delta_{xY} - Y\gamma_{XY} \\ O_{yY} + Y + \delta_{yY} \\ O_{zY} + \delta_{zY} \\ 1 \end{bmatrix} \begin{bmatrix} 1 & -\varepsilon_{zZ} & \beta_{XZ} + \varepsilon_{yZ} & O_{xZ} + \delta_{xZ} + Z\beta_{XZ} \\ \varepsilon_{zZ} & 1 & -\alpha_{YZ} - \varepsilon_{xZ} & O_{yZ} + \delta_{yZ} - Z\alpha_{YZ} \\ -\varepsilon_{yZ} - \beta_{XZ} & \alpha_{YZ} + \varepsilon_{xZ} & 1 & O_{zZ} + Z + \delta_{zZ} \\ 0 & 0 & 0 & 1 \end{bmatrix} \quad (4-7)$$

$$= \begin{bmatrix} 1 & 0 & 0 & O_{xS} \\ 0 & 1 & 0 & O_{yS} \\ 0 & 0 & 1 & O_{zS} \\ 0 & 0 & 0 & 1 \end{bmatrix} \begin{bmatrix} 1 & 0 & 0 & O_{xt} \\ 0 & 1 & 0 & O_{yt} \\ 0 & 0 & 1 & O_{zt} \\ 0 & 0 & 0 & 1 \end{bmatrix}$$

Also, formulas for the homogeneous transformation matrix under rigid body motion assumption in the workpiece side loop can be obtained as below:

$${}^R T = {}^R T_{pc} \cdot {}^R T_{oe} \cdot {}^R T_{ce}$$

$$= \begin{bmatrix} 1 & 0 & 0 & O_{xB} \\ 0 & 1 & 0 & O_{yB} \\ 0 & 0 & 1 & O_{zB} \\ 0 & 0 & 0 & 1 \end{bmatrix} \begin{bmatrix} 1 & -\gamma_{XB} & 0 & \delta x_{yB} \\ \gamma_{XB} & 1 & -\alpha_{zB} & 0 \\ 0 & \alpha_{zB} & 1 & \delta z_{yB} \\ 0 & 0 & 0 & 1 \end{bmatrix} \quad (4-8)$$

$$= \begin{bmatrix} \cos(\theta_B + \varepsilon_{yB}) & -\varepsilon_{zB} \cos(\theta_B + \varepsilon_{yB}) & \sin(\theta_B + \varepsilon_{yB}) & 0 \\ \varepsilon_{xB} \sin(\theta_B + \varepsilon_{yB}) + \varepsilon_{zB} & 1 & -\varepsilon_{xB} \cos(\theta_B + \varepsilon_{yB}) & 0 \\ -\sin(\theta_B + \varepsilon_{yB}) & \varepsilon_{zB} \sin(\theta_B + \varepsilon_{yB}) + \varepsilon_{xB} & \cos(\theta_B + \varepsilon_{yB}) & 0 \\ 0 & 0 & 0 & 1 \end{bmatrix}$$

$$\begin{aligned}
 {}^B_C T &= {}^B_C T_{pc} \cdot {}^B_C T_{oe} \cdot {}^B_C T_{ce} \\
 &= \begin{bmatrix} 1 & 0 & 0 & O_{xC} \\ 0 & 1 & 0 & O_{yC} \\ 0 & 0 & 1 & O_{zC} \\ 0 & 0 & 0 & 1 \end{bmatrix} \begin{bmatrix} 1 & 0 & \beta_{XC} & \delta x_{ZC} \\ 0 & 1 & -\alpha_{YC} & \delta y_{ZC} \\ -\beta_{XC} & \alpha_{YC} & 1 & 0 \\ 0 & 0 & 0 & 1 \end{bmatrix} \\
 &\begin{bmatrix} \cos(\theta_C + \varepsilon_{zC}) & & & -\sin(\theta_C + \varepsilon_{zC}) \\ \sin(\theta_C + \varepsilon_{zC}) & & & \cos(\theta_C + \varepsilon_{zC}) \\ \varepsilon_{xC} \sin(\theta_C + \varepsilon_{zC}) - \varepsilon_{yC} \cos(\theta_C + \varepsilon_{zC}) & \varepsilon_{yC} \sin(\theta_C + \varepsilon_{zC}) + \varepsilon_{xC} \cos(\theta_C + \varepsilon_{zC}) & & \\ 0 & & & 0 \end{bmatrix} \quad (4-9) \\
 &\begin{bmatrix} \varepsilon_{yC} & 0 \\ -\varepsilon_{xC} & 0 \\ 1 & 0 \\ 0 & 1 \end{bmatrix} \\
 {}^C_W T &= \begin{bmatrix} 1 & 0 & 0 & O_{xW} \\ 0 & 1 & 0 & O_{yW} \\ 0 & 0 & 1 & O_{zW} \\ 0 & 0 & 0 & 1 \end{bmatrix} \quad (4-10)
 \end{aligned}$$

Similarly, a homogenous transformation matrix from a reference frame to a workpiece can be described by:

$$\begin{aligned}
 {}^R_W T &= {}^R_B T \cdot {}^B_C T \cdot {}^C_W T \\
 &= \begin{bmatrix} 1 & -\gamma_{XB} & 0 & O_{xB} + \delta x_{YB} \\ \gamma_{XB} & 1 & -\alpha_{ZB} & O_{yB} \\ 0 & \alpha_{ZB} & 1 & O_{zB} + \delta z_{YB} \\ 0 & 0 & 0 & 1 \end{bmatrix} \begin{bmatrix} \cos(\theta_B + \varepsilon_{yB}) & & & -\varepsilon_{zB} \cos(\theta_B + \varepsilon_{yB}) \\ \varepsilon_{xB} \sin(\theta_B + \varepsilon_{yB}) + \varepsilon_{zB} & & & 1 \\ -\sin(\theta_B + \varepsilon_{yB}) & & & \varepsilon_{zB} \sin(\theta_B + \varepsilon_{yB}) + \varepsilon_{xB} \\ 0 & & & 0 \end{bmatrix} \\
 &\begin{bmatrix} \sin(\theta_B + \varepsilon_{yB}) & 0 \\ -\varepsilon_{xB} \cos(\theta_B + \varepsilon_{yB}) & 0 \\ \cos(\theta_B + \varepsilon_{yB}) & 0 \\ 0 & 1 \end{bmatrix} \begin{bmatrix} 1 & 0 & \beta_{XC} & O_{xC} + \delta x_{ZC} \\ 0 & 1 & -\alpha_{YC} & O_{yC} + \delta y_{ZC} \\ -\beta_{XC} & \alpha_{YC} & 1 & O_{zC} \\ 0 & 0 & 0 & 1 \end{bmatrix} \quad (4-11) \\
 &\begin{bmatrix} \cos(\theta_C + \varepsilon_{zC}) & & & -\sin(\theta_C + \varepsilon_{zC}) \\ \sin(\theta_C + \varepsilon_{zC}) & & & \cos(\theta_C + \varepsilon_{zC}) \\ \varepsilon_{xC} \sin(\theta_C + \varepsilon_{zC}) - \varepsilon_{yC} \cos(\theta_C + \varepsilon_{zC}) & \varepsilon_{yC} \sin(\theta_C + \varepsilon_{zC}) + \varepsilon_{xC} \cos(\theta_C + \varepsilon_{zC}) & & \\ 0 & & & 0 \end{bmatrix} \\
 &\begin{bmatrix} \varepsilon_{yC} & 0 \\ -\varepsilon_{xC} & 0 \\ 1 & 0 \\ 0 & 1 \end{bmatrix} \begin{bmatrix} 1 & 0 & 0 & O_{xW} \\ 0 & 1 & 0 & O_{yW} \\ 0 & 0 & 1 & O_{zW} \\ 0 & 0 & 0 & 1 \end{bmatrix}
 \end{aligned}$$

For reference  $O_{x\#}$ ,  $O_{y\#}$ , and  $O_{z\#}$  are the values of topological position between each coordinate frame of adjacent bodies, where  $\#$  is a character for representing coordinate frames. The cutting tool and

workpiece are firmly mounted on the Z-axis and C-axis, respectively, which is assumed as none-error as described earlier. And  $O_{xw}$ ,  $O_{yw}$ , and  $O_{zw}$  are the relative location for each orthogonal direction between the coordinate frames' center of the workpiece and the C-axis.  $O_{xt}$ ,  $O_{yt}$ , and  $O_{zt}$  are the relative location for each orthogonal direction between the coordinate frames' center of the cutting tool and spindle(head). In this connection, distributions of the coordinate frame in each rigid body composing a 5-axis machine tool are established, which is depicted in Fig. 4-2.

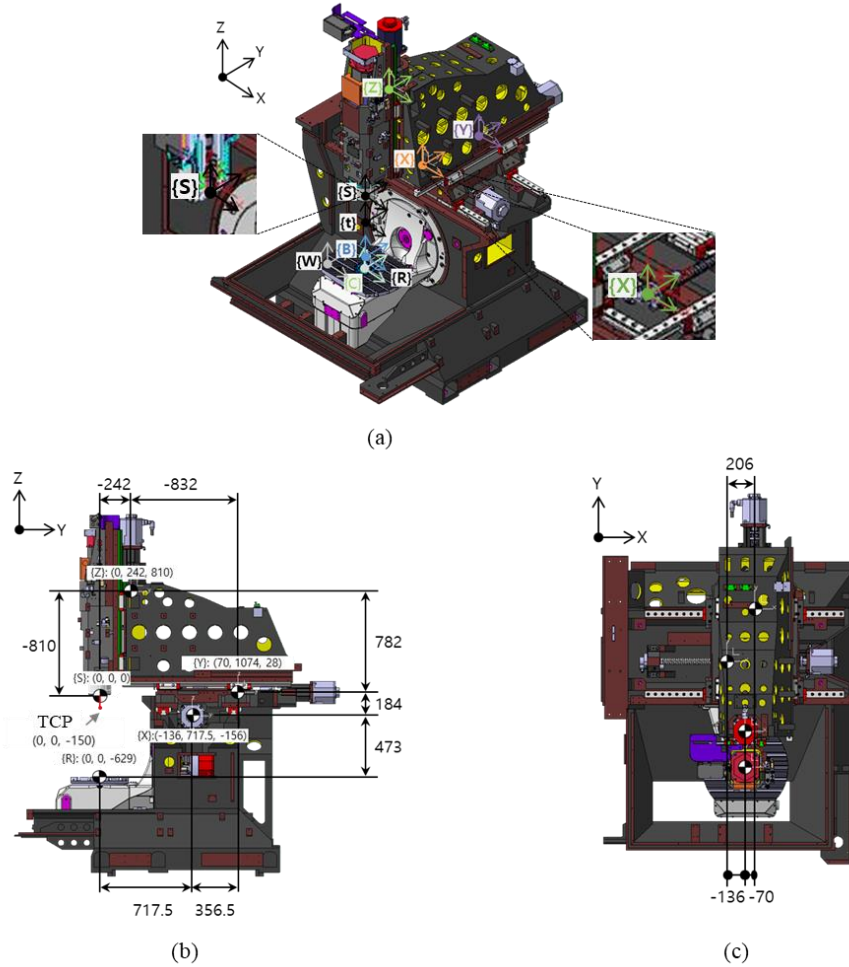


Fig. 4-2 Distribution of coordinate frames in each rigid body; (a) Isometric view, (b) Right side view, and (c) Plane view

$P_t$  and  $P_w$  are the position vectors of a certain point within the machine coordinate frame of the cutting tool and workpiece, which are expressed below;

$$P_t = [X_t \quad Y_t \quad Z_t]^T \tag{4-12}$$

$$P_w = [X_w \quad Y_w \quad Z_w]^T \quad (4-13)$$

Therefore, the volumetric error vector,  $E_v$ , between the tool and workpiece at certain functional points(TCP, tool contact point on TWP, etc.) of 5-axis machine tools is described as Eq. 4-14, and which can be calculated by utilizing Eq. 4-15 to Eq. 4-17 according to a domain of attention to analyzing.

$$E_v = [E_{vx} \quad E_{vy} \quad E_{vz}] \quad (4-14)$$

$$\begin{aligned} [E_v \quad 1]_{tool}^T &= [E_{vx} \quad E_{vy} \quad E_{vz} \quad 1]_{tool}^T \\ &= {}^R_t T_{actual} \cdot [P_t \quad 1]^T - {}^R_t T_{nominal} \cdot [P_t \quad 1]^T \end{aligned} \quad (4-15)$$

$$\begin{aligned} [E_v \quad 1]_{workpiece}^T &= [E_{vx} \quad E_{vy} \quad E_{vz} \quad 1]_{workpiece}^T \\ &= {}^R_w T_{actual} \cdot [P_w \quad 1]^T - {}^R_w T_{nominal} \cdot [P_w \quad 1]^T \end{aligned} \quad (4-16)$$

$$\begin{aligned} [E_v \quad 1]^T &= [E_{vx} \quad E_{vy} \quad E_{vz} \quad 1]^T \\ &= {}^R_t T \cdot [P_t \quad 1]^T - {}^R_w T \cdot [P_w \quad 1]^T \end{aligned} \quad (4-17)$$

#### 4.2 Determination of Key Error for a Practical 5-Axis Machine Tool

One of the most considerable preliminary measures to enhance the machine tools' spatial performance like volumetric accuracy is the identification, and control of the key geometric error parameters contributing dominantly to a volumetric accuracy in advance. In particular, 5-axis machine tools have multiple coupling relationships between geometric errors as the kinematic structure is more complex, the determination of key geometric error parameters influencing dominantly comprehensive accuracy in spatial becomes an intractable challenge. Hence, a well-defined volumetric error model for 5-axis machine tools is essential to make it possible to identify the effect of propagation from each error parameter and quantify the coupling relationships between machine tools' components, which will be helpful in the strategy for allocation of the 5-axis machine tools' accuracy during conceptual design. And the error gain matrix, which is composed of error gain that are the polynomial coefficients of each systematic geometric error, serves to call attention to errors that may dominantly affect cutting tool

points regarding each geometric error that can occur at motion components.

Thus, this section studies key contributing error analysis using the volumetric error model established beforehand for the purpose of machine tools design and production. Specifically, a systematic analysis method for assembly errors of a 5-axis machine tool and the countermeasure strategies such as estimating the manufacturing allowance reflecting each error characteristic is presented.

Axial direction	Parameter	Dimension(mm)
X	$O_{xw}, O_{xc}, O_{xb}, O_{xx}, O_{xy}, O_{xz}, O_{xs}, O_{xt}$	0, 0, 0, -136, 206, -70, 0, 0, 0
Y	$O_{yw}, O_{yc}, O_{yb}, O_{yx}, O_{yy}, O_{yz}, O_{ys}, O_{yt}$	0, 0, 0, 717.5, 356.5, -832, -242, 0
Z	$O_{zw}, O_{zc}, O_{zb}, O_{zx}, O_{zy}, O_{zz}, O_{zs}, O_{zt}$	0, 0, 0, 50, 423, 184, 782, -810, -150

Table 4-1 Relative coordinate values between the origin of each coordinate frame

Axis	PIGEs	Number of errors	PDGEs	Number of errors
X	$\delta_{xx}, \delta_{yx}, \delta_{zx}$ $\varepsilon_{xx}, \varepsilon_{yx}, \varepsilon_{zx}$	6	-	-
Y	$\delta_{xy}, \delta_{yy}, \delta_{zy}$ $\varepsilon_{xy}, \varepsilon_{yy}, \varepsilon_{zy}$	6	$\gamma_{xy}$	1
Z	$\delta_{xz}, \delta_{yz}, \delta_{zz}$ $\varepsilon_{xz}, \varepsilon_{yz}, \varepsilon_{zz}$	6	$\alpha_{yz}, \beta_{xz}$	2
B	$\delta_{xB}, \delta_{yB}, \delta_{zB}$ $\varepsilon_{xB}, \varepsilon_{yB}, \varepsilon_{zB}$	6	$\alpha_{zB}, \gamma_{xB}$	2
C	$\delta_{xC}, \delta_{yC}, \delta_{zC}$ $\varepsilon_{xC}, \varepsilon_{yC}, \varepsilon_{zC}$	6	$\alpha_{yC}, \beta_{xC}$	2

Table 4-2 List of considered error parameters for 5-axis machine tool

In this study, a key factor determination and analysis for volumetric error in a functional point of a 5-axis machine tool(e.g., TCP) is carried out for the error allocation design for the assembly process of machine tools as shown in Fig. 4-1. For this purpose, first, the coordinate frame' origin of each component under the assumption of a rigid body behavior is set up on the center of motion and the characters represent each body distributed, which is shown in Fig. 4-2. Then, dimensions considering the topology distance of the structure for this 5-axis machine tool, and the relative coordinate distance between the adjacent coordinate frames' origin are distinguished as shown in Table 4-1. Lastly, a total of 37 error parameters, as listed in the Table 4-2, are considered for individual error identification in whether having potentially crucial deviations associated with the propagation of spatial errors as translational deviation.



In a structural loop of three sequential translatory axes for tool carrying, the errors in each motion component(i.e., carriage) are identical to those of the translatory joint shown in Fig 3-3, and orientation errors between the linear axes' mutual motion occurred by inaccuracies of the linkage are the same as those shown in Fig 3-5. And by keeping axes parallelism of all the coordinate frames, the HTM given by Eq. 4-7 can be used for each of the motion axes. Then proceeding with the logic used to obtain Eq. 4-15, for a tool point(i.e.,  $t_x, t_y, t_z$ ) located at an arbitrary spot, the cutting tool point's actual coordinates with respect to the reference coordinate frame are given by;

$$\begin{aligned}
 \begin{bmatrix} P_t \\ 1 \end{bmatrix}_{\text{actual}} &= {}^R T \begin{bmatrix} t_x \\ t_y \\ t_z \\ 1 \end{bmatrix} \\
 &= \begin{bmatrix} 1 & -\varepsilon_{zX} & \varepsilon_{yX} & O_{xX} + X + \delta_{xX} \\ \varepsilon_{zX} & 1 & -\varepsilon_{xX} & O_{yX} + \delta_{yX} \\ -\varepsilon_{yX} & \varepsilon_{xX} & 1 & O_{zX} + \delta_{zX} \\ 0 & 0 & 0 & 1 \end{bmatrix} \begin{bmatrix} 1 & -\gamma_{XY} - \varepsilon_{zY} & \varepsilon_{yY} \\ \varepsilon_{zY} + \gamma_{XY} & 1 & -\varepsilon_{xY} \\ -\varepsilon_{yY} & \varepsilon_{xY} & 1 \\ 0 & 0 & 0 & 1 \end{bmatrix} \\
 &= \begin{bmatrix} O_{xY} + \delta_{xY} - Y\gamma_{XY} \\ O_{yY} + Y + \delta_{yY} \\ O_{zY} + \delta_{zY} \\ 1 \end{bmatrix} \begin{bmatrix} 1 & -\varepsilon_{zZ} & \beta_{XZ} + \varepsilon_{yZ} & O_{xZ} + \delta_{xZ} + Z\beta_{XZ} \\ \varepsilon_{zZ} & 1 & -\alpha_{YZ} - \varepsilon_{xZ} & O_{yZ} + \delta_{yZ} - Z\alpha_{YZ} \\ -\varepsilon_{yZ} - \beta_{XZ} & \alpha_{YZ} + \varepsilon_{xZ} & 1 & O_{zZ} + Z + \delta_{zZ} \\ 0 & 0 & 0 & 1 \end{bmatrix} \\
 &= \begin{bmatrix} 1 & 0 & 0 & O_{xS} \\ 0 & 1 & 0 & O_{yS} \\ 0 & 0 & 1 & O_{zS} \\ 0 & 0 & 0 & 1 \end{bmatrix} \begin{bmatrix} 1 & 0 & 0 & O_{xT} \\ 0 & 1 & 0 & O_{yT} \\ 0 & 0 & 1 & O_{zT} \\ 0 & 0 & 0 & 1 \end{bmatrix} \begin{bmatrix} t_x \\ t_y \\ t_z \\ 1 \end{bmatrix}
 \end{aligned} \tag{4-18}$$

The nominal coordinates of the tool point, which do not contain any error parameter, would be the sum of relative coordinate values between the origins of every individual motion component along their respective axes;

$$\begin{bmatrix} P_t \\ 1 \end{bmatrix}_{\text{nominal}} = \begin{bmatrix} O_{xS} + O_{xX} + O_{xY} + O_{xZ} + O_{xT} + X + t_x \\ O_{yS} + O_{yX} + O_{yY} + O_{yZ} + O_{yT} + Y + t_y \\ O_{yT} + O_{zS} + O_{zX} + O_{zY} + O_{zZ} + Z + t_z \\ 1 \end{bmatrix} \tag{4-19}$$

Therefore, The volumetric errors as the translational deviation in the tool point position are thus given by:

$$\begin{bmatrix} E_{vx} \\ E_{vy} \\ E_{vz} \\ 1 \end{bmatrix} = \begin{bmatrix} P_t \\ 1 \end{bmatrix}_{\text{actual}} - \begin{bmatrix} P_t \\ 1 \end{bmatrix}_{\text{nominal}} \quad (4-20)$$

Deriving Eq. 4-20 with neglecting second-order terms gives  $E_x$ ,  $E_y$ , and  $E_z$  following.

$$\begin{aligned} E_{vx} = & \delta_{xX} + \delta_{xY} + \delta_{xZ} + Z\beta_{XZ} - Y\gamma_{XY} - (\varepsilon_{zY} + \gamma_Y)(O_{yS} + O_{yZ} + O_{yI} + \delta_{yZ} + t_y - Z\alpha_{YZ} \\ & + \varepsilon_{zZ}(O_{xS} + O_{xI} + t_x) - (\alpha_{YZ} + \varepsilon_{xZ})(O_{yI} + O_{zS} + t_z)) + \varepsilon_{yY}(O_{yI} + O_{zS} + O_{zZ} + Z + \delta_{zZ} + t_z \\ & + (\alpha_{YZ} + \varepsilon_{xZ})(O_{yS} + O_{yI} + t_y) - (\beta_{XZ} + \varepsilon_{yZ})(O_{xS} + O_{xI} + t_x)) - \varepsilon_{zZ}(O_{yS} + O_{yI} + t_y) - \varepsilon_{zX} \\ & (O_{yS} + O_{yY} + O_{yZ} + O_{yI} + Y + \delta_{yY} + \delta_{yZ} + t_y - Z\alpha_{YZ} - \varepsilon_{xY}(O_{yI} + O_{zS} + O_{zZ} + Z + \delta_{zZ} + t_z \\ & + (\alpha_{YZ} + \varepsilon_{xZ})(O_{yS} + O_{yI} + t_y) - (\beta_{XZ} + \varepsilon_{yZ})(O_{xS} + O_{xI} + t_x)) + \varepsilon_{zZ}(O_{xS} + O_{xI} + t_x) - (\alpha_{YZ} \\ & + \varepsilon_{xZ})(O_{yI} + O_{zS} + t_z) + (\varepsilon_{zY} + \gamma_{XY})(O_{xS} + O_{xZ} + O_{xI} + \delta_{xZ} + t_x + Z\beta_{XZ} - \varepsilon_{zZ}(O_{yS} + O_{yI} \\ & + t_y) + (\beta_{XZ} + \varepsilon_{yZ})(O_{yI} + O_{zS} + t_z))) + \varepsilon_{yX}(O_{yI} + O_{zS} + O_{zY} + O_{zZ} + Z + \delta_{zY} + \delta_{zZ} + t_z - \varepsilon_{yY} \\ & (O_{xS} + O_{xZ} + O_{xI} + \delta_{xZ} + t_x + Z\beta_{XZ} - \varepsilon_{zZ}(O_{yS} + O_{yI} + t_y) + (\beta_{XZ} + \varepsilon_{yZ})(O_{yI} + O_{zS} + t_z)) \\ & + \varepsilon_{xY}(O_{yS} + O_{yZ} + O_{yI} + t_y + \varepsilon_{zZ}(O_{xS} + O_{xI} + t_x) - (\alpha_{YZ} + \varepsilon_{xZ})(O_{yI} + O_{zS} + t_z)) + (\alpha_Z + \varepsilon_{xZ}) \\ & (O_{yS} + O_{yI} + t_y) - (\beta_{XZ} + \varepsilon_{yZ})(O_{xS} + O_{xI} + t_x) + (\beta_{XZ} + \varepsilon_{yZ})(O_{yI} + O_{zS} + t_z) \end{aligned} \quad (4-21)$$

$$\begin{aligned} E_{vy} = & \delta_{yX} + \delta_{yY} + \delta_{yZ} - Z\alpha_{YZ} - \varepsilon_{xY}(O_{yI} + O_{zS} + O_{zZ} + Z + \delta_{zZ} + t_z + (\alpha_{YZ} + \varepsilon_{xZ})(O_{yS} \\ & + O_{yI} + t_y) - (\beta_{XZ} + \varepsilon_{yZ})(O_{xS} + O_{xI} + t_x)) + \varepsilon_{zZ}(O_{xS} + O_{xI} + t_x) - \varepsilon_{xX}(O_{yI} + O_{zS} + O_{zY} \\ & + O_{zZ} + Z + \delta_{zY} + \delta_{zZ} + t_z + \varepsilon_{xY}(O_{yS} + O_{yZ} + O_{yI} + \delta_{yZ} + t_y + \varepsilon_{zZ}(O_{xS} + O_{xI} + t_x) - (\alpha_{YZ} \\ & + \varepsilon_{xZ})(O_{yI} + O_{zS} + t_z)) - \varepsilon_{yY}(O_{xS} + O_{xZ} + O_{xI} + \delta_{xZ} + t_x + Z\beta_{XZ} - \varepsilon_{zZ}(O_{yS} + O_{yI} + t_y) \\ & + (\beta_{XZ} + \varepsilon_{yZ})(O_{yI} + O_{zS} + t_z)) + (\alpha_{YZ} + \varepsilon_{xZ})(O_{yS} + O_{yI} + t_y) - (\beta_{XZ} + \varepsilon_{yZ})(O_{xS} + O_{xI} \\ & + t_x) + \varepsilon_{zX}(O_{xS} + O_{xY} + O_{xZ} + O_{xI} + \delta_{xY} + \delta_{xZ} + t_x + Z\beta_{XZ} - Y\gamma_{XY} + \varepsilon_{yY}(O_{yI} + O_{zS} + O_{zZ} \\ & + Z + \delta_{zZ} + t_z + (\alpha_{YZ} + \varepsilon_{xZ})(O_{yS} + O_{yI} + t_y) - (\beta_{XZ} + \varepsilon_{yZ})(O_{xS} + O_{xI} + t_x)) - \varepsilon_{zZ}(O_{yS} \\ & + O_{yI} + t_y) + (\beta_{XZ} + \varepsilon_{yZ})(O_{yI} + O_{zS} + t_z) - (\varepsilon_{zY} + \gamma_{XY})(O_{yS} + O_{yZ} + O_{yI} + \delta_{yZ} + t_y - Z\alpha_{YZ} \\ & + \varepsilon_{zZ}(O_{xS} + O_{xI} + t_x) - (\alpha_{YZ} + \varepsilon_{xZ})(O_{yI} + O_{zS} + t_z)) - (\alpha_{YZ} + \varepsilon_{xZ})(O_{yI} + O_{zS} + t_z) + (\varepsilon_{zY} \\ & + \gamma_{XY})(O_{xS} + O_{xZ} + O_{xI} + \delta_{xZ} + t_x + Z\beta_{XZ} - \varepsilon_{zZ}(O_{yS} + O_{yI} + t_y) + (\beta_{XZ} + \varepsilon_{yZ})(O_{yI} + O_{zS} \\ & + t_z)) \end{aligned} \quad (4-22)$$

$$\begin{aligned}
 E_{vz} = & \delta_{zX} + \delta_{zY} + \delta_{zZ} + \varepsilon_{xY}(O_{yS} + O_{yZ} + O_{yT} + t_y + \varepsilon_{zZ}(O_{xS} + O_{xT} + t_x) - (\alpha_{YZ} + \varepsilon_{xZ})(O_{yT} \\
 & + O_{zS} + t_z)) - \varepsilon_{yY}(O_{xS} + O_{xZ} + O_{xT} + \delta_{xZ} + t_x + Z\beta_{XZ} - \varepsilon_{zZ}(O_{yS} + O_{yT} + t_y) + (\beta_{XZ} + \varepsilon_{yZ}) \\
 & (O_{yT} + O_{zS} + t_z)) - \varepsilon_{yX}(O_{xS} + O_{xY} + O_{xZ} + O_{xT} + \delta_{xY} + \delta_{xZ} + t_x + Z\beta_{XZ} - Y\gamma_{XY} + \varepsilon_{yY}(O_{yT} \\
 & + O_{zS} + O_{zZ} + Z + \delta_{zZ} + t_z + (\alpha_{YZ} + \varepsilon_{xZ})(O_{yS} + O_{yT} + t_y) - (\beta_{XZ} + \varepsilon_{yZ})(O_{xS} + O_{xT} + t_x)) \\
 & - \varepsilon_{zZ}(O_{yS} + O_{yT} + t_y) + (\beta_{XZ} + \varepsilon_{yZ})(O_{yT} + O_{zS} + t_z) - (\varepsilon_{zY} + \gamma_{XY})(O_{yS} + O_{yZ} + O_{yT} + \delta_{yZ} \\
 & + t_y - Z\alpha_{YZ} + \varepsilon_{zZ}(O_{xS} + O_{xT} + t_x) - (\alpha_{YZ} + \varepsilon_{xZ})(O_{yT} + O_{zS} + t_z))) + \varepsilon_{xX}(O_{yS} + O_{yY} + O_{yZ} \\
 & + O_{yT} + Y + \delta_{yY} + \delta_{yZ} + t_y - Z\alpha_{YZ} - \varepsilon_{xY}(O_{yT} + O_{zS} + O_{zZ} + Z + \delta_{zZ} + t_z + (\alpha_{YZ} + \varepsilon_{xZ}) \\
 & (O_{yS} + O_{yT} + t_y) - (\beta_{XZ} + \varepsilon_{yZ})(O_{xS} + O_{xT} + t_x)) + \varepsilon_{zZ}(O_{xS} + O_{xT} + t_x) - (\alpha_{YZ} + \varepsilon_{xZ}) \\
 & (O_{yT} + O_{zS} + t_z) + (\varepsilon_{zY} + \gamma_{XY})(O_{xS} + O_{xZ} + O_{xT} + \delta_{xZ} + t_x + Z\beta_{XZ} - \varepsilon_{zZ}(O_{yS} + O_{yT} + t_y) \\
 & + (\beta_{XZ} + \varepsilon_{yZ})(O_{yT} + O_{zS} + t_z))) + (\alpha_{YZ} + \varepsilon_{xZ})(O_{yS} + O_{yT} + t_y) - (\beta_{XZ} + \varepsilon_{yZ})(O_{xS} + O_{xT} + t_x)
 \end{aligned} \tag{4-23}$$

Since  $E_{vx}$ ,  $E_{vy}$ , and  $E_{vz}$  mean the volumetric translational error on an arbitrary point, like a tool point, in the cartesian coordinate axis respectively, and  $E_v$ , the resultant volumetric error, is defined as follows.

$$|E_v| = \sqrt{(E_{vx})^2 + (E_{vy})^2 + (E_{vz})^2} \tag{4-24}$$

And applying the coordinate dimension values that are designedly determined as a constant gives a matrix constructed with error gains for the coefficients of each variable as shown in Table 4-3 below.

Axis	$E_v$	$E_{vx}$	$E_{vy}$	$E_{vz}$
<b>X Axis errors</b>				
$\varepsilon_{xX}$	1.05	0	0.47	0.94
$\varepsilon_{yX}$	0.49	0.47	0	0.14
$\varepsilon_{zX}$	0.95	0.94	0.14	0
<b>Y Axis errors</b>				
$\varepsilon_{xY}$	1.26	0	0.66	1.07
$\varepsilon_{yY}$	0.66	0.66	0	0.07
$\varepsilon_{zY}$	1.08	1.07	0.07	0
<b>Z Axis errors</b>				
$\varepsilon_{xZ}$	0.99	0	0.96	0.24
$\varepsilon_{yZ}$	0.96	0.96	0	0
$\varepsilon_{zZ}$	0.24	0.24	0	0
<b>Perpendicularity</b>				
$\gamma_{XY}$	1.3	1.3	0.07	0
$\alpha_{YZ}$	1.46	0	1.44	0.24
$\beta_{XZ}$	1.44	1.44	0	0

Table 4-3 Error gain matrix for translatory axes of a 5-axis machine tool, DVF5000

For reference, each type of translational error, such as kinds of  $\delta x\#$ ,  $\delta y\#$ , and  $\delta z\#$ , does not represent

any amplification by distance, so, the coefficients of these errors equal 1 and were not expressed in a table of error gain matrix. And in the analysis procedure for crucial error parameters, every error parameter is considered as the uniform unit dimensions and treated the same (i.e., '1' as 1 $\mu$ m for position and straightness errors, 1 $\mu$ rad for angular and squareness errors).

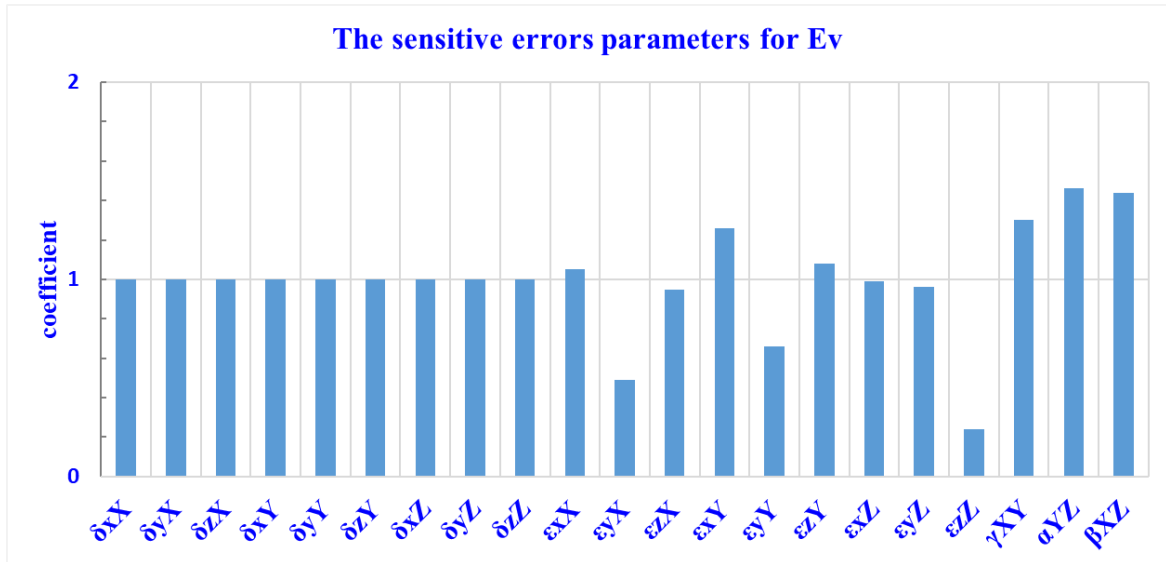


Fig. 4-3 The analysis result of sensitive error parameters for  $E_v$

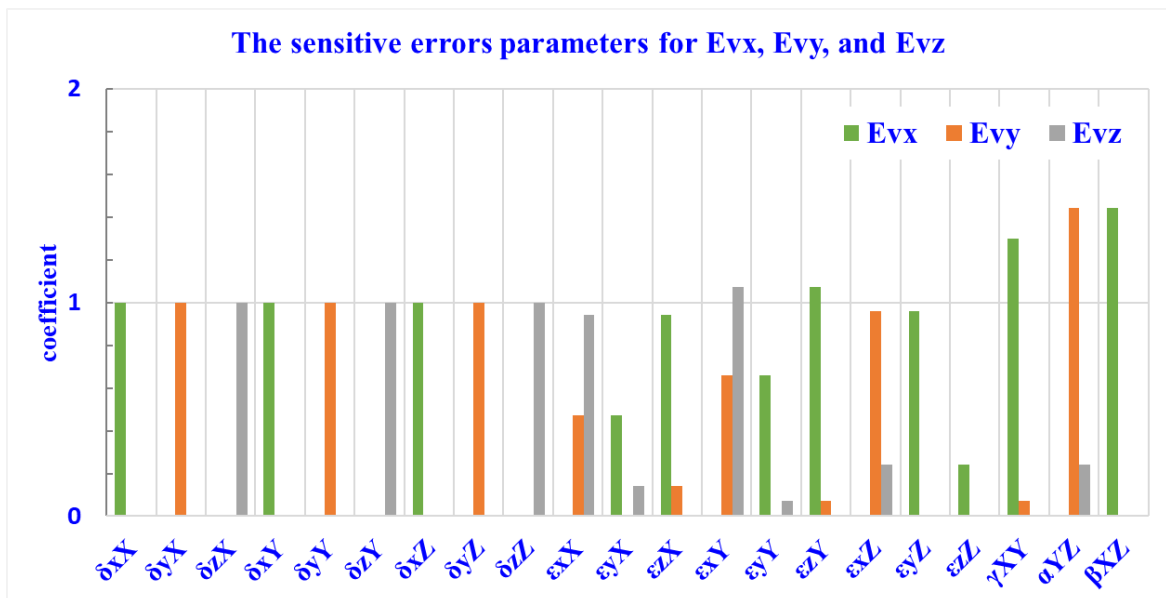


Fig. 4-4 The analysis result of sensitive error parameters for  $E_{vx}$ ,  $E_{vy}$ , and  $E_{vz}$

The outcome of determining the analysis for key error of a 5-axis machine tool, DVF5000, are shown in Fig. 4-3, and 4-4, where Fig. 4-3 shows the result of analysis for  $E_v$ , and Fig. 4-4 shows the sensitivity for  $E_{vx}$ ,  $E_{vy}$ , and  $E_{vz}$ . The analysis result of sensitive error parameters of a 5-axis machine tool, DVF5000, reveals that the key error factors propagating to the end-point's volumetric error are angular motion and orthogonality(squareness errors) related to the orientation of the motion components. In other words, kinds of angular errors, e.i., Abbe offset errors, are key factors that can contain potentially dominant effects propagated to the spatially translational deviation. On the contrary, the sensitivity of translational errors like a form of position errors and straightness errors is relatively small. Specifically, the 5-axis machine tool, DVF5000, examined by this study, involves in the order of  $\alpha_{YZ}$ ,  $\beta_{XZ}$ ,  $\gamma_{XY}$ ,  $\varepsilon_{xY}$ ,  $\varepsilon_{zY}$ , and  $\varepsilon_{xX}$  as the key error parameters for  $E_v$ . And  $\beta_{XZ}$ ,  $\gamma_{XY}$ , and  $\varepsilon_{zY}$  are the key error parameters for  $E_{vx}$ ,  $\alpha_{YZ}$  is the key error parameters for  $E_{vy}$ , and  $\varepsilon_{xY}$  is the key error parameters for  $E_{vz}$  the respectively.

In a structural loop of two sequential rotary axes for workpiece carrying, the errors in each motion component(i.e., tilting table) are the same as those of the rotational joint shown in Fig. 3-4, and orientation errors occurred by the inaccuracy of link are the same to those of the shown in Fig. 3-5. Then the HTM given by Eq. 4-11 is used for the rotary motion axes and can be developed as a formula like Eq. 4-16, therefore, the actual point coordinate on the workpiece (i.e.,  $W_x$ ,  $W_y$ ,  $W_z$ ) with respect to the reference coordinate frame is described by;

$$\begin{aligned}
 \begin{bmatrix} P_W \\ 1 \end{bmatrix}_{\text{actual}} &= {}^R_W T \begin{bmatrix} W_x \\ W_y \\ W_z \\ 1 \end{bmatrix} \\
 &= \begin{bmatrix} 1 & -\gamma_{XB} & 0 & O_{xB} + \delta x_{yB} \\ \gamma_{XB} & 1 & -\alpha_{ZB} & O_{yB} \\ 0 & \alpha_{ZB} & 1 & O_{zB} + \delta z_{yB} \\ 0 & 0 & 0 & 1 \end{bmatrix} \begin{bmatrix} \cos(\theta_B + \varepsilon_{yB}) \\ \varepsilon_{xB} \sin(\theta_B + \varepsilon_{yB}) + \varepsilon_{zB} \\ -\sin(\theta_B + \varepsilon_{yB}) \\ 0 \end{bmatrix} \\
 &\quad -\varepsilon_{zB} \cos(\theta_B + \varepsilon_{yB}) \quad \sin(\theta_B + \varepsilon_{yB}) \quad 0 \\
 &\quad 1 \quad -\varepsilon_{xB} \cos(\theta_B + \varepsilon_{yB}) \quad 0 \\
 &\quad \varepsilon_{zB} \sin(\theta_B + \varepsilon_{yB}) + \varepsilon_{xB} \quad \cos(\theta_B + \varepsilon_{yB}) \quad 0 \\
 &\quad 0 \quad 0 \quad 0 \quad 1 \begin{bmatrix} 1 & 0 & \beta_{XC} & O_{xC} + \delta x_{zC} \\ 0 & 1 & -\alpha_{YC} & O_{yC} + \delta y_{zC} \\ -\beta_{XC} & \alpha_{YC} & 1 & O_{zC} \\ 0 & 0 & 0 & 1 \end{bmatrix} \quad (4-25) \\
 &\quad \begin{bmatrix} \cos(\theta_C + \varepsilon_{zC}) & & & -\sin(\theta_C + \varepsilon_{zC}) \\ \sin(\theta_C + \varepsilon_{zC}) & & & \cos(\theta_C + \varepsilon_{zC}) \\ \varepsilon_{xC} \sin(\theta_C + \varepsilon_{zC}) - \varepsilon_{yC} \cos(\theta_C + \varepsilon_{zC}) & \varepsilon_{yC} \sin(\theta_C + \varepsilon_{zC}) + \varepsilon_{xC} \cos(\theta_C + \varepsilon_{zC}) \\ 0 & & & 0 \end{bmatrix} \\
 &\quad \varepsilon_{yC} \quad 0 \quad \begin{bmatrix} 1 & 0 & 0 & O_{xW} \\ 0 & 1 & 0 & O_{yW} \\ 0 & 0 & 1 & O_{zW} \\ 0 & 0 & 0 & 1 \end{bmatrix} \begin{bmatrix} W_x \\ W_y \\ W_z \\ 1 \end{bmatrix}
 \end{aligned}$$

The nominal coordinates of the arbitrary point on a workpiece would be the sum of relative coordinate values between the origin of all the individual motion components along their respective axes;

$$\begin{bmatrix} P_W \\ 1 \end{bmatrix}_{\text{nominal}} = \begin{bmatrix} O_{xB} + \cos\theta_B (O_{xC} + \cos\theta_C (O_{xW} + W_x) - \sin\theta_C (O_{yW} + W_y)) + \sin\theta_B (O_{zC} + O_{zW} + W_z) \\ O_{yB} + O_{yC} + \cos\theta_C (O_{yW} + W_y) + \sin\theta_C (O_{xW} + W_x) \\ O_{zB} - \sin\theta_B (O_{xC} + \cos\theta_C (O_{xW} + W_x) - \sin\theta_C (O_{yW} + W_y)) + \cos\theta_B (O_{zC} + O_{zW} + W_z) \\ 1 \end{bmatrix} \quad (4-26)$$

The volumetric errors as the translational deviation in the tool point position are thus given by:

$$\begin{bmatrix} E_{vx} \\ E_{vy} \\ E_{vz} \\ 1 \end{bmatrix} = \begin{bmatrix} P_W \\ 1 \end{bmatrix}_{\text{actual}} - \begin{bmatrix} P_W \\ 1 \end{bmatrix}_{\text{nominal}} \quad (4-27)$$

Deriving Eq. 4-27 with neglecting second-order terms gives  $E_x$ ,  $E_y$ , and  $E_z$  following.

$$\begin{aligned} E_{vx} = & (\cos\theta_B - \varepsilon_{yB} \sin\theta_B) (O_{xC} + (O_{xW} + W_x) (\cos\theta_C - \varepsilon_{zC} \sin\theta_C) - (O_{yW} + W_y) (\sin\theta_C \\ & + \varepsilon_{zC} \cos\theta_C) + (O_{zW} + W_z) (\beta_{xC} + \varepsilon_{yC} \cos\theta_C + \varepsilon_{xC} \sin\theta_C) + \delta_{xC} \cos\theta_C - \delta_{yC} \sin\theta_C) - \\ & (\gamma_{xB} + \varepsilon_{zB} \cos\theta_B - \varepsilon_{xB} \sin\theta_B) (O_{yC} + (O_{xW} + W_x) (\sin\theta_C + \varepsilon_{zC} \cos\theta_C) + (O_{yW} + W_y) \\ & (\cos\theta_C - \varepsilon_{zC} \sin\theta_C) - (O_{zW} + W_z) (\alpha_{yC} + \varepsilon_{xC} \cos\theta_C - \varepsilon_{yC} \sin\theta_C) + \delta_{yC} \cos\theta_C + \delta_{xC} \sin\theta_C \\ & - \cos\theta_B (O_{xC} + \cos\theta_C (O_{xW} + W_x) - \sin\theta_C (O_{yW} + W_y)) + \delta_{xB} \cos\theta_B - \sin\theta_B (O_{zC} + O_{zW} \\ & + W_z) + \delta_{zB} \sin\theta_B + (\sin\theta_B + \varepsilon_{yB} \cos\theta_B) (O_{zC} + O_{zW} + W_z + \delta_{zC} - (O_{xW} + W_x) (\varepsilon_{yC} + \\ & \beta_{xC} \cos\theta_C - \alpha_{yC} \sin\theta_C) + (O_{yW} + W_y) (\varepsilon_{xC} + \alpha_{yC} \cos\theta_C + \beta_{xC} \sin\theta_C)) \end{aligned} \quad (4-28)$$

$$\begin{aligned}
E_{vy} = & \delta_{yB} - \cos\theta_C (O_{yW} + W_y) + (O_{xW} + W_x)(\sin\theta_C + \varepsilon_{zC}\cos\theta_C) + (O_{yW} + W_y)(\cos\theta_C \\
& - \varepsilon_{zC}\sin\theta_C) - \sin\theta_C (O_{xW} + W_x) + (\varepsilon_{zB} + \gamma_{XB}\cos\theta_B + \alpha_{ZB}\sin\theta_B)(O_{xC} + (O_{xW} + W_x) \\
& (\cos\theta_C - \varepsilon_{zC}\sin\theta_C) - (O_{yW} + W_y)(\sin\theta_C + \varepsilon_{zC}\cos\theta_C) + (O_{zW} + W_z)(\beta_{XC} + \varepsilon_{yC}\cos\theta_C \\
& + \varepsilon_{xC}\sin\theta_C) + \delta_{xC}\cos\theta_C - \delta_{yC}\sin\theta_C) - (O_{zW} + W_z)(\alpha_{YC} + \varepsilon_{xC}\cos\theta_C - \varepsilon_{yC}\sin\theta_C) \\
& + \delta_{yC}\cos\theta_C + \delta_{xC}\sin\theta_C - (\varepsilon_{xB} + \alpha_{ZB}\cos\theta_B - \gamma_{XB}\sin\theta_B)(O_{zC} + O_{zW} + W_z + \delta_{zC} - \\
& (O_{xW} + W_x)(\varepsilon_{yC} + \beta_{XC}\cos\theta_C - \alpha_{YC}\sin\theta_C) + (O_{yW} + W_y)(\varepsilon_{xC} + \alpha_{YC}\cos\theta_C + \beta_{zC}\sin\theta_C))
\end{aligned} \tag{4-29}$$

$$\begin{aligned}
E_{vz} = & (\alpha_{ZB} + \varepsilon_{xB}\cos\theta_B + \varepsilon_{zB}\sin\theta_B)(O_{yC} + (O_{xW} + W_x)(\sin\theta_C + \varepsilon_{zC}\cos\theta_C) + (O_{yW} + W_y) \\
& (\cos\theta_C - \varepsilon_{zC}\sin\theta_C) - (O_{zW} + W_z)(\alpha_{YC} + \varepsilon_{xC}\cos\theta_C - \varepsilon_{yC}\sin\theta_C) + \delta_{yC}\cos\theta_C + \delta_{xC}\sin\theta_C) \\
& - (\sin\theta_B + \varepsilon_{yB}\cos\theta_B)(O_{xC} + (O_{xW} + W_x)(\cos\theta_C - \varepsilon_{zC}\sin\theta_C) - (O_{yW} + W_y)(\sin\theta_C + \\
& \varepsilon_{zC}\cos\theta_C) + (O_{zW} + W_z)(\beta_{XC} + \varepsilon_{yC}\cos\theta_C + \varepsilon_{xC}\sin\theta_C) + \delta_{xC}\cos\theta_C - \delta_{yC}\sin\theta_C) + \sin\theta_B \\
& (O_{xC} + \cos\theta_C (O_{xW} + W_x) - \sin\theta_C (O_{yW} + W_y)) - \cos\theta_B (O_{zC} + O_{zW} + W_z) + \delta_{zB}\cos\theta_B - \\
& \delta_{xB}\sin\theta_B + (\cos\theta_B - \varepsilon_{yB}\sin\theta_B)(O_{zC} + O_{zW} + W_z + \delta_{zC} - (O_{xW} + W_x)(\varepsilon_{yC} + \beta_{XC}\cos\theta_C - \\
& \alpha_{YC}\sin\theta_C) + (O_{yW} + W_y)(\varepsilon_{xC} + \alpha_{YC}\cos\theta_C + \beta_{XC}\sin\theta_C) + \alpha_{YC}\delta_{xC}\sin\theta_C)
\end{aligned} \tag{4-30}$$

Similarly to the process for the induction of a formula of the tool side loop, applying the coordinate dimension values that are designedly determined as a constant gives a matrix constructed with error gains for the coefficients of each variable as shown in Table 4-4 below.

Axis	$E_v$	$E_{vx}$	$E_{vy}$	$E_{vz}$
B Axis errors				
$\varepsilon_{xB}$	0.49	0.27	0.4	0.27
$\varepsilon_{yB}$	0.49	0.48	0	0.48
$\varepsilon_{zB}$	0.27	0.27	0.27	0.27
C Axis errors				
$\varepsilon_{xC}$	0.53	0.53	0.45	0.53
$\varepsilon_{yC}$	0.45	0.45	0.45	0.45
$\varepsilon_{zC}$	0.27	0.27	0.27	0.27
Perpendicularity				
$\alpha_{ZB}$	0.49	0	0.48	0.27
$\gamma_{XB}$	0.49	0.27	0.48	0
$\alpha_{YC}$	0.53	0.27	0.45	0.27
$\beta_{XC}$	0.53	0.53	0	0.53

Table 4-4 Error gain matrix for rotary axes of a 5-axis machine tool, DVF5000

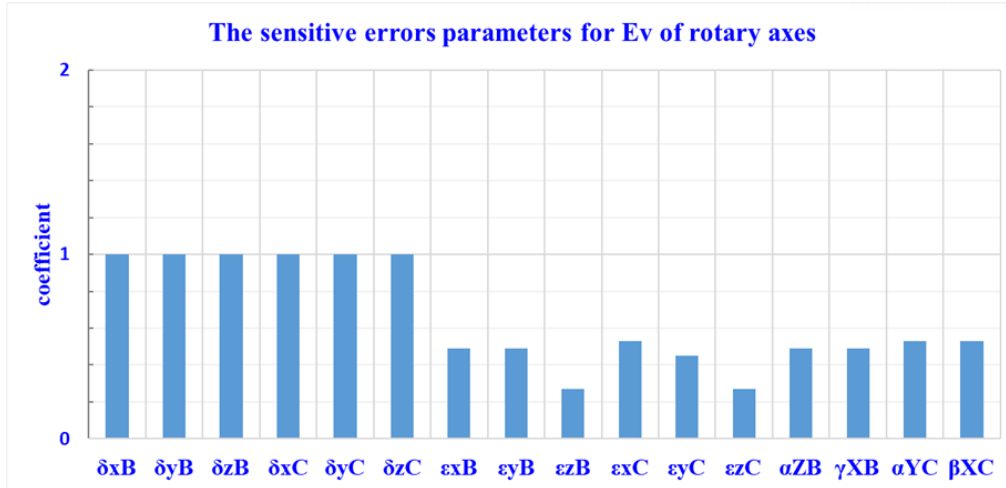


Fig. 4-5 The analysis result of sensitive error parameters for  $E_v$  of rotary axes

The consequence of determining the analysis for critical error of rotary components of a 5-axis machine tool, DVF5000, are shown in Fig. 4-5, and 4-6, where Fig. 4-5 show the result of analysis for  $E_v$ , and Fig. 4-6 shows the sensitivity for  $E_{vx}$ ,  $E_{vy}$ , and  $E_{vz}$ . The analysis result of sensitive error parameters of rotary axes of a 5-axis machine tool, DVF5000, reveals that unlike the configuration of the linear motion axis, the angular error parameters propagating with amplification do not exist in the designated workspace of this machine tool. Hence, the sensitivity of translational errors such as axial and radial errors is relatively more influential than angular errors, even though translational errors are reflected without amplification to the volumetric error at all.

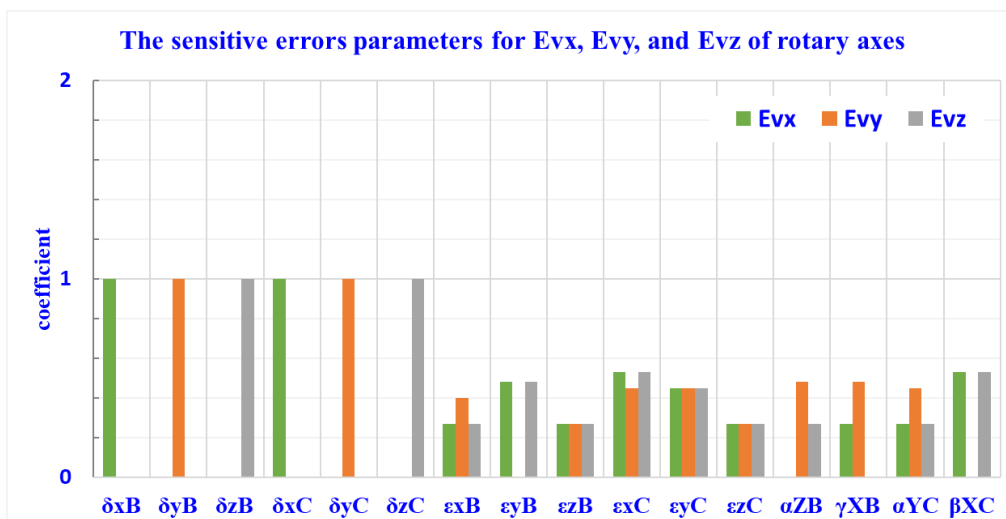


Fig. 4-6 The analysis result of sensitive error parameters for  $E_{vx}$ ,  $E_{vy}$ , and  $E_{vz}$  of rotary axes



### 4.3 Estimation of Volumetric Error for a Practical 5-Axis Machine Tool

The machine tools' geometric and volumetric errors are mainly used as post-performance measures that are inspected for real-world machine tools that are assembled already. In addition, it is very difficult to estimate this performance related to the machine tools' accuracy in the conceptual design or development stage and to correct defects found after the design or during the assembly process as well. Hence, estimating machine tools' spatial performance in advance is an assignment that must be done to improve the volumetric error of the machine tool, although it is a difficult and complicated task. The 5-axis machine tool is mainly composed of a machine bed, a column, saddles, carriages, linear motion guide rails, sliders, rollers, and other machinery parts, the motion components reciprocate along the guide system(e.g., box guide, linear motion guide, etc.)'s direction. Therefore the kinematic and geometric error of the motion axis depends on the geometric error contained in the motion guide system and deformations of the structural components composing the machine tool. These geometric or kinematic errors of the machinery parts and motion guide systems that govern movement are difficult to know in the design stage, while can manage the extent that restricts its fluctuation by specifying its tolerance.

The geometric tolerance of machine tools is easier to obtain through standards about machine tool verification such as ISO 230 or 10791 series, but it is tough for estimating precisely the volumetric error's distribution functions which is a comprehensive error indicator caused by the complex interrelationship of every geometric error. The sampling statistical analysis method is one of the useful approaches to analyze its hard-to-estimate parameters under the uncertain distribution function like estimating the volume error of machine tools. Therefore, the interval parameters and function for the error gain model of a subject 5-axis machine tools' volumetric error are adopted to describe the predicting distribution of spatial performance under the occurrence of uncertain geometric error. Besides, the Monte Carlo Simulation method is employed for estimating the spatial performance of a 5-axis machine tool, DVF5000; subject machine tools' volumetric error distribution is obtained under constraints ranging from the geometric error tolerance.

Monte Carlo simulations, as is well known, are methodologies for obtaining approximate solutions to problems through statistical analysis of random variables and stochastic simulations[61], it has numerous advantages such as powerful adaptability, the simpleness of calculation, and the independency of problem dimensions[60]. Thus, in order to estimate the machine tools' volumetric error in advance and decide the range of geometric error tolerance considering the kinematic structure characteristics of each machine tool, normally distributed random numbers of geometric error parameters are sampled and the spatial performance's response is investigated by applying the principle of the Monte Carlo Simulation. The procedures to estimate the variation range of the machine tool's volumetric error according to the tolerance of each geometric and kinematic error have proceeded as

follows.

First, the geometric errors' probability distribution model is determined. As usual, the normal distribution is the most widely used probability distribution since it can describe many natural phenomena, The geometric error distribution of manufactured mechanical parts also follows the principle of normal distribution[62]. And the assumption for the probability density function is described as follows:

$$f(x) = \frac{1}{\sqrt{2\pi\sigma^2}} e^{-\frac{(x-\mu)^2}{2\sigma^2}} \tag{4-31}$$

Where  $\mu$  is the mean of the distribution, and  $\sigma^2$  is the variance.

Secondly, the mean value and variance of the geometric error parameters' probability distribution were determined, and from the viewpoint of a reasonable convention for engineering, the distribution range of the normal distribution was considered as  $\pm 3\sigma$ . For reference, Table 4-5 gives the probability of a value occurring within a number of standard deviations of its expected value.

k	N(%) Chance of occurrence
1.0	68.2689
2.0	95.4500
3.0	99.7300
4.0	99.9937
5.0	99.9999
6.0	100.0000

Table 4-5 Chance of a value falling within k  $\sigma$  of its expected value for random processes[19]

Last, the parameters of geometric errors are sampled according to the two conditions of constraint, one is general tolerance referring to standards such as ISO widely used by general machine tool builders without consideration for the effect of sensitive errors and another is the range of geometric error considering the consequence of analyzing crucial geometric errors that reflected the kinematic structure characteristics of the targeted 5-axis machine tool. Each sampling range of each geometric and kinematic error of a linear motion component is chosen as Table 4-6 and Table 4-7 respectively. The total sample size in this study was set at 100,000, besides that all the motion components behave like rigid bodies and keep balance was assumed, also the effect of thermal behavior was excluded.

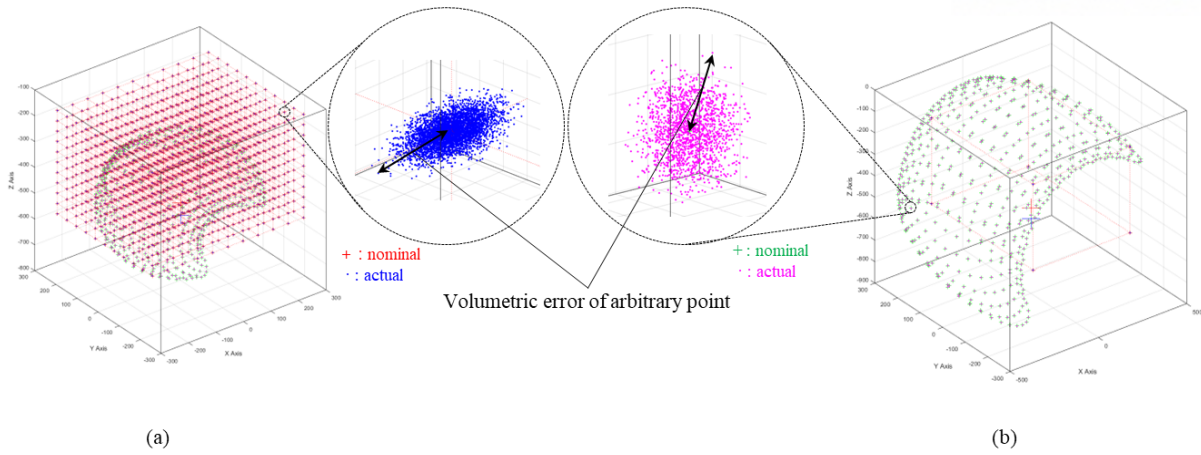


Fig. 4-7 Illustration of the simulation of the traces at arbitrary point; (a) tool point, (b) workpiece point

The illustration of the simulation of traces at each tool point that is affected by the geometric and kinematic error occurring within the tolerance range in the working volume,  $550 \times 450 \times 400\text{mm}^3$ , of this 5-axis machine tool, is as depicted in Fig. 4-7 (a). And the traces at a certain point equivalent to the allowed height and radius of the maximum workpiece,  $\text{Ø}550 \times 450\text{mm}^3$ , which is affected by the geometric and kinematic error occurring within the tolerance range when rotating in the limit of the angle of each rotary component, is as shown in Fig. 4-7 (b).

Parameters	Targeted tolerance	Parameters	Targeted tolerance	Parameters	Targeted tolerance	Parameters	Targeted tolerance
$\delta_{xX}$	$\pm 10\mu\text{m}$	$\epsilon_{zX}$	$\pm 20\mu\text{rad}$	$\delta_{xB}$	$\pm 10\mu\text{m}$	$\epsilon_{zC}$	$\pm 20\mu\text{rad}$
$\delta_{yX}$	$\pm 10\mu\text{m}$	$\epsilon_{xY}$	$\pm 20\mu\text{rad}$	$\delta_{yB}$	$\pm 10\mu\text{m}$	$\alpha_{zB}$	$\pm 25\mu\text{rad}$
$\delta_{zX}$	$\pm 10\mu\text{m}$	$\epsilon_{yY}$	$\pm 20\mu\text{rad}$	$\delta_{zB}$	$\pm 10\mu\text{m}$	$\gamma_{xB}$	$\pm 25\mu\text{rad}$
$\delta_{xY}$	$\pm 10\mu\text{m}$	$\epsilon_{zY}$	$\pm 20\mu\text{rad}$	$\delta_{xC}$	$\pm 10\mu\text{m}$	$\alpha_{yC}$	$\pm 25\mu\text{rad}$
$\delta_{yY}$	$\pm 10\mu\text{m}$	$\epsilon_{xZ}$	$\pm 20\mu\text{rad}$	$\delta_{yC}$	$\pm 10\mu\text{m}$	$\beta_{xC}$	$\pm 25\mu\text{rad}$
$\delta_{zY}$	$\pm 10\mu\text{m}$	$\epsilon_{yZ}$	$\pm 20\mu\text{rad}$	$\delta_{zC}$	$\pm 10\mu\text{m}$		
$\delta_{xZ}$	$\pm 10\mu\text{m}$	$\epsilon_{zZ}$	$\pm 20\mu\text{rad}$	$\epsilon_{xB}$	$\pm 20\mu\text{rad}$		
$\delta_{yZ}$	$\pm 10\mu\text{m}$	$\gamma_{XY}$	$\pm 25\mu\text{rad}$	$\epsilon_{yB}$	$\pm 20\mu\text{rad}$		
$\delta_{zZ}$	$\pm 10\mu\text{m}$	$\alpha_{YZ}$	$\pm 25\mu\text{rad}$	$\epsilon_{zB}$	$\pm 20\mu\text{rad}$		
$\epsilon_{xX}$	$\pm 20\mu\text{rad}$	$\beta_{XZ}$	$\pm 25\mu\text{rad}$	$\epsilon_{xC}$	$\pm 20\mu\text{rad}$		
$\epsilon_{yX}$	$\pm 20\mu\text{rad}$			$\epsilon_{yC}$	$\pm 20\mu\text{rad}$		

Table 4-6 Ranges of sampling tolerance of geometric and kinematic errors; general case

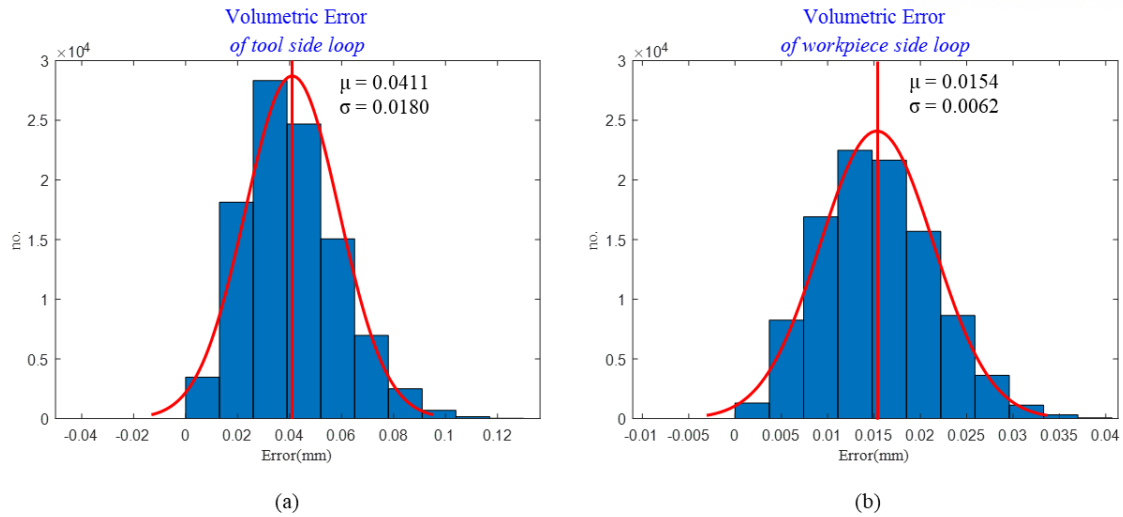


Fig. 4-8 Frequency distribution of predicting volumetric errors propagated through (a) the tool side loop, (b) the workpiece side loop under the general tolerance

According to the estimation for the subject 5-axis machine tools' volumetric error under the tolerance of general case as Table 4-6, the volumetric error of the tool point which is propagated through the tool side loop is predicted as about  $41\mu\text{m}$ , and the volumetric error of the workpiece point which is propagated through the workpiece side loop is predicted as about  $15\mu\text{m}$ . Moreover, the frequency distribution expressing each simulated volumetric error related to the tool side loop and workpiece side loop is shown in Fig. 4-8 (a) and (b) respectively.

Parameters	Targeted tolerance	Parameters	Targeted tolerance
$\epsilon_{xX}$	$-8\pm 6\ \mu\text{rad}$	$\delta_{xB}$	$\pm 5\ \mu\text{m}$
$\epsilon_{xY}$	$-8\pm 6\ \mu\text{rad}$	$\delta_{yB}$	$\pm 5\ \mu\text{m}$
$\epsilon_{zY}$	$-8\pm 6\ \mu\text{rad}$	$\delta_{zB}$	$\pm 5\ \mu\text{m}$
$\epsilon_{xZ}$	$-8\pm 6\ \mu\text{rad}$	$\delta_{xC}$	$\pm 5\ \mu\text{m}$
$\gamma_{XY}$	$17\pm 4\ \mu\text{rad}$	$\delta_{yC}$	$\pm 5\ \mu\text{m}$
$\alpha_{YZ}$	$17\pm 4\ \mu\text{rad}$	$\delta_{zC}$	$\pm 5\ \mu\text{m}$
$\beta_{XZ}$	$17\pm 4\ \mu\text{rad}$		

Table 4-7 Key errors and ranges of sampling tolerance; case considering coefficient of errors

Subsequently, to confirm the effect under the condition of suppressing the critical geometric error parameters which propagate to the end of the functional point sensitively, key error parameters, which are magnified by the distance between error sources and the end functional point, are determined to

$\varepsilon_{xx}$ (X-axis's roll),  $\varepsilon_{xy}$ (Y-axis's pitch),  $\varepsilon_{zy}$ (Y-axis's yaw),  $\varepsilon_{xz}$ (Z-axis' pitch),  $\gamma_{xy}$ (squareness between X and Y),  $\alpha_{yz}$ (i.e., squareness between Y and Z), and  $\beta_{xz}$ (i.e., squareness between X and Z). And key errors parameters for rotary motion axes such as the B or C axis are axial errors and radial errors. The target tolerance proposed for key geometric errors is set based on the coefficient of error gain respectively and is shown in Table 4-7. The predicted volumetric error under the condition of suppressing the key geometric errors with the proposed range through the assembly process is about  $24\mu\text{m}$  for the tool side loop, and about  $10\mu\text{m}$  for the workpiece side loop; moreover, the frequency distribution expressing each simulated volumetric error related to the tool side loop and workpiece side loop under the condition of suppressing the key errors is shown in Fig. 4-9 (a) and (b) respectively.

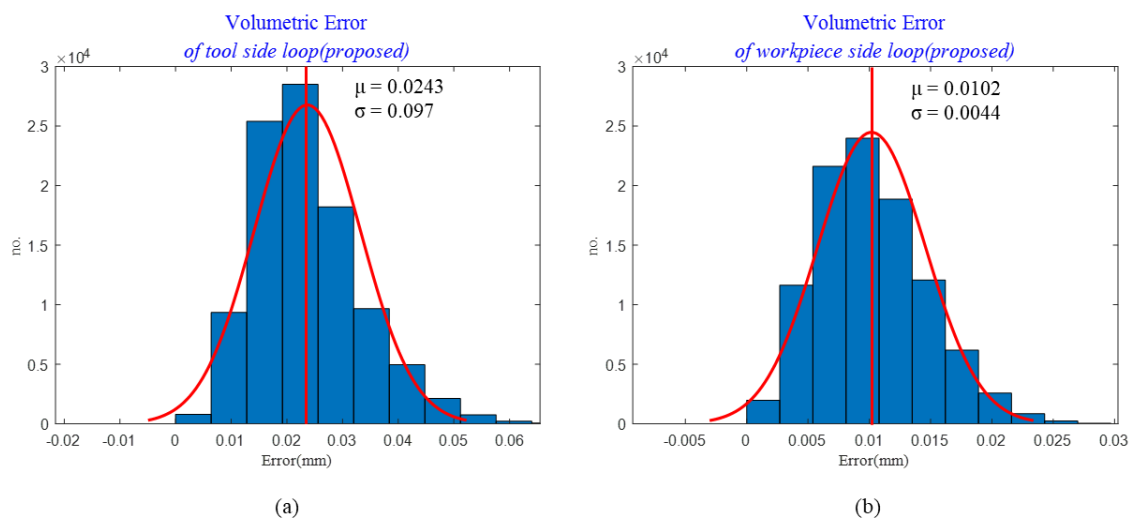


Fig. 4-9 Frequency distribution of predicting volumetric errors propagated through (a) the tool side loop, (b) the workpiece side loop under the condition of suppressing the key errors

Consequently, based on the results of the estimation and analysis for volumetric error, two useful significances can be confirmed about the precise design and assembly of the 5-axis machine tools. First, these results reveal that the 5-axis machine tools' volumetric error can be predicted by establishing the mathematical model for volumetric error and applying stochastic simulation of random variables. Secondly, as well as, it also predicted that the achievable effect via identifying and ranging the key geometric errors properly and then suppressing them during the assembly process is considerable. Therefore, it is expected that if the assembly process is managed within the tolerance range proposed for the key error parameters, the volumetric error of this a 5-axis machine tool, DVF5000, can be achieved at less than  $24\mu\text{m}$  without measures of compensation using the software.

In this regard, the comparison results show that for 4 categories of key errors parameters of the subject 5-axis machine tool and the effect that can be obtained by restraining them, and is shown in Table 4-8. For reference, the comparison mainly focused on the value of predicted volumetric error at the peak of

frequency distribution, namely the average value of volumetric error.

Classification	Key errors parameters	General tolerance	Proposed target tolerance
Angular errors of linear motion	$\varepsilon_{xX}, \varepsilon_{xY}, \varepsilon_{zY}, \varepsilon_{xZ}$	$\pm 20\mu\text{rad}$	$-8\pm 6\mu\text{rad}$
Squareness errors between linear motion	$\gamma_{XY}, \alpha_{YZ}, \beta_{XZ}$	$\pm 25\mu\text{rad}$	$17\pm 4\mu\text{rad}$
Predicted volumetric error by linear motion		$41\mu\text{m}$	$24\mu\text{m}$
Axial error of rotary motion	$\delta_{yB}, \delta_{zC}$	$\pm 10\mu\text{m}$	$\pm 5\mu\text{m}$
Radial error of rotary motion	$\delta_{xB}, \delta_{zB}, \delta_{xC}, \delta_{yC}$	$\pm 10\mu\text{m}$	$\pm 5\mu\text{m}$
Predicted volumetric error by rotary motion		$15\mu\text{m}$	$10\mu\text{m}$

Table 4-8 Comparison of the predicted volumetric error under the general and proposed tolerance

## Chapter 5. EXPERIMENTAL RESULTS AND DISCUSSION

### 5.1 Experiment Setup

As it is well known in the research conducted previously, thermal-induced errors are one of the major causes of deviations in machining tools[63], and one of the possible heat sources that lead to the machining tools' thermal-induced errors is the room environment classified as the external heat source[64]. Therefore, it is necessary to control the installation environment such as ambient temperature so that the machine is not directly exposed to changes in the atmosphere that may directly affect the machining tools' geometric and kinematic behavior. Accordingly, the experiment was conducted under conditions that minimize the effect of environmental variables on the machining tools' accuracy by installing the vertical 5-axis machine tool, DVF5000 series, in the environmental chamber as shown in Fig. 5-1.

The chamber used in the experiment was manufactured in the shape of a rectangular parallelepiped with an internal volume of  $5,000 \times 7,000 \times 5,000\text{mm}^3$ , and is operated by a forced convection method. The reference temperature for industrial dimensional measurements in accordance with ISO 230-1 is  $20^\circ\text{C}$ . Therefore, measurement devices and measurement targets should be in equilibrium with the environment where the temperature is maintained at  $20^\circ\text{C}$ [65]. Thus, during the experiment the atmospheric temperature in the chamber was set to maintain  $20^\circ\text{C}$ . In addition, the discharge wind speed was limited to not exceed 1 m/s in order to prevent causing temperature distribution in the machining tools' structure due to the direct blowing of the wind cooled/heated to a specific area. Table 5-1 contains information about the specifications of the environmental chamber used and the setup condition of the experiment.



Fig. 5-1 Preparation for experiments using the environmental chamber; (a) installation of DVF5000 before tests, (d) state of the environmental chamber during the experiment

	Internal size (W×D×H mm <sup>3</sup> )	Limit of weight (ton/m <sup>2</sup> )	Range of temp control (°C)	Setup of Temp (°C)	Range of wind speed (m/s)	Setup of wind speed (m/s)
Specification	5,000×7,000×5,000	5	-70~60	20	0~20	≤1

Table 5-1 Specification of a Walk-in environmental chamber and setup condition

According to ISO 230-1[65], the linear axis's geometric error consists of 6 motion errors covering the 3 linear motion errors including position and straightness errors, and the 3 angular motions error, the so-described roll, pitch, and yaw. Measurement guidance and approaches for these linear motion's geometric errors are well defined in ISO 230-1 above mentioned. In this study, to measure the linear axis's geometric error motion, XM-60, a multi-axis calibrator manufactured by RENISHAW with a laser interferometer, was utilized as a measuring instrument to carry out the experiments. The XM-60 is a measurement system that is capable of simultaneously measuring 6-DOF errors along a linear axial direction through only a single set-up, so, it is a measuring instrument suitable for assessing and correcting during assembly or product inspection the overall error of linear motion components related to volumetric error evaluation of machining tools; some performance specification about this measuring instrument is listed in Table 5-2.

Errors motion	Accuracy	Resolution	Range
Linear	±0.5ppm	1 nm	0m to 4m
Straightness	Typical range: ±0.01A ±1μm	0.03μrad	±50μm
Angular (pitch/yaw)	±0.004A ±(0.5μrad +0.11M μrad)	0.25μm	±500μrad
Angular (Roll)	±0.01A ±6.3μrad	0.12μrad	±500μrad

※ A = displayed error reading, M = measured distance in meters

Table 5-2 Performance specification of an XM-60, a multi-axis calibrator

To install a measurement device for linear error, a typical laser interferometer consists of a combination of elements such as a laser head, a beam splitter, and 2 linear reflectors, and one linear reflector among 2 reflectors should be mounted to the beam splitter to make the reference path for the laser beam. And then the beam splitter is located in the path of the laser beam between a laser transmitter and the linear reflector. In this study, the laser launch unit which adopts the built-in interferometer is kept stationary, whereas the laser receiver which contains built-in a retro-reflector is located on a spindle, the moving components, of this 5-axis machine tool. An example of installation for a typical 5-axis machine tool is given in Fig. 5-2, the figure depicts a setup for linear motions error of the X-, Y-, and



Z-axal directions in order.

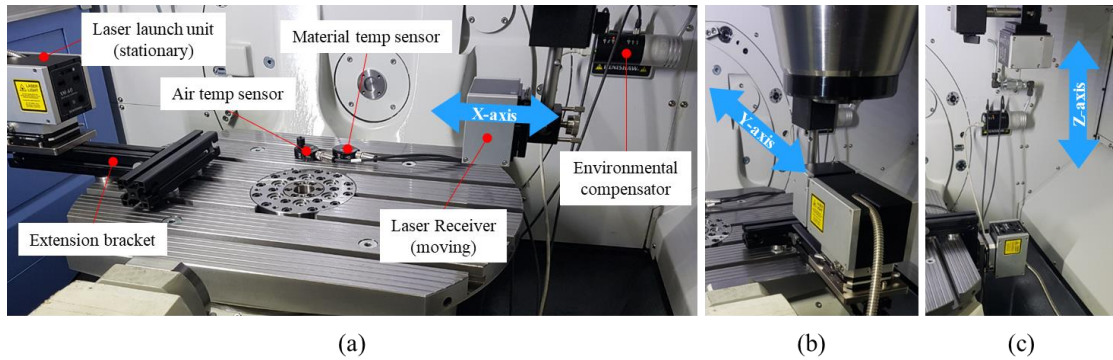


Fig. 5-2 Experimental setup for measuring linear errors of (a) X-axis, (b) Y-axis, and (c) Z-axis

The circular trajectory test, described in ISO 230-4[40], provides the estimation of the CNC machining tool's contouring performance, errors in circular interpolation trajectories are influenced by geometric errors including squareness, and a machining tool's dynamic behavior. In particular, a circular test utilizing a double ball bar(i.e., DBB) is one of the most widely used by machine builders for detecting geometric errors. In this study, to assess the squareness error between orthogonal linear axes a wireless double ball bar system, QC20-W manufactured by RENISHAW, was utilized.

For example, when the squareness error exists between the X- and Y-axial direction motion, the obtained circular contour in a polar plot is tilted in the X or Y direction, as is shown by a typical instance of the measured result in Fig. 5-3. And this well illustrates the basic concept of approaches for identifying the squareness error. An example of the setup for the circular test of the typical type of vertical machining tool is given in Fig. 5-4, and a figure depicts a preparation according to the contour motions of the XY, XZ, and YZ in order.

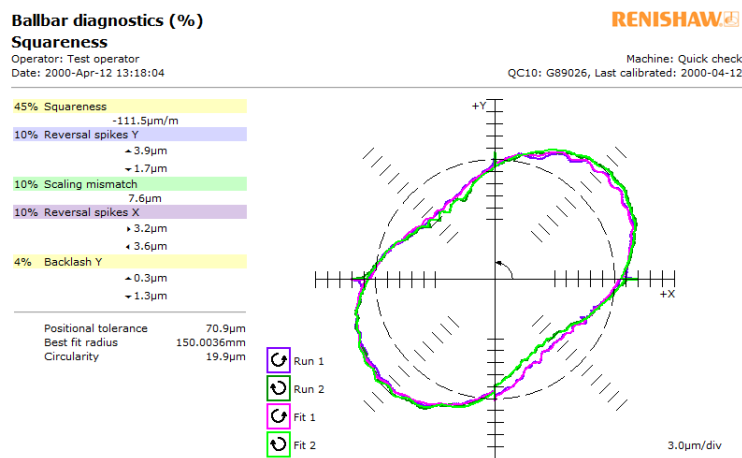


Fig. 5-3 A measured error profile affected by the squareness error dominantly

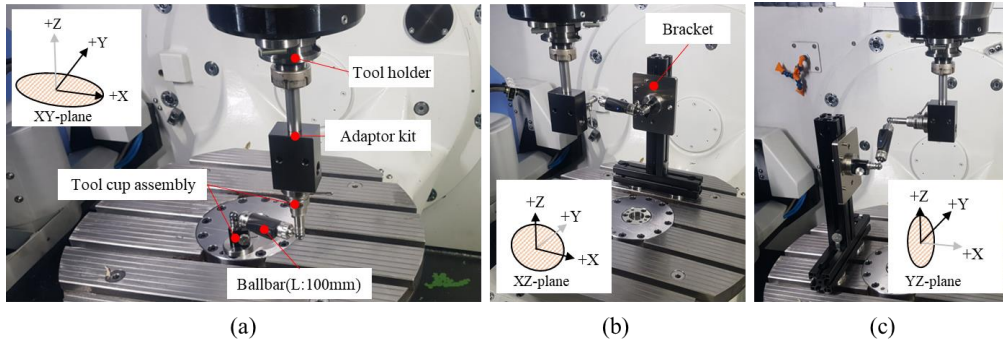


Fig. 5-4 Experimental setup for the circular test of each plane of (a) XY, (b) XZ, and (c) YZ

The 3 orthogonal linear axes' volumetric error is the maximum range of relative translational deviations between nominal and actual positions in X-, Y- and Z-axial directions in the working volume interested, where the deviations are defined as the relative extent of discrepancy between the machining tool's cutting tool side and the workpiece side for the alignment of specified axes[65]. Diagonal displacement tests have been utilized as means for estimating the CNC machining tools' spatial performance quickly among the methods of verification for volumetric error. However, the disadvantages exist in that it is unsuitable to assess the machining tools' volumetric error directly and to identify individual geometric error parameters through only 4 body diagonal measurements[41]. On the contrary, a measuring instrument using a measurement technology based on multilateration with a fiber-based laser interferometer and steering mechanism, the so-named Lasertracer, tracks the targeted reflector positioned in a spatial grid and acquires the spatial displacement directly. Owing to these features, measurements for targeted spatial points can easily be performed even exists a large number of target positions that cover the entire working volume. And since the laser tracer measures a stationary sphere directly, it can significantly decrease the uncertainty related to the radial measurement of the system compared to conventional laser trackers[39]. In this study, therefore, a laser tracer is utilized as a means to finally assess the 5-axis machining tool's volumetric error to prove the usefulness of restraint measures for key errors and enhancement of volumetric error accordingly, an instance of the setup of laser trace for assessing the volumetric error is given in Fig. 5-5.

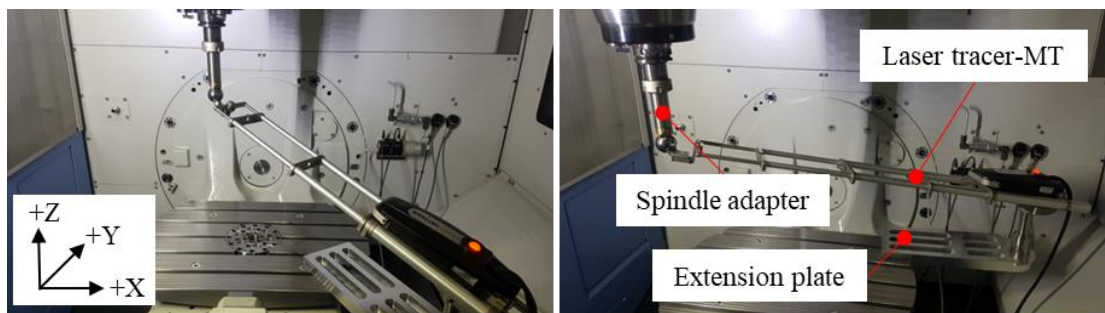


Fig. 5-5 Experimental setup of laser trace for assessing the volumetric error

## 5.2 Experiment Results of a 5-Axis Machine Tool, DVF5000

The results of the experiments conducted on a 5-axis machine tool are given in this section. First, the measurement results of each evaluation item before applying the proposed tolerance and the points of improvement to enhance the volumetric errors of this machining tools are presented. Then, the measurement results performed on the same model of a machining tool after undergoing remedial measures which satisfied the proposed tolerance based on the prediction of volumetric error are presented. Finally, through the comparison of the results before and after, the validity of the error model for a targeted 5-axis machine and the practicality of restraint measures for key errors are confirmed.

### 5.2.1 Assessment for Errors Before Application of Proposed Tolerance

#### (1) Geometric Errors of the Individual Linear Axis

The geometric errors of the individual linear axis were taken along the X, Y, and Z axes in the DVF5000, a 5-axis machining tool, and the direction of the detection of the laser system was set to be the same as the machine under test. The values for three translational and three angular errors of each axis were shown in the same plot, and since the effects related to a reversal error and thermal drift along linear motion were not considered in this study, the error data acquired runs in a forward(i.e., positive) direction are only represented.

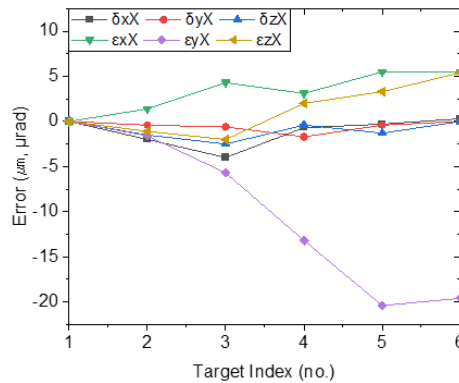


Fig. 5-6 Geometric errors along the X-axis before applying the proposed tolerance

First, the geometric error data measured along the X-axis are shown in Fig. 5-6, a total of six error parameters,  $\delta_{xX}$ ,  $\delta_{yX}$ ,  $\delta_{zX}$ ,  $\epsilon_{xX}$ ,  $\epsilon_{yX}$ , and  $\epsilon_{zX}$ , are represented according to each color of the line. The error expressed by the purple line, e.i.,  $\epsilon_{yX}$ , due to the pitch motion according to the forward/backward motion of the X-axis stands out among the error parameters. Since this error parameter, however, is an error that is not highly sensitive to propagation as a volumetric error of this machining tool, it can be estimated that the effect on the volumetric error of the machining tool under test is not dominant based on the analysis for key error parameter.

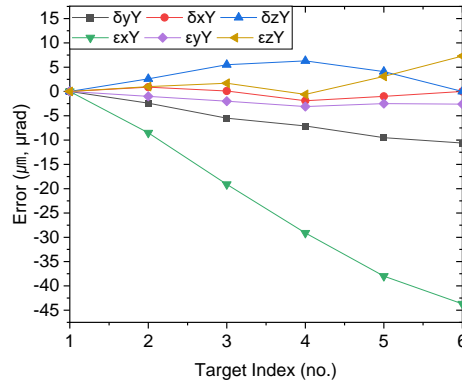


Fig. 5-7 Geometric errors along the Y-axis before applying the proposed tolerance

Secondly, the geometric error data measured along the Y-axis are shown in Fig. 5-7. A total of six error parameters,  $\delta_{xY}$ ,  $\delta_{yY}$ ,  $\delta_{zY}$ ,  $\epsilon_{xY}$ ,  $\epsilon_{yY}$ , and  $\epsilon_{zY}$ , are represented according to each color of the line. The error parameters to note in this plot presenting the result of error motions along the Y-axis is the error expressed by the green line, i.e.,  $\epsilon_{xY}$ , due to the pitch motion according to the forward/backward motion of the Y-axis. This error is one of the key errors, which is magnified to the tool point error, hence, remedial measures to restrain this error motion are required in order to enhance volumetric error.

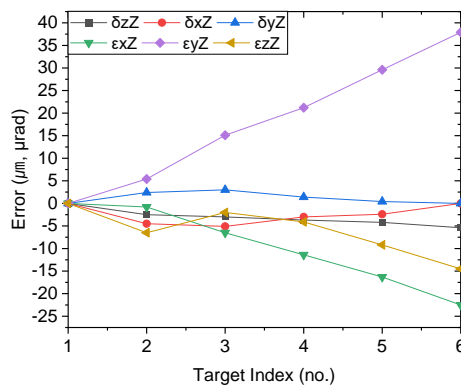


Fig. 5-8 Geometric errors along the Z-axis before applying the proposed tolerance

Last, the geometric error data measured along the Z-axis are shown in Fig. 5-8, and a total of six errors,  $\delta_{xZ}$ ,  $\delta_{yZ}$ ,  $\delta_{zZ}$ ,  $\epsilon_{xZ}$ ,  $\epsilon_{yZ}$ , and  $\epsilon_{zZ}$ , are represented according to each color of the line. The parameters to note in the result of error motions along the Z-axis are the errors expressed by the purple and green line, i.e.,  $\epsilon_{yZ}$  and  $\epsilon_{xZ}$ , due to the yaw and pitch motion according to the motion of the Z-axis. These two errors are classified also key errors based on the analysis of key error parameters, hence, improvement measures to restrain these errors are also required.

## (2) Squareness Errors between the Linear Axis

As mentioned earlier, a circular test using a double ball bar was utilized in a way to confirm the squareness error of the machining tool under test, and an example of the measurement result as shown in Fig. 5-9 is obtained. The measurement result below is a circular trajectory acquired by simultaneous motion between the Y- and Z-axis, as indicated in the results, various errors as well as squareness errors can be detected and diagnosed.

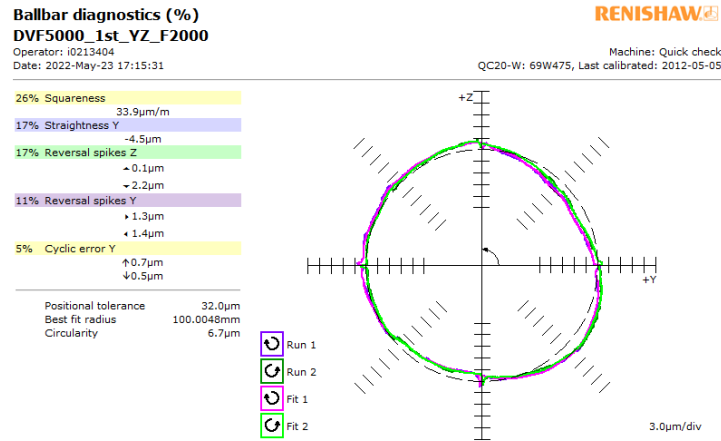


Fig. 5-9 Squareness errors between the Y- and Z-axis before applying the proposed tolerance

The results of the circular test obtained by simultaneously contouring the X and Y axes, the X and Z axes, and the Y and Z axes are listed in Table 5-3. All three of the error parameters related to squareness error are classified as key errors that could dominate the volumetric error of the targeted machining tool based on the determination of key contributing errors influencing volumetric error. And as can be seen from Table 5-3, the two squareness error parameters such as  $\gamma_{XY}$  and  $\alpha_{YZ}$  are identified as errors that need improvement which aligns the mutual relation between the two linear axes in this machining tool under test.

Parameters	$\gamma_{XY}$	$\beta_{XZ}$	$\alpha_{YZ}$
Squareness errors	23.1µrad	18.1µrad	33.9µrad
Tolerance proposed	17±4µrad	17±4µrad	17±4µrad

Table 5-3 Results of squareness errors between the linear axes before applying the proposed tolerance

## (3) Volumetric Error within the Working Space

The volumetric error within the working space of the machining tool is a comprehensive evaluation

index of errors of the machining tool, in that the effects of the geometric and squareness errors measured in the previous step are directly reflected. Thus, in order to directly compare the effects of restraining each key error parameter, the volumetric error of the machining tool produced in the condition without the application of optimized tolerances to reflect the kinematic characteristics of this machining tool was confirmed using Lasertracer-MT manufactured by eTALON, and the result is shown in Fig. 5-10. As can be seen from the measurement results, the volumetric error of the test machining tool is  $32\mu\text{m}$  within the entire working space. And it is figured out that the YZ-plane has been distorted into a rhombus shape caused by,  $\alpha_{YZ}$ , the squareness error parameter, which was previously confirmed in the circular test, is directly reflected in to result of this assessment. Thus, based on the results of this assessment, the volumetric error of the machining tool assembled with the proposed tolerance is compared in the aspect of the shape of the three-dimensional space composed of each plane and the volumetric error level, and the validity of the new tolerance is determined through this comparison of differences.

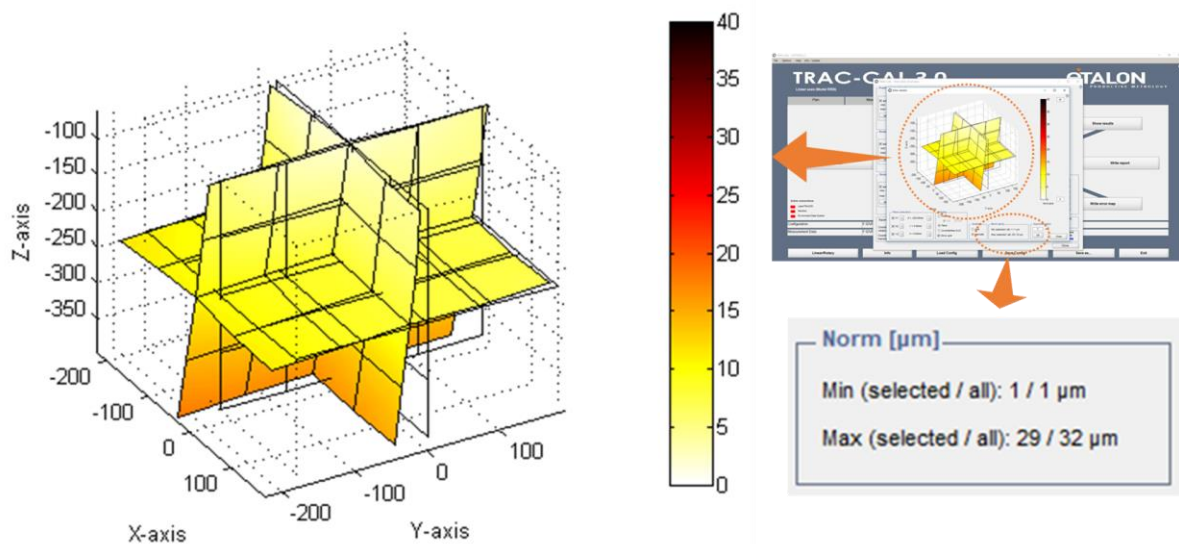


Fig. 5-10 Result of volumetric errors before applying the proposed tolerance

## 5.2.2 Assessment for Errors After Application of Proposed Tolerance

### (1) Geometric Errors of the Individual Linear Axis

The measurement result of geometric errors along the X-, Y, and Z-axis to which the proposed tolerance is applied to improve the volumetric error of the target machining tool is shown in Fig. 5-11 (a), (B), and (C). And all the crucial error parameters such as  $\epsilon_{xx}$  (i.e., the roll motion of the X-axis),  $\epsilon_{xy}$  (i.e., the yaw motion of the X-axis),  $\epsilon_{xy}$  (i.e., the pitch motion of the Y-axis),  $\epsilon_{zy}$  (i.e., the yaw motion of the Y-axis),  $\epsilon_{xz}$  (i.e., the pitch motion of the Z-axis), and  $\epsilon_{yz}$  (i.e., the yaw motion of the Z-axis), which

were classified as a kind of key error parameters of the test machining tool, are confirmed to have been assembled in a well-suppressed within the proposed tolerance through this assessment.

For reference, as shown in Fig. 5-11(a), the pitch motion error of the X-axis,  $\epsilon_{yX}$ , expressed by the purple line is relatively prominent compared to other error parameters in both the two machining tools selected for this experiment though, further step for modification is not taken as it is considered that it would not significantly affect volumetric error according to the analysis for key error parameters.

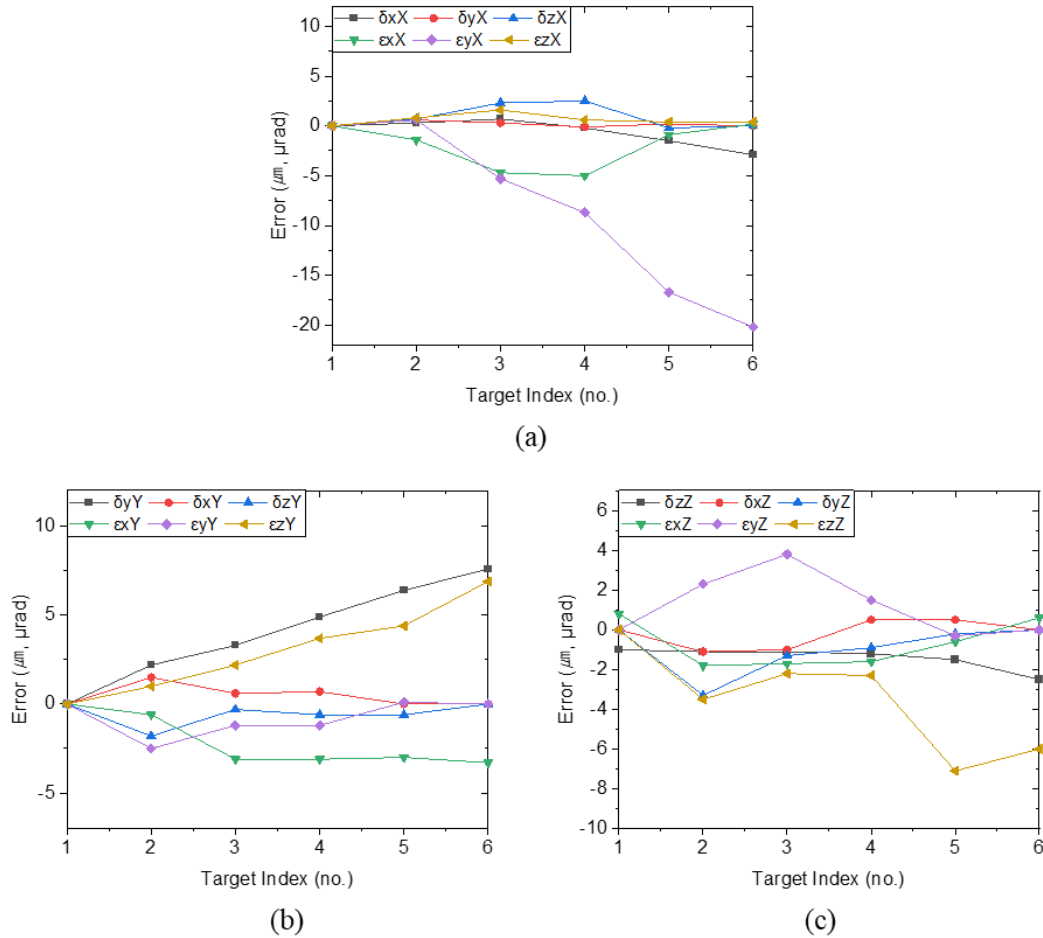


Fig. 5-11 Geometric errors of the (a) X-, (b) Y-, and (c) Z- axis, after applying the proposed tolerance

## (2) Squareness Errors between the Linear Axis

The values of squareness error obtained from the results of the circular test under the condition adopting tolerance proposed are listed in Table 5-4, and based on this result that all three squareness error parameters that could affect the volumetric error of the targeted machining tool have been in a well-suppressed during assembly can be confirmed. Hence, it can be expected that the volumetric error of test 5- axis machining tool might have been sufficiently improved under the condition that all key

error components are properly controlled.

Parameters	$\gamma_{XY}$	$\beta_{XZ}$	$\alpha_{YZ}$
Squareness errors	13.2 $\mu$ rad	19.6 $\mu$ rad	13.8 $\mu$ rad
Tolerance proposed	17 $\pm$ 4 $\mu$ rad	17 $\pm$ 4 $\mu$ rad	17 $\pm$ 4 $\mu$ rad

Table 5-4 Results of squareness errors between the linear axes after applying the proposed tolerance

### (3) Volumetric Error within the Working Space

The volumetric error as a comprehensive evaluation index of errors of the machining tool directly reflects the condition depending on how the machine builder keeps controlling the error caused by the motion components of the machining tool during design and assembly. Thus, assessing and comparing machining tool precision through volumetric error measurement is an effective quality management measure, it is suitable for identifying the effects of the well-managed key geometries through the assembly process.

Consequently, the volumetric error of the machining tool produced with the application of optimized tolerances to reflect the kinematic characteristics of this machining tool is 15 $\mu$ m within the entire working space, and the result is shown in Fig. 5-11. Compared to the comparative test machining tool produced without the application of the proposed tolerance, it can be confirmed that the value of volumetric error in the entire working space has been significantly improved, and it is judged that the overall shape of the space has also been remarkably in good form visually.

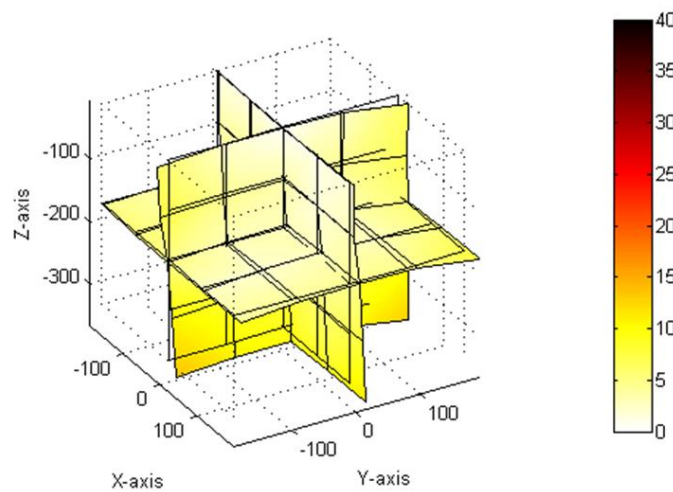


Fig. 5-12 Result of volumetric errors after applying the proposed tolerance



### 5.3 Comparison of Experiment Results and Discussion

As written in the previous sections, error parameters that affect the volumetric error of machining tool tolerance have been identified and classified, and the actual effect of these errors was evaluated through measurements of various errors. From this section, the error evaluation data measured on the two sample machining tools, one without the application of optimization tolerance and another with the adoption of the tolerance proposed, are directly compared. And through comparison, whether the assembly tolerance control of key error parameters reflecting the characteristics of the machining tools has had a practical effect on the volumetric error of the machining tool is examined.

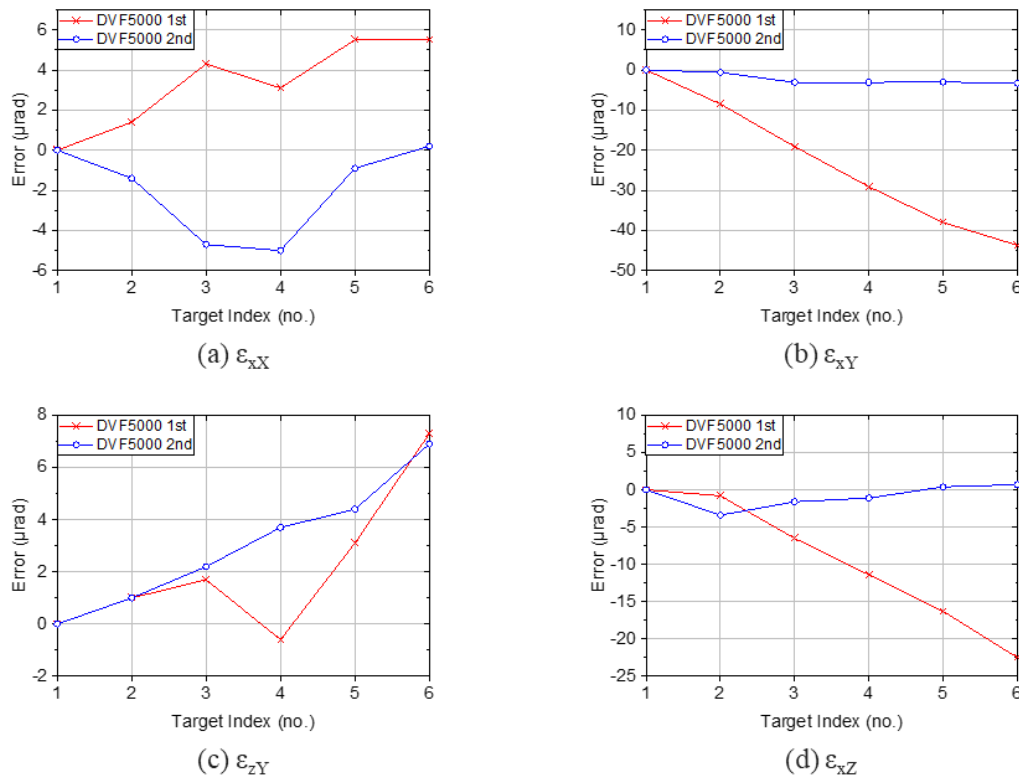


Fig. 5-13 Comparison of key errors for individual motions of two machine tools tested

First, key error parameters for individual motions were extracted and compared from the measurement results of the two test machining tools. The classification of the two machining tools was marked with a subscript as '1st' marked with a red line, and '2nd' marked with a blue line respectively for convenience in comparison, where, data marked with a subscript as '1st' points to a result measured at the machining tool without optimizing tolerance, and another data marked with a subscript as '2nd' points to a result measured at the machining tool with optimizing tolerance. The key error parameters for individual

motions of DVF5000, which is a 5-axis machining tool to have been studied and tested, were identified as  $\epsilon_{xX}$ ,  $\epsilon_{xY}$ ,  $\epsilon_{zY}$ , and  $\epsilon_{xZ}$  through the analysis for determination of key error, and the measurement results for these errors are shown in Fig. 5-13. It is confirmed that all key error parameters of the '2nd' machining tool are well-managed, that is, well-suppressed, compared to the '1st' machining tool. In particular, improvements in the  $\epsilon_{xY}$  shown (b) error parameters corresponding to the Y-axis pitch motion and the  $\epsilon_{xZ}$  shown (d) error parameters corresponding to the Z-axis pitch motion are clearly observed. These pitch motion errors are errors that are mainly affected by the shape of the bottom machining surface of the structure in which the linear motion guide(i.e., LMG) is installed and the deflection caused by the deadweight of the components. Therefore, in order to minimize these errors during the manufacturing process, precision adjustment using dummy loads during assembly and optimization of the shape of the machining surface seem to have been effective.

Then, key error parameters for mutually simultaneous motions were acquired by circular tests and the test results compared to the two machining tools are shown in Fig. 5-14. Comparing the perpendicularity for each measurement plane, it is confirmed that the squareness error for XY and YZ planes of the '2nd' compared to '1st' is assembled under remarkably well-managed. and the squareness error for the XZ plane of '2nd' is observed to be slightly inferior though, it is not only a range that satisfies the proposed tolerance but also not riskful enough to wreck the volumetric error of the targeted 5-axis machining tool. Through these results, it was confirmed that the proposed tolerances of squareness error, which is an influenceable factor on the volumetric error, have been properly applied to the intended machining tool. Therefore, the effectiveness of controlling the squareness error for the enhancement of the volumetric error of the machining tool can be distinguished through these comparative experiments of the two sampled machining tools.

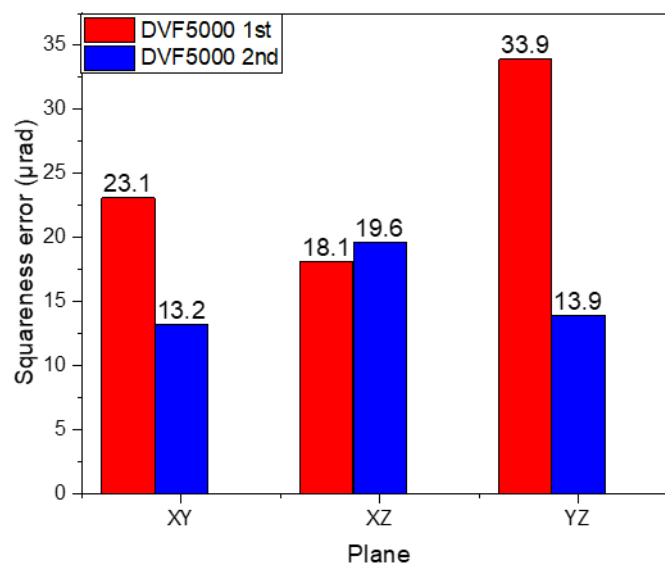


Fig. 5-14 Comparison of key errors for mutually simultaneous motions of two machine tools tested

Consequently, the key error components and the spatial error measured in the two machining tools are summarized and compared as shown in Table 5-5. As can be seen from the comparison, among the two machines used for this verification, the machining tool marked with "2nd" subscripts is a machine that has been put in the effort to assemble according to the optimized tolerance ranges, and another machine marked with "1st" subscripts is not a machining tool produced with this proposed tolerance. These differences in whether to determine and control key parameters have been evidently demonstrated that it is revealed as a volumetric error, a comprehensive precision evaluation index for machining tools. While the measurement value of the volumetric error of a machining tool that does not adopt assembly tolerance improved is  $32\mu\text{m}$ , the measurement value of another machining tool that has undergone determination of key error and tolerance range and application to the practical assembly process is  $15\mu\text{m}$  without post-process such as any numerical error compensation through controllers. Furthermore, it can be seen that not only the difference in measurement value but also the shape of the entire working space shows an explicit difference in quality as seen in Fig. 5-10, and Fig. 5-12. And in the end, it can conjecture that shape of the working space would be directly projected onto the workpiece during machining, which has a decisive effect on distorting the shape of the final products machined.

Key error parameters	Proposed tolerance	Measured value of errors and fulfillment			
		Test machine tools 1st		Test machine tools 2nd	
$\epsilon_{xx}$	$-8\pm 6\mu\text{rad}$	$5.5\mu\text{rad}$	X	$-5.0\mu\text{rad}$	O
$\epsilon_{xy}$	$-8\pm 6\mu\text{rad}$	$-43.7\mu\text{rad}$	X	$-3.3\mu\text{rad}$	O
$\epsilon_{zy}$	$-8\pm 6\mu\text{rad}$	$7.3\mu\text{rad}$	X	$6.9\mu\text{rad}$	X
$\epsilon_{xz}$	$-8\pm 6\mu\text{rad}$	$-22.5\mu\text{rad}$	X	$-3.3\mu\text{rad}$	O
$\gamma_{xy}$	$17\pm 4\mu\text{rad}$	$23.1\mu\text{rad}$	X	$13.2\mu\text{rad}$	O
$\alpha_{yz}$	$17\pm 4\mu\text{rad}$	$18.1\mu\text{rad}$	O	$19.6\mu\text{rad}$	O
$\beta_{xz}$	$17\pm 4\mu\text{rad}$	$33.9\mu\text{rad}$	X	$13.9\mu\text{rad}$	O
Measured volumetric error		$32\mu\text{m}$		$15\mu\text{m}$	

Table 5-5 Comparison of key errors and the resulting volumetric error of two machine tools tested

## Chapter 6. CONCLUSION AND FUTURE WORKS

This thesis described practical methods for analysis concerning the classification of the 5-axis machining tools' geometric errors, the modeling method for machining tools' volumetric, the determination of key errors, and finally the methods for estimation and verification of machining tools' volumetric error. In order to obtain these insights into machining tools' spatial performance within the entire working volume due to the geometric error of individual components and kinematic error on a 5-axis machining tool, study and experiments to demonstrate were conducted through the following procedures.

First, the individual error parameters that could occur in the 5-axis machining tool were classified into errors due to linear motion components, errors due to rotary motion components, and errors due to mutually linked relationships, and error matrices composed of these error parameters were defined. A kinematic chain of the RRTTT type machining tool under this study was constructed according to the sequential linked relationship of each motion component, and an error model using a homogeneous transformation matrix (HTM) and assuming rigid body motion was established.

Second, an error model of the machining tools targeted was developed by deriving the gain equation for volumetric error, which is composed of each error parameter as a variable, of the machining tool. And the coefficients of the polynomial were compared for each variable, and the errors propagating sensitively to volumetric errors were determined as key errors. Through the key error analysis, the fact that the key error parameters of the machining tool to be studied are  $\varepsilon_{xx}$ ,  $\varepsilon_{xy}$ ,  $\varepsilon_{zy}$ ,  $\varepsilon_{xz}$ ,  $\gamma_{xy}$ ,  $\alpha_{yz}$ , and  $\beta_{xz}$  has been revealed, and the sensitivity, namely the extent to which propagate to the functional end-point, of translation errors such as position and straightness errors are relatively small, and can be disregarded compared with sort of angular error parameters including angular motion and squareness errors.

Third, to confirm the effect of applying the measures to restrain the key geometric errors which propagate to the end of the functional point sensitively, the range of tolerances for key errors has been selected considering kinematic characteristics. And then volumetric errors within the entire workspace under the range of general tolerance and the proposed tolerance were predicted through simulation in the working volume,  $550 \times 450 \times 400\text{mm}^3$ . According to the simulation, the volumetric error of the targeted 5-axis machine under the tolerance of the general case is predicted as about  $41\mu\text{m}$ , and it is expected that the volumetric error of DVF5000 can be achieved at around  $24\mu\text{m}$  without any compensation through the software if the assembly process is managed within the tolerance range proposed for the key geometric errors.

Last, In order to demonstrate whether the volumetric error has been improved through the process for determination and suppression of key errors reviewed previously, experiments for each error assessment

were conducted on two machining tools. Each error evaluation before applying the proposed tolerance has been conducted for a machining tool called sample '1st', and the measurement after undergoing measures that satisfied the proposed tolerance based on the prediction of the volumetric error has been conducted for the same model of a machining tool called sample '2nd'. Prior to the volumetric error, which is the means for resultant error evaluation, whether each key error parameter was properly suppressed has been evaluated. Each key error parameter was measured using a laser interferometer which can measure six-degree-of-freedom error, and a double ball bar, which are instruments commonly used by machining tool manufacturers or users. Through the comparison of the measurement results of two machining tools, the '2nd' machining tool confirmed that the key error parameters were well suppressed within the intended tolerance range, and the measurement results of the volumetric error were also  $15\mu\text{m}$  and  $32\mu\text{m}$ , respectively, showing a significant difference between the '1st' machining tool and the '2nd' machining tool which did not adopt the proposed tolerance.

Therefore, it was confirmed that if machining tools' key error parameters can be classified in advance from the design or production step of the machining tool and then manage properly during the machining tools' assembly process, the machining tools' volumetric accuracy can be significantly enhanced without error compensation methods which are kinds of post-process through the machining tools' controller. And for this, developing a multi-axis machining tools' error model which allows for the calculation of the effects from geometric inaccuracies in the structural geometry or motion of the components composing the machining tools, using the kinematics of rigid body motion and Homogenous Transformation Matrix is needed. and estimation for volumetric error at any arbitrary point in the working space of machining tools is important for establishing an effective strategy for enhancing machining tools' volumetric accuracy.

In order to enhance the volumetric error of the multi-axis machining tools, an error model for the target machining tool is essential. There is no generic error model, especially since the 5-axis machining tool has a complex kinematic structure and configuration. This is why it is difficult to predict and improve performance related to accuracy in advance, and an error model that reflects each kinematic characteristic of each multi-axis machining tool is needed as well. Therefore, since this study and experiment were conducted based on conditions limited to one type of 5-axis machining tool such as RRTTT type, error models for various practical machining tools regardless of horizontal 5-axis machining tools and vertical 5-axis machining tools are going to construct. Furthermore, even if the key error parameter is suppressed through manufacturing processes for machining tools, a compensation strategy is developed as a post-processing method to eliminate the influence of errors that still exist, and an overall strategy for machining tools with stable precision performance is going to establish.

## REFERENCES

- [1] Bohez, Erik L.J. "Five-axis milling machine tool kinematic chain design and analysis." *International Journal of Machine Tools and Manufacture* 42.4 (2002): 505-520.
- [2] Damsohn, Herbert. *Fünffachsiges NC-Fräsen: Beitrag zur Technologie, Teileprogrammierung und Postprozessorverarbeitung*. Vol. 14. Springer-Verlag, 2013.
- [3] Ramesh, R., M. A. Mannan, and A. N. Poo. "Error compensation in machine tools—a review: part I: geometric, cutting-force induced and fixture-dependent errors." *International Journal of Machine Tools and Manufacture* 40.9 (2000): 1235-1256.
- [4] Hocken, R. J. *Technology of machine tools*. Volume 5. Machine tool accuracy. No. UCRL-52960-5. California Univ., Livermore (USA). Lawrence Livermore Lab., 1980.
- [5] Lin, YI, and Y. Shen. "Modelling of five-axis machine tool metrology models using the matrix summation approach." *The International Journal of Advanced Manufacturing Technology* 21.4 (2003): 243-248.
- [6] Postlethwaite, S. R., and D. G. Ford. "Geometric error analysis software for CNC machine tools." *WIT Transactions on Engineering Sciences* 16 (1970).
- [7] Kiridena, V. F. P. M., and P. M. Ferreira. "Mapping the effects of positioning errors on the volumetric accuracy of five-axis CNC machine tools." *International Journal of Machine Tools and Manufacture* 33.3 (1993): 417-437.
- [8] Kiridena, V. S. B., and P. M. Ferreira. "Kinematic modeling of quasistatic errors of three-axis machine tools." *International Journal of Machine Tools and Manufacture* 34.1 (1994): 85-100.
- [9] Srivastava, A. K., S. C. Veldhuis, and M. A. Elbestawit. "Modelling geometric and thermal errors in a five-axis CNC machine tool." *International Journal of Machine Tools and Manufacture* 35.9 (1995): 1321-1337.
- [10] Abbaszadeh-Mir, Yousefali, et al. "Theory and simulation for the identification of the link geometric errors for a five-axis machine tool using a telescoping magnetic ball-bar." *International Journal of Production Research* 40.18 (2002): 4781-4797.
- [11] Lin, YI, and Y. Shen. "Modelling of five-axis machine tool metrology models using the matrix summation approach." *The International Journal of Advanced Manufacturing Technology* 21.4 (2003): 243-248.
- [12] Tsutsumi, M., and A. Saito. "Identification and compensation of systematic deviations particular to 5-axis machine tools." *International Journal of Machine Tools and Manufacture* 43.8 (2003): 771-

780.

- [13] BOHEZ, Erik LJ, et al. Systematic geometric rigid body error identification of 5-axis milling machines. *Computer-Aided Design*, 2007, 39.4: 229-244.
- [14] Uddin, M. Sharif, et al. "Prediction and compensation of machining geometric errors of five-axis machine tools with kinematic errors." *Precision engineering* 33.2 (2009): 194-201.
- [15] Khan, Abdul Wahid, and Wuyi Chen. "A methodology for systematic geometric error compensation in five-axis machine tools." *The International Journal of Advanced Manufacturing Technology* 53.5 (2011): 615-628.
- [16] Lee, Rong-Shean, and Y. H. Lin. "Applying bidirectional kinematics to assembly error analysis for five-axis machine tools with general orthogonal configuration." *The International Journal of Advanced Manufacturing Technology* 62.9 (2012): 1261-1272.
- [17] Zhou, Baocang, et al. "Geometric error modeling and compensation for five-axis CNC gear profile grinding machine tools." *The International Journal of Advanced Manufacturing Technology* 92.5 (2017): 2639-2652.
- [17] Zha, Jun, et al. "Volumetric error compensation of machine tool using laser tracer and machining verification." *The International Journal of Advanced Manufacturing Technology* 108.7 (2020): 2467-2481.
- [18] Khan, Abdul Wahid, and Chen Wuyi. "Systematic geometric error modeling for workspace volumetric calibration of a 5-axis turbine blade grinding machine." *Chinese Journal of Aeronautics* 23.5 (2010): 604-615.
- [19] Slocum, Alexander H. *Precision machine design*. Society of Manufacturing Engineers, 1992.
- [20] Denavit, Jacques, and Richard S. Hartenberg. "A kinematic notation for lower-pair mechanisms based on matrices." (1955): 215-221.
- [21] Paul, Richard P. *Robot manipulators: mathematics, programming, and control: the computer control of robot manipulators*. Richard Paul, 1981.
- [22] Donmez, M. Alkan, et al. "A general methodology for machine tool accuracy enhancement by error compensation." *Precision Engineering* 8.4 (1986): 187-196.
- [23] Ferreira, P. M., C. R. Liu, and E. Merchant. "A contribution to the analysis and compensation of the geometric error of a machine tool." *CIRP Annals* 35.1 (1986): 259-262.
- [24] Kiridena, V. S. B., and P. M. Ferreira. "Kinematic modeling of quasistatic errors of three-axis

- machine tools." *International Journal of Machine Tools and Manufacture* 34.1 (1994): 85-100.
- [25] Ehmann, Kornel F. "Solution principles for a new generation of precision self-correcting multi-axis machines." *Robotics and Computer-Integrated Manufacturing* 7.3-4 (1990): 357-364.
- [26] Soons, J. A., F. C. Theuws, and P. H. Schellekens. "Modeling the errors of multi-axis machines: a general methodology." *Precision engineering* 14.1 (1992): 5-19.
- [27] Kiridena, V. F. P. M., and P. M. Ferreira. "Mapping the effects of positioning errors on the volumetric accuracy of five-axis CNC machine tools." *International Journal of Machine Tools and Manufacture* 33.3 (1993): 417-437.
- [28] Ahn, Kyoung Gee, and Dong Woo Cho. "Proposition for a volumetric error model considering backlash in machine tools." *The International Journal of Advanced Manufacturing Technology* 15.8 (1999): 554-561.
- [29] Lin, Y., and Y. Shen. "Modelling of Five-axis Machine Tool Metrology Models Using the Matrix Summation Approach." *International Journal of Advanced Manufacturing Technology* 21.4 (2003): 243-48. Web.
- [30] Fan, J. W., et al. "A universal modeling method for enhancement the volumetric accuracy of CNC machine tools." *Journal of Materials Processing Technology* 129.1-3 (2002): 624-628.
- [31] Chen, Guoda, et al. "Volumetric error modeling and sensitivity analysis for designing a five-axis ultra-precision machine tool." *The International Journal of Advanced Manufacturing Technology* 68.9 (2013): 2525-2534.
- [32] Bohez, Erik LJ. "Five-axis milling machine tool kinematic chain design and analysis." *International Journal of Machine Tools and Manufacture* 42.4 (2002): 505-520.
- [33] Brecher, Christian, and Manfred Weck. *Machine Tools Production Systems 2: Design, Calculation and Metrological Assessment*. Springer, 2021.
- [34] SO/FDIS 230-1, "Test code for machine tools – Part 1: Geometric accuracy of machines operating under no-load or quasi-static conditions," 2011.
- [35] ISO 230-7, "Test code for machine tools – Part 7: Geometric accuracy of axes of rotation," 2006
- [36] Erkan, T., and J. R. R. Mayer. "A cluster analysis applied to volumetric errors of five-axis machine tools obtained by probing an uncalibrated artefact." *CIRP annals* 59.1 (2010): 539-542.
- [37] Li, Qingzhao, et al. "Measurement method for volumetric error of five-axis machine tool considering measurement point distribution and adaptive identification process." *International Journal*



of Machine Tools and Manufacture 147 (2019): 103465.

[38] Gao, Weiguo, et al. "An improved machine tool volumetric error compensation method based on linear and squareness error correction method." *The International Journal of Advanced Manufacturing Technology* 106.11 (2020): 4731-4744.

[39] Schwenke, Heinrich, et al. "Geometric error measurement and compensation of machines—an update." *CIRP annals* 57.2 (2008): 660-675.

[40] ISO 230-4, "Test code for machine tools – Part 4: Circular tests for numerically controlled machine tools," 2005.

[41] Ibaraki, Soichi, and Wolfgang Knapp. "Indirect measurement of volumetric accuracy for three-axis and five-axis machine tools: a review." *International Journal of Automation Technology* 6.2 (2012): 110-124.

[42] Kakino, Yoshiaki, et al. *Accuracy inspection of NC machine tools by double ball bar method*. New York: Hanser, 1993.

[43] Lai, J-M., J-S. Liao, and W-H. Chieng. "Modeling and analysis of nonlinear guideway for double-ball bar (DBB) measurement and diagnosis." *International Journal of Machine Tools and Manufacture* 37.5 (1997): 687-707.

[44] Florussen, G. H. J., et al. "Assessing geometrical errors of multi-axis machines by three-dimensional length measurements." *Measurement* 30.4 (2001): 241-255.

[45] ISO 230-6, "Test code for machine tools – Part 6: Determination of positioning accuracy on body and face diagonals (Diagonal displacement tests)," 2002.

[46] Kruth, J-P., et al. "A method for squareness error verification on a coordinate measuring machine." *The International Journal of Advanced Manufacturing Technology* 21.10 (2003): 874-878.

[47] Morris, T. J. "A new slant on diagonal laser testing." *WIT Transactions on Engineering Sciences* 34 (1970).

[48] Chapman, Mark AV. "Limitations of laser diagonal measurements." *Precision Engineering* 27.4 (2003): 401-406.

[49] Ibaraki, Soichi, and Takafumi Hata. "A new formulation of laser step diagonal measurement—Three-dimensional case." *Precision Engineering* 34.3 (2010): 516-525.

[50] ISO/CD 10791-6, "Test conditions for machining centres – Part 6: Accuracy of feeds, speeds and interpolations, 2011.

- [51] Tsutsumi, M., and A. Saito. "Identification and compensation of systematic deviations particular to 5-axis machine tools." *International Journal of Machine Tools and Manufacture* 43.8 (2003): 771-780.
- [52] Kakino, Y. "A Study on the motion accuracy of NC machine tools (7th report)-Measurement of motion accuracy of 5-axis machine by DBB tests." *J Jpn Soc Precision Eng* 60.5 (1994): 718-723.
- [53] Lei, W. T., I. M. Paung, and Chen-Chi Yu. "Total ballbar dynamic tests for five-axis CNC machine tools." *International Journal of Machine Tools and Manufacture* 49.6 (2009): 488-499.
- [54] Weikert, S. "R-test, a new device for accuracy measurements on five axis machine tools." *CIRP annals* 53.1 (2004): 429-432.
- [55] Bringmann, Bernhard, and Wolfgang Knapp. "Model-based 'chase-the-ball' calibration of a 5-axes machine tool." *CIRP annals* 55.1 (2006): 531-534.
- [56] Andolfatto, Loïc, J. R. R. Mayer, and Sylvain Lavernhe. "Adaptive Monte Carlo applied to uncertainty estimation in five axis machine tool link errors identification with thermal disturbance." *International Journal of Machine Tools and Manufacture* 51.7-8 (2011): 618-627.
- [57] Bringmann, B., and W. Knapp. "Machine tool calibration: Geometric test uncertainty depends on machine tool performance." *Precision Engineering* 33.4 (2009): 524-529.
- [58] Schwenke, H., et al. "On-the-fly calibration of linear and rotary axes of machine tools and CMMs using a tracking interferometer." *CIRP annals* 58.1 (2009): 477-480.
- [59] Bal, Evren. Modeling and compensation of machine tool volumetric errors for virtual CNC environment. Diss. University of British Columbia, 2003.
- [60] Xinxin, L. I., et al. "A Novel Error Equivalence Model on the Kinematic Error of the Linear Axis of High-End Machine Tool." (2021).
- [61] Zhong X, Yang R, Zhou B. "Accuracy analysis of assembly success rate with Monte Carlo simulations." *J DongHua Univer* 20(4):128–131 (2003): 128-131.
- [62] Jia, Z., and F. Wang. "Foundation of machine manufacturing technology." (2011).
- [63] Mayr, Josef, et al. "Thermal issues in machine tools." *CIRP annals* 61.2 (2012): 771-791.
- [64] Bryan, Jim. "International status of thermal error research (1990)." *CIRP annals* 39.2 (1990): 645-656.
- [65] ISO 230-1, "Test code for Machine Tools – Part 1: Geometric Accuracy of Machines Operating Under No-load or Quasi-static Conditions," (2012).

## ACKNOWLEDGEMENT

My study aimed to study how individual geometric errors of machine tools are magnified to machine tools' functional point volumetric error as a result of their propagation through a kinematic structure system. And insights and experiences attained through study at UNIST make me realize that what I have achieved can be possible thanks to the help of the following people rather than my sole efforts.

I want to thank the members of my thesis committee. First and foremost, I would like to appreciate Professor Hyung-Wook Park as a great teacher who introduced structural error analysis of machine tools, and an advisor who advised error model for machine tools from scratch. I will try harder in the future to become a person like my professor. I want to thank Professor Namhoon Kim for having commented on my paper at the thesis examining and teaching me 'Advanced Additive Manufacturing' in my first semester. And also I want to thank Professor Im doo Jung for giving heartfelt advice and helpful comment on my paper at the thesis examining.

Since I first came to UNIST, MHM lab. members(Bros.) have supported and helped me in many aspects and helped me prepare for my thesis examining as well. Thanks for their advice and consistent support; Dong-Chan who is a great leader of our lab., Hyun-Min who didn't hesitate to help me, Sang-Min who always treated me with a smile, Hee-Chan who does his best in everything, Jong-Woo who is always humble and gentle, Yoon-Seok who is a native of Europe, Sin-Won who will be the number one in tantalum machining, and Yoon-Jae who is a smart and romantic guy. And I want to thank Chang-Hyun, who seat next to me in the office for the past two years, for always giving me help and caring about me with all his heart. You guys are indeed the best friends I have ever met. I will remember the precious time I spent with you guys around Ulsan and Eon-yang for the rest of my life.

I owe debts to many co-workers in my company and my graduate studies would not have been possible without the encouragement and support of my company. In particular, I am incredibly grateful to Kyuho Pae, vice president of my company, and Wonjin Sung who used to be my team leader for standing behind me even though I was not good enough in many ways and encouraging me on studying mechanical engineering again.

Lastly, but most importantly, thanks to my family for their support throughout my studies. My parents, Jae-Hoon Jang and Soon-Ae Kim, my younger brother Soo-Won Jang, and my parents-in-law, Jong-Do Lim and Hyun-Ok Choi, have always supported me to do whatever I want to do. My wife, Hee-Jeong Rim, and Sein Jang who is my lovely daughter and a treasure, I could not complete graduate school without their cheer and love, and they are the most important existence in my life and a true pillar of support for me in my life journey. I know that is not possible that me to pay off all these debts I have received. However, whenever I have a chance, I will help others just as they helped me and repay their kindness for the rest of my life.